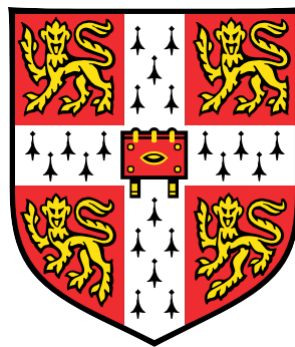


# **Arenaviruses: the Role of Antigen Presenting Cells (APC) in Persistence and Immunopathology**



**Ugwu Alphonsus Chinedu**

Department of Veterinary Medicine

University of Cambridge

This thesis is submitted for the degree of

*Doctor of Philosophy*

**Fitzwilliam College**

**October 2020**

## **Declaration**

I hereby declare that this dissertation is the result of my own work and includes nothing which is the outcome of work done in collaboration except as specified in the text.

It is not substantially the same as any that I have submitted or is being concurrently submitted for a degree or diploma or other qualification at the University of Cambridge or any other University or similar institution except as declared in the preface and specified in the text. I further state that no substantial part of my dissertation has already been submitted, or is being concurrently submitted for any such degree, diploma, or other qualification at the University of Cambridge or any other University or similar institution except as specified in the text

This dissertation contains less than 65,000 words including appendices, bibliography, footnotes, tables, and equations, and has less than 150 figures.

Alphonsus Chinedu Ugwu

# **Arenaviruses: the Role of Antigen Presenting Cells (APC) in Persistence and Immunopathology**

**Alphonsus Chinedu Ugwu**

## **Summary**

Viruses are major contributors to global health crises. Many of the disease pandemics the world has experienced were caused by viruses from smallpox to Spanish flu, Ebola (Public health emergency of international concern), SARS, West Nile, Zika and currently SARS-CoV-2 the aetiology of COVID19. At the centre of the virus-host interaction is a unique group of cells called the antigen presenting cells (APC). APC play a significant role in immune response, as the receptionist, they are the first cells to detect pathogen invasion and present the antigen to the cells of the adaptive immune system for activation and clearance of the pathogen. This unique function as the receptionist and coordinator of signals makes them critical players in directing the outcome of an immune response. Therefore, they are critical in understanding the dynamics of viral infection, why certain viruses are cleared while others persist; the study of virus interaction with APC is a vital area to start.

This thesis investigates the role of APC in virus infection, persistence and immunopathology using the LCMV model. The LCMV model is a well-established model system for studying the immune system and its interaction with pathogen. It has contributed to some fundamental discoveries in the field of immunology and virology; for example, understanding the role of the major histocompatibility complex. Though the LCMV model has been a critical player in the field of immunology and virology, most of the data from the model are from bulk analyses and made use of available resources at the time. With the advent of high throughput technologies such as the single cell RNA sequencing, this thesis revisits the LCMV-APC (DC and macrophage/monocytes) interaction at the *in vitro*, *in vivo* and single-cell level.

The findings from the *in vitro* study confirmed the heterogeneity of *in vitro* bone marrow derived cells as opposed to the previous view that they were mainly DC whilst macrophages are generated only by M-CSF growth factor. This heterogeneity was present after differentiating cells in the presence of all the growth factors commonly used for generating *in vitro* BM-DC. Moreso, the result confirmed functional

differences between the DC (BM-DC) and macrophage (BM-M) subsets. While BM-DC were better at antigen presentation to T cells, BM-M were more efficient cytokine producers.

The *in vivo* study validated the immunosuppressive nature of LCMV in virus persistence. LCMV clone 13 infected all subsets of splenic DC and macrophages and impaired expression of antiviral and inflammatory cytokine genes as well as antigen presentation genes in APC. However, this impairment was temporary and was overridden by secondary stimulation with poly (I:C).

Taken together, this thesis has shown the division of labour amongst APC in their interaction with the virus. It also demonstrated the power of single-cell sequencing technology and how it is helping to recognise the dynamic nature of the immune response at the single-cell transcriptome level. With more availability of high-throughput technology, there is a need to revisit some of the previous studies that were based on bulk analyses of the immune response to viruses. Understanding the dynamic nature of immunity and the individual contribution at the cellular level will improve our efficiency and precision in designing intervention measures.

## **Acknowledgements**

I am eternally grateful to everyone that contributed to making this project a reality. In particular: My PhD supervisor Jonathan Heeney. Jon provided both scientific and emotional support throughout this journey. I am glad our relationship has grown beyond this PhD studies and now for life. If I will have to choose a supervisor for this journey again, I will choose Jon.

My second supervisor Dr Barbara Blacklaw who provided critical review of this project at every step from the beginning to the end. I am grateful she is still supporting me beyond this PhD.

My special gratitude also goes to my friend and lab manager Paul Tonks. Paul supported me with setting up all the technical aspects of the experiments for this project. I am grateful for all the extra working hours you put in just to see this work come to fruition.

To my PhD predecessors and Postdocs (Dr Ed Greenwood, Dr Fabian Schmidt, Dr James Chettle, Dr Osama Eisa, Dr Sam Stubbs, Dr David Wells), research assistants (Sheryl Baptista), and administrative staff (Dr Rebecca Kingsley) and new graduate students' members of the LVZ lab and department of the Veterinary medicine, I met during this journey, thank you for all your support and guidance. Also, thank you to Dr Julien Bauer and Dr Katarzyna Kania for helping with my bioinformatic analysis and single RNA sequencing respectively.

Further appreciation goes to my Fitz family (from the college Master -Nicky Padfield, my college Mentor-Jonathan Cullen and other members of the college administration), thank you for providing a warm and conducive home for an international student.

I am grateful to Dr Goodluck Jonathan and the Federal republic of Nigeria under the presidential scholarship for innovation and development (PRESSID) for providing the scholarship that supported this project.

Finally, my sincere appreciation to my family and friends especially my mother (Christiana Ugwu- Odiichenwanyi) to whom I dedicate this project. Thank you.

## Abbreviations

APC – Antigen presenting cell

BCR – B-cell receptor

BDCA2 - Blood DC antigen 2

BMP-2 – Bone morphogenetic protein 2

BST2 - Bone marrow stromal antigen 2

CBS – Cambridge biomedical centre

CD – Cluster of differentiation

cDC - Conventional/Classical dendritic cells

cDNA – Complementary DNA

cGAS - cyclic GMP-AMP synthase (cGAS)

CMV – Cytomegalovirus

CDP – Common DC progenitor

CH25H - Cholesterol-25-hydroxylase

cMOP – Common monocyte progenitor

CMP – Common myeloid progenitor

CSF – Colony stimulating factor

DC – Dendritic cell

DCP – DC progenitor

DAI - DNA-dependent activator of IRFs

DMEM-Dulbecco's modified Eagle's medium

DN – Double negative

ELISA – Enzyme-linked immunosorbant assay

FACS – Fluorescent activated cell sorting

FCS - foetal calf serum

FDR – False discovery rate

FLT3 – FMS-like tyrosine kinase 3

FOXP3 – Forkhead box P3

GFP – Green fluorescent protein

GO1 – Gene of interest

GM-CSF – granulocyte-monocyte colony stimulating factor

HIV – Human immunodeficiency virus

HLA – Human leukocyte antigen

HSC – Haematopoietic stem cell

IFN – Interferon

IL – Interleukin

IMDM - Iscove's modified Dulbecco's medium

IPC - Interferon-producing cells

IPS - Inositol-3-phosphate synthase isozyme 1

Ig(A-E) – Immunoglobulin (isotype A-E)

IRF7 – Interferon regulatory factor 7

LC – Langerhans cell

LCMV - Lymphocytic choriomeningitis virus

LGP-2 - Laboratory of genetics and physiology-2

LPS – Lipopolysaccharide

MAPK - Mitogen-activated protein kinase

MAVS - Mitochondrial anti-viral signaling proteins

MDA5 - Melanoma differentiation factor-5

MDP – Macrophage-DC progenitor

MHC – Major histocompatibility complex

MIIC – MHC II compartment

MOI – Multiplicity of infection

NFκB - Nuclear factor-κB

NGS – Next generation sequencing

NK cell – Natural killer cell

NLR – Nod like receptors

OAS - Oligoadenylate synthetase

PAMP – Pathogen associated molecular pattern

PBMC – Peripheral blood mononuclear cell

PCR – Polymerase chain reaction

pDC – Plasmacytoid DC

PRR – Pattern recognition receptor

qPCR – Quantitative polymerase chain reaction

RCA – Rolling circle amplification

RLR - Retinoic acid-inducible gene I (RIG-I)-like receptors

RT-PCR – Reverse-transcription PCR

rRNA – Ribosomal RNA

SCSA – Signal computing system architecture

Siglec-H – Sialic acid-binding immunoglobulin-like lectin H

TBK1 - TANK-binding kinase 1

TCF4 - Transcription factor 4

TCR – T cell receptor

TGF-β – Transforming growth factor beta

TLR – Toll like receptor

UMAP – Uniform manifold approximation projection

VHF – Viral haemorrhagic fever

ZBTB46 - Zinc finger and BTB domain containing 46

# Contents

<b>Arenaviruses: the Role of Antigen Presenting Cells (APC) in Persistence and Immunopathology .....</b>	<b>1</b>
<i>Summary.....</i>	<i>3</i>
<i>Acknowledgements.....</i>	<i>5</i>
<i>Abbreviations.....</i>	<i>6</i>
<i>Contents.....</i>	<i>10</i>
<i>List of Tables .....</i>	<i>13</i>
<i>List of Figures .....</i>	<i>14</i>
<b>Chapter 1 .....</b>	<b>15</b>
<b>Introduction .....</b>	<b>15</b>
<b>1.1 The Immune System and The Role of Antigen Presenting Cells (APC).....</b>	<b>15</b>
1.1.1 Overview of Antigen Presenting Cells (APC) .....	18
1.1.2 APCs and Viral Infections .....	26
<b>1.2 Arenavirus Overview .....</b>	<b>37</b>
1.2.1 Classification and Virus Replication.....	37
1.2.2 Arenavirus infection: The Role of APC.....	44
1.2.3 Arenaviruses and Viral Haemorrhagic Fever Syndrome.....	45
1.2.4 LCMV as a Model of Virus Persistence in APCs.....	47
<b>1.3 Hypothesis and Aims.....</b>	<b>49</b>
1.3.1 Hypotheses: .....	49
1.3.2 Aims and Objectives: .....	49
<b>Chapter 2 .....</b>	<b>51</b>
<b>General Materials and Methods .....</b>	<b>51</b>
<b>2.1 Cell Lines.....</b>	<b>51</b>
<b>2.2 Mice .....</b>	<b>52</b>
<b>2.3 Viruses.....</b>	<b>52</b>
2.3.1 Generation and Quantitation of High-Titre Virus Stocks .....	54
<b>2.4 In vitro Infection of Bone Marrow Derived Cells.....</b>	<b>55</b>
2.4.1 Generation of Bone marrow (BM) Derived Cells.....	55
2.4.2 LCMV Infection of BM Derived Cells .....	55
2.4.3 Infection Assays on RAW and BV-2 Cells.....	56
2.4.4 Treatment of BM Derived Cells with Poly(I:C) .....	56
<b>2.5 In vivo Infection of Mice.....</b>	<b>56</b>
2.5.1 Intraperitoneal Infection with r3LCMV/CI13 Cre or Stimulation with Poly (I:C) .	56
2.5.2 Isolation of Mouse Splenic Mononuclear Cells .....	57
<b>2.6 Flow Cytometry .....</b>	<b>57</b>
2.6.1 Surface Staining of BM Derived and Splenic DCs and Macrophages.....	57
2.6.2 Detection of Cell surface Markers by Flow Cytometry .....	58
2.6.3 Sorting of BM Derived and Splenic DCs and Macrophages .....	58

2.6.4	Antibodies .....	59
<b>2.7</b>	<b>RNA Extraction.....</b>	<b>64</b>
2.7.1	Cells in Culture .....	65
<b>2.8</b>	<b>Reverse Transcription and Gene Expression Assays.....</b>	<b>65</b>
2.8.1	Reverse Transcription .....	65
2.8.2	Gene Expression Analysis.....	65
<b>2.9</b>	<b>Statistical Analysis .....</b>	<b>66</b>
<b>Chapter 3 .....</b>		<b>67</b>
<b>Infection of <i>in vitro</i> Bone Marrow Derived APC with LCMV Virus .....</b>		<b>67</b>
<b>3.1</b>	<b>Background.....</b>	<b>67</b>
<b>3.2</b>	<b>Materials and Methods .....</b>	<b>68</b>
3.2.1	Generation of Bone-marrow (BM) Derived Cells .....	68
3.2.2	Flow Cytometry Analysis .....	69
3.2.3	BM derived cell morphology by light microscope .....	72
3.2.4	LCMV infection of BM derived cells .....	73
3.2.5	Quantification of LCMV-GFP infectious units in Vero cell.....	73
3.2.6	Treatment of BM derived cells with poly (I:C) .....	73
3.2.7	Gene expression analysis .....	73
3.2.8	IFN- $\beta$ Enzyme-Linked Immunosorbent Assay (ELISA).....	75
3.2.9	Single cell RNA sequencing of LCMV infected bone marrow derived cells.....	75
3.2.9	Antigen presentation assays .....	75
<b>3.3</b>	<b>Results .....</b>	<b>76</b>
3.3.1	Description of <i>In vitro</i> Bone Marrow Derived Cell Heterogeneity .....	76
3.3.2	Susceptibility of BM derived cells to LCMV infection.....	82
3.3.3	LCMV impairs cytokine production and antigen presentation in <i>in vitro</i> BM derived cells .....	84
<b>3.4</b>	<b>Discussion.....</b>	<b>98</b>
<b>3.5</b>	<b>Conclusion .....</b>	<b>101</b>
<b>Chapter 4 .....</b>		<b>102</b>
<b>Dissecting LCMV <i>In vivo</i> Infection of APC using Single Cell RNA Sequencing .....</b>		<b>102</b>
<b>4.1</b>	<b>Background.....</b>	<b>102</b>
<b>4.2</b>	<b>Materials and Methods .....</b>	<b>103</b>
4.2.1	Animals .....	103
4.2.2	Experimental procedure .....	103
4.2.3	Hashtag labelling of mouse splenic cells .....	106
4.2.4	Sorting of Mouse Splenic DCs and Monocytes .....	107
4.2.5	Library Preparation and Sequencing of Mouse Splenic Cells using the 10x Genomics Platform .....	107
4.2.6	Bioinformatics and data analysis .....	108
4.2.7	Comparison between the clusters and treatment.....	113
4.2.8	Statistical Analysis.....	114
<b>4.3</b>	<b>Results .....</b>	<b>114</b>
4.3.1	Cell hashing approach in single cell RNA sequencing.....	114

4.3.2	LCMV Infects all Splenic DC and Monocytes .....	115
4.3.3	Cytokine Gene Expression Kinetics of DC and Monocytes Following LCMV clone 13 Infection .....	117
4.3.3	Biological consequences of LCMV infection in APC .....	123
<b>4.4</b>	<b><i>Discussion</i></b> .....	<b>123</b>
<b>4.5</b>	<b><i>Conclusion</i></b> .....	<b>127</b>
<b>Chapter 5 .....</b>		<b>129</b>
<b>General Discussion and Concluding remarks .....</b>		<b>129</b>
<b>5.1</b>	<b><i>Summary of results</i></b> .....	<b>129</b>
<b>5.2</b>	<b><i>Limitations to this study</i></b> .....	<b>131</b>
<b>5.5</b>	<b><i>Concluding remarks and future work</i></b> .....	<b>133</b>
<b>Bibliography .....</b>		<b>134</b>
<b><i>Appendix 1. A summary table for all the comparisons between different cell clusters and treatments .....</i></b>		<b>160</b>
<b>4.2.9.2</b>	<b><i>Library 4</i></b> .....	<b>163</b>
<b>4.2.9.3</b>	<b><i>Library 5</i></b> .....	<b>164</b>
<b>4.2.9.4</b>	<b><i>Library 6</i></b> .....	<b>165</b>

# List of Tables

## Chapter 1

1: Table 1.1:	Summary of Viral Agents of Haemorrhagic Fevers .....	39
2: Table 1.2:	Comparison Between the Acute Strain (LCMV Armstrong) and the Persistent Strain (LCMV clone13) of LCMV .....	48

## Chapter 2

3: Table 2.1	Aria III Configuration and Set up .....	58
4: Table 2.2	List of Antibodies.....	60

## Chapter 3

5: Table 3.1	Experimental Procedure for Bone Marrow Derived Cell Phenotyping (Plate Map)	70
6: Table 3.2	Bone Marrow Derived Cell Sorting Procedure.....	71
7: Table 3.3	Quantitect Primer Assays (Qiagen) used for Gene Expression Analysis.....	74

## Chapter 4

8: Table 4.1.	Treatment Groups and Their Hashtags (summary).....	106
9: Table 4.2	Summary of Cellranger and Library Performance.....	108
10: Table 4.3	Summary of Cell Clusters and Their Top Five Genes (fold change log2) ...	111

## List of Figures

### Chapter 1

1: Figure 1.1:	The interplay between the innate and adaptive immune system.....	17
2: Figure 1.2:	Maturation of Dendritic cells and Macrophages .....	20
3: Figure 1.3:	Arenavirus Structure.....	42
4: Figure 1.4:	Arenavirus replication cycle .....	44

### Chapter 2

5: Figure 2.1:	Recombinant LCMV Arm and Clone 13 construct (with GFP).....	53
6: Figure 2.2:	Trisegmented recombinant LCMV Clone 13 construct (with Cre recombinase)	54

### Chapter 3

7: Figure 3.1	Bone Marrow Derived Cell Sorting Procedure.....	72
8: Figure 3.2	CD11b+ Expression on CD11c+MHC class II+ Bone Marrow Derived Cells Differentiated with Various Growth Factors .....	77
9: Figure 3.3A	Dendritic Cell Associated Receptor.....	78
10: Figure 3.3B	Macrophage Associated Receptors.....	79
11: Figure 3.3C	Costimulatory Receptors.....	79
12: Figure 3.4.	Morphology of the Three Groups of Bone Marrow Derived Cells Differentiated with Different Growth Factors .....	80
13:Figure 3.5	Transcription Factor Expression of Three Groups of CD11c+ MHC class II+ and/or CD11b+ Bone Marrow Derived Cells Differentiated with Various Growth Factors .....	81
14: Figure 3.6	LCMV (Armstrong and clone 13) Infection of BM Derived Cells .....	83
15: Figure 3.7	Productive Infection of BM Derived Cells by LCMV (ARM and clone 13).....	84
16: Figure 3.8.	Ifnb1 and Tnfa mRNA Expression in BM Derived Cells after Poly (I:C) Stimulation.....	85
17: Figure 3.9	Mx1 and Isg15 mRNA Expression in BM Derived Cells after Poly (I:C) Stimulation.....	86
18: Figure 3.10	ELISA for IFN- $\beta$ Production after Poly (I:C) Stimulation of BM Derived Cells .....	87
19: Figure 3.11	RT-qPCR-based Gene Expression Analysis of BM Derived Cells Following LCMV Infection.....	89
20: Figure 3.12A	BM-M: LCMV vs Poly (I:C).....	90
21: Figure 3.12B	DN: LCMV vs Poly (I:C).....	90
22: Figure 3.12C	LCMV clone 13 (GFP) infection then Poly (I:C) stimulation .....	91
23: Figure 3.13A	Antigen Presentation and T cell Activation by LCMV Infected BM Derived Cell Subsets	93
24: Figure 3.13B	Percentage CD25 expression.....	93
25: Figure 3.14 A	CD80 Expression.....	95
26: Figure 3.14 B	CD86 Expression.....	96
27: Figure 3.14C	CD40 Expression.....	97

### Chapter 4

28: Figure 4.1A	Uninfected Mouse Splenic Cells Sorting Procedure .....	104
29: Figure 4.1B	Infected Mouse Splenic Cells Sorting Procedure.....	105
30: Figure 4.2	Mouse Splenic Cell Clustering.....	113
31: Figure 4.3	Cell Hashing Approach in Single Cell RNA Sequencing .....	115
32: Figure 4.4	LCMV clone 13 Infection of DC and Monocytes Subsets In vivo .....	117
33: Figure 4.5A	Antiviral Gene Expression (fold change Log2) .....	120
34: Figure 4.5B	Antigen presentation gene expression (fold change Log2) .....	121
35: Figure 4.5C	Inflammatory gene expression (fold change Log2).....	122

# Chapter 1

## Introduction

### 1.1 The Immune System and The Role of Antigen Presenting Cells (APC)

Living organisms are constantly exposed to foreign microorganisms such as viruses, bacteria, and fungi as well as insults from dangerous self-tissues. The immune system is the body's defense system designed to protect the host from attack by these local and foreign agents. The interaction of the microbes and the immune system may result in pathology depending on two factors: the pathogenic properties of the microbe (including virulence factors at its disposal) and the types of host defence mechanisms induced (1). The goal of an intact immune system is to neutralise and eliminate these assaults without causing harm to self-tissue (2). There are three levels of the immune response: (a) anatomical and physiological barriers; (b) innate immunity; and (c) adaptive immunity.

Anatomical and physiological barriers are the first line of defence against pathogens. These barriers include intact skin, mucociliary clearance, stomach acid, and bacteriolytic lysozyme in tears, saliva, and other secretions. The intact skin and mucociliary movement of secretory surfaces prevent pathogens from entering the body. If the pathogens penetrate these layers and gain entry, they are faced with bacteriolytic enzymes that will neutralise them. The importance of the anatomical and physiological barriers in the immune response is well illustrated in the extreme susceptibility to infections observed in subjects with severe cutaneous burns or primary ciliary dyskinesia (3).

The next layer of defence is the innate immune system. This relies on a limited repertoire of receptors called pattern recognition receptors (PRR) to detect invading pathogens. The PRR target conserved microbial components that are shared by large groups of pathogens. The innate immune system is made up of cells and molecules that act within minutes of exposure to generate a protective inflammatory response. Speed is a defining characteristic of the innate immune system (3). The cells include macrophages, dendritic cells, mast cells, neutrophils, eosinophils, natural killer (NK) cells, NK T cells and epithelial cells lining the mucosal surfaces. The effector molecules include complement proteins, PRR, LPS binding protein, C-

reactive protein and other pentraxins, collectins, and antimicrobial peptides, including defensins. They are involved in both the sensing of microbes and damaged 'self' as well as being effector mechanisms to facilitate clearance of the infection. For example, activation of the complement cascade when mannose-binding lectin binds to carbohydrates on the microbe helps in clearance of pathogen as well as generating protein products that will activate and augment the adaptive immune response. Thus, innate immunity plays an essential role in activating the subsequent adaptive immune response.

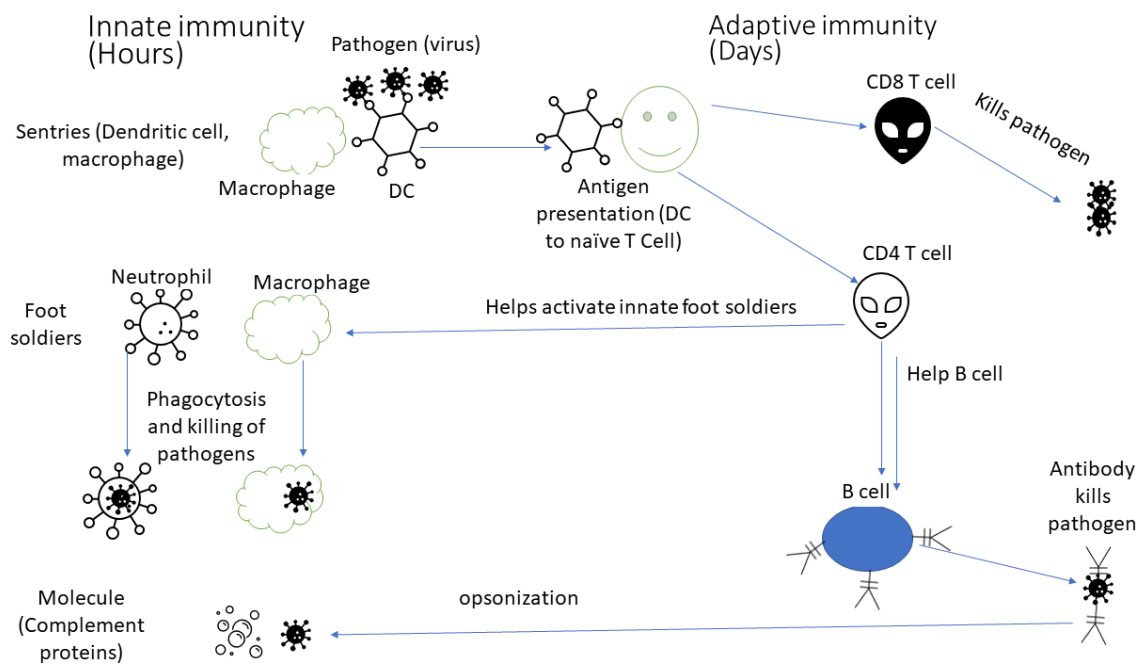
Adaptive or acquired immune responses are considered the last line of defense, arising late and becoming measurable after a few days of exposure. They are highly specific and able to build on previous exposure (memory). They involve the activation of antigen-specific B and T lymphocytes via their antigen receptors: surface immunoglobulin or T cell receptor (TCR) respectively. Lymphocyte antigen receptors are rearranged from germline genes during lymphocyte development. T cells are activated via interaction with antigen presenting cells (APCs) such as dendritic cells (DCs) and macrophages and collaborate with them to generate a specific response that may lead to the elimination of the antigen. There are two major types of T lymphocytes in adaptive immunity: CD4<sup>+</sup> helper T cells and CD8<sup>+</sup> cytotoxic T cells. CD4<sup>+</sup> helper T cells, as the name implies, assist other cells in executing immune function as well as regulating the type of immune response that develops. For example, CD4<sup>+</sup> helper T cells help B cells make antibody. CD8<sup>+</sup> T cells directly kill infected cells. CD4<sup>+</sup> T cells bind peptide bound to major histocompatibility complex class II antigen (MHC-II) expressed mostly on APC, while CD8<sup>+</sup> T cells bind peptide bound to major histocompatibility complex class I antigen (MHC-I) expressed on most nucleated cells. B cells, on the other hand, bind native antigens, differentiate into plasma cells and secrete immunoglobulins/antibodies. Antibodies are useful in blocking infection by pathogens or elimination of extracellular microorganisms.

Linking the innate and adaptive arm of the immune system are a unique group of cells called antigen presenting cells (APC). APC survey the host environment for the presence of foreign and self-antigens which are harmful to the host. Upon detection, they process these antigens and present them to T (and B) cells thereby activating adaptive immunity which will result in either clearance, pathology, or tolerance. Professional APC include dendritic cells (DCs), monocytes/macrophages, B cells and recent literature now also includes granulocytes (4).

The focus of my work was on how infection of mononuclear APC modulates the outcome of RNA virus infection and persistence using the lymphocytic choriomeningitis virus (LCMV)

model.

In summary, all the components of the immune system act individually or synergistically to maintain order and protect the host from invading microbes and dangerous self-tissues. The classic demarcation between innate and adaptive immunity is overly simplistic as it does not take into account the crosstalk between the two arms of the immune system. The adaptive immune response build on the foundation of the innate immune response, but the adaptive immune response may also augment the innate response. For example, the capacity of neutrophils to kill bacteria is enhanced when bacteria are opsonised by antibodies produced through the coordinated efforts of T and B cells. Similarly, the C3d fragment that is generated in the course of complement activation acts as a molecular adjuvant to influence the subsequent adaptive immune response. The activation of adaptive immune cells can only occur following antigen presentation by the cells of the innate immune system e.g. DCs (3). The essential function of the immune system in host defence is best illustrated when it goes wrong; under-activity (immunodeficiency) results in severe infections, and over-activity in allergy and autoimmune disease (1). Understanding the relationships between the different immune effector pathways will permit improved immunomodulatory therapeutics, development of improved vaccines, and avoidance of unintended reaction to self-antigens.



**1: Figure 1.1: The interplay between the innate and adaptive immune system**

The innate immunity made of cells (the sentries, and the foot soldiers) and molecules (complement proteins) and the adaptive immunity comprising the T and B lymphocytes. Following an infection, the sentries recognize the presence of foreign or unwanted self-tissue and present it to the T cells of the adaptive immunity. While CD 4 T cells will help in killing of the pathogen by activating the foot soldiers of the innate immunity, the CD8 T cells directly kills the pathogen. The antibody produced from B cells helps complement proteins of the innate immunity kill pathogen more efficiently.

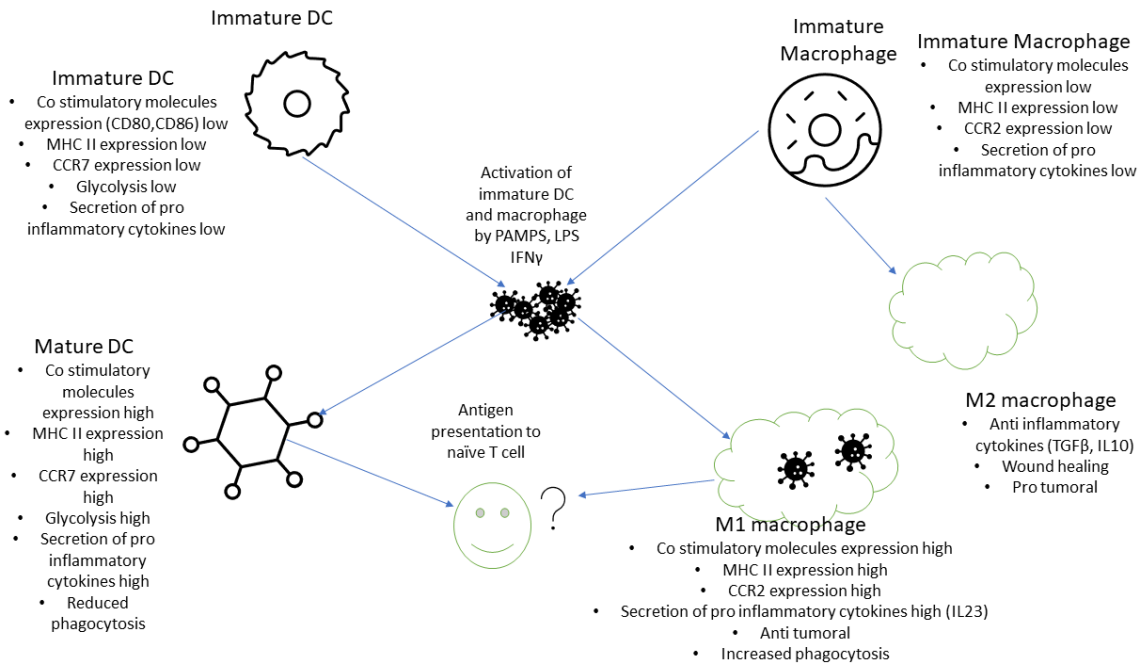
### **1.1.1 Overview of Antigen Presenting Cells (APC)**

APC are a group of cells that patrol the host environment for foreign and 'dangerous' self-antigens. They act as sentinels of the immune system and their interactions with antigens either induce adaptive immune responses or tolerance. Antigen presentation is a fundamental process of the immune response serving as the bridge between the innate and adaptive immune response. It involves the interaction of MHC class I and II and their corresponding T cell receptors. MHC-I is found on all nucleated cells of the body while MHC-II is found on select cells of the immune system called professional APC. Professional APC function is usually defined by the "three-signal model" (signal 1 – TCR - peptide/MHC complex; signal 2 - CD28 - CD80/CD86, signal 3 – IL-12 or IL-4) required for the activation of T cells (5). DC are the most potent APC due to their superior ability to prime naïve T cells(6). Though, this is debatable as a study by Pozzi et al. (2005) showed that macrophages are equally capable of activating naïve T cells(7). While DC are known for their ability to induce and coordinate adaptive T cell responses, macrophages are recognised for their phagocytic activity, antigen presentation in sites of immune responses and ability to mediate wound repair. Several explanations have been postulated to explain why DC are better antigen presenting cells than macrophages. Chang et al. (2005) demonstrated that DC have reduced proteolysis because they express reduced levels of proteolytic enzymes that break down peptide compared to macrophages. Thus, antigenic peptide stays longer in DC, allowing enough time for presentation to specific T cells compared to macrophages (8,9). In addition to this, phagosomal pH in DC is higher compared to macrophages, which explains why peptides are stable, survive longer and can be presented to T cells. However, in times of need such as inflammation, other cells in the body acquire the capacity to present antigens and initiate adaptive immune responses. These cells are called non-professional APC and include epithelial cells, plasmacytoid DC, monocytes, and granulocytes

(4,10,11). Because of their specialised status, DCs and macrophages will be the focus of my introduction.

### **1.1.1.1 DC as Professional APC**

In 1973, Ralph Steinmann, in his quest to unravel the initiators of immunity, discovered unique cells with a stellate appearance in the mouse spleen and called them DC (12). Subsequently, efforts have been channelled towards understanding the biology and function of DC using mouse models and to a lesser extent, human cells. DC are classified based on their anatomic location, phenotype, ontogeny, function and transcriptional profile. There are two major classes: plasmacytoid (pDC) and conventional/classical dendritic cells (cDC). DCs can be found in both non-lymphoid and lymphoid tissues where they exist as immature or mature dendritic cells depending on an encounter with pathogen-associated molecular patterns (PAMPs) or inflammatory mediators. Their core function is antigen presentation which can result in tolerance or activation of the adaptive immune response. In steady-state, immature DC patrol the body, take up and present self-antigen to naive T cells, but because they lack expression of activating co-stimulatory receptors, this interaction induces IL-10 producing suppressor T cells resulting in tolerogenic responses (13). On encounter with foreign antigen and inflammatory signals, they mature. DC maturation involves decrease in antigen uptake activity, translocation of MHC-II from the MHC-II compartment (MIIC) to the surface, up-regulation of maturation markers (co-stimulatory molecules) such as CD80 and CD86, leading to activation of naive T cells through cognate TCRs and proliferation of different types of CD4<sup>+</sup> T cells based on the signal received (14). The half-life of MHC-II on the surface of the DC is extended upon maturation, an important difference between mature and immature DC. Transition from the immature to the mature state in DC also involves a change in cellular metabolism from fatty acid oxidation to glycolysis and lactate production (15). These changes culminate in the ability to productively activate T cells.



## 2: Figure 1.2: Maturation of Dendritic cells and Macrophages

DC and macrophage mature when they encounter pathogen. Maturation involves upregulation of MHC II and co-stimulatory receptors (CD80, CD86), increase glycolytic activity and secretion of inflammatory cytokines. While DC matures and present antigen to T cell, macrophage maturation can either result in M1 or M2 macrophage depending on the cue from the environment.

DC develop from CD34<sup>+</sup> haematopoietic stem cells (HSC), which give rise to the common myeloid progenitor (CMP) in the bone marrow. The CMP then gives rise to macrophage-DC progenitor cells (MDP). MDP give rise to the common DC progenitor cell (CDP) and common monocyte progenitor (cMoP) which generate DC and macrophages respectively. Few studies have questioned the role of MDP as an intermediate cell in DC and macrophage development (16,17). There is no debate that cMoP exclusively generate macrophages while CDP generate DC (plasmacytoid and conventional DC precursors (pre-cDC)). CDP are defined as a Lin<sup>-</sup> CD117<sup>int</sup> CD135<sup>+</sup> CD115<sup>+</sup> BM population. An interplay between different transcription factors directs the differentiation of CDP to either plasmacytoid or conventional DCs. The expression of the transcription factors zinc finger and BTB domain containing 46 (ZBTB46) and ID2 drive differentiation into a cDC-precursor whereas transcription factor 4 (TCF4) and E2-2 expression

led to pDC commitment. Thus, an antagonistic relationship exists between transcription factor E2-2 and ID2 that, alongside other factors, controls the differentiation of DCPs to plasmacytoid or classical DCs. Recent work by Murphy et al. (2019) identified a subset of DCP that is destined to give rise to cDC1 cells using single-cell RNA transcriptomics (18). The cells are known to express ZBTB46.

Plasmacytoid DCs (pDCs), also known as interferon-producing cells (IPCs), produce large amounts of interferon-alpha (IFN- $\alpha$ ) when activated. pDCs make up about 50 % of total DCs in blood and 1 % of the total blood mononuclear phagocytes (19). pDCs have dual origin. As previously noted, they develop from the DCP depending on increased expression of the transcription factor E2-2 compared to ID2 for classical DC. They can also arise from lymphoid progenitors delineated as LIN<sup>-</sup>KIT<sup>+</sup>SCA1<sup>+</sup>CD34<sup>+</sup>FLT3<sup>+</sup>. However, only myeloid derived pDC can process and present antigen (20). The transcription factor E2-2 has been identified as the master regulator that drives the differentiation and maturation of pDC in mice and humans (21). A heterozygous mutation or loss of E2-2 causes a syndrome called Pitt-Hopkins syndrome, characterised by reduction in the number of IFN- $\alpha$  producing pDCs. In mice, pDCs are identified by expression of CD11c, B220, Ly6C, bone marrow stromal antigen 2 (BST2) and sialic acid-binding immunoglobulin-like lectin H (Siglec-H); while in humans, pDCs lack CD11c and Siglec-H but express BDCA-2 (also known as CD303), BDCA-3 (also known as thrombomodulin or CD141) and CD123 (22). pDCs participate in diverse functions in the immune system such as anti-viral immune responses, antigen presentation and tolerance (22). pDCs robust and early production of IFN- $\alpha$  during viral infection has been attributed to their constitutive expression of IRF7, which is downstream of Toll-like receptor (TLR)-7 and TLR-9 signaling pathways. TLR-7 and TLR-9 sense viral RNA and DNA, respectively (23). For example, early production of IFN- $\alpha$  by gut pDCs helps in control of HIV virus in elite controllers. However, late production IFN- $\alpha$  can lead to persistence in chronic hepatitis and LCMV infection. Expression of other toll-like receptors, such as TLR-11, TLR-12 (in mice) and cytosolic PRRs for microbial sensing, have also been described in pDCs (24–26). Because of the copious amounts of IFN- $\alpha$  produced by pDCs following activation, they are implicated in some autoimmune diseases that involve type I IFN, collectively called type I interferonopathies (27). However, pDCs also participate in immuno-tolerance, which can counteract exaggerated immune responses in autoimmune diseases. Chappel et al. (2014) demonstrated that coupling an antigen to BDCA-2, which is specifically expressed in human pDC, reduces effector CD4<sup>+</sup> T cells while preserving FOXP3<sup>+</sup> T regulatory cells thereby

maintaining tolerance (28). Recently, a study by Alculumbre et al. (2018) showed heterogeneity of pDCs in response to viral infection (10). Three subsets of pDCs were identified based on expression of PD-L1 and CD80 with one of the subsets more efficient in antigen presentation to T cells while the other was better at IFN production (10). The role of pDCs in antigen presentation has been questioned following identification of pre-DCs in blood, which express similar surface markers as pDCs (29). Using single-cell RNA sequence technology, Villani et al. (2017) isolated a pure culture of pDCs that was attenuated for antigen presentation after separating away a contaminating subset of cDCs called AXL<sup>+</sup>SIGLEC6<sup>+</sup> cells (“AS DCs”) (30). Thus, the pDC role may remain as IFN- $\alpha$  producing cells while antigen presentation is the remit of cDCs.

Conventional DCs arise from a pre-DC precursor in blood. This is a down-stream product from the common DCP in the bone marrow. There are two classes of pre-DCs: pre-DC1, which are committed to produce cDC1, and pre-DC2 which give rise to the cDC2 subset (31). Various subsets of conventional DCs exist and are present in both lymphoid and non-lymphoid tissues. They vary in their phenotypes, transcriptomic profile and functional specialisation within and across different tissues. They are now broadly classified into two populations: XCR1<sup>+</sup> (cDC1) and CD11b<sup>+</sup> (cDC2) conventional DC (32–35). IRF8-BATF3-ID2 controls cDC1 development while cDC2 is dependent on IRF4, Notch2, RBP-J, IRF2 and RELB (34). Understanding the exact role of these transcription factors has been very daunting due to their effects on other cells of the body. For example, mice lacking IRF8, which is used to classify cDC1, also suffer from neutrophilia and monocyte defects (36), thus showing that IRF8 also has an effect on neutrophil development. With advancements in technology especially single cell transcriptomics and multiplex cytometry technology, these two broad DC groups can be further classified to reflect variation in their surface markers, anatomic location and functional specialisation within and across different tissues (29). Recent work by Murphy et al. (2019) used single-cell RNA transcriptomics to explain the interaction between the transcription factors (IRF8-BATF3-ID2-NFIL3-ZEB-2) involved in the development of cDC1 (18).

cDC1 include the CD8 $\alpha$ <sup>+</sup> classical DCs in lymphoid tissue, CD103<sup>+</sup> classical DCs in non-lymphoid tissue and BDCA-3<sup>+</sup> classical DCs in mice and humans (37,38). cDC2 are less well characterised and comprise the CD8 $\alpha$ <sup>-</sup> lymphoid tissue resident classical DCs, the CD11b<sup>+</sup> classical DCs in non-lymphoid tissue in mice and CD1c<sup>+</sup> classical DCs in humans (32). cDC1 are very efficient in cross presenting antigen to CD8<sup>+</sup> T cells and share similar PRRs and genetic profiles in mice and humans (39). They express high levels of TLR-3, -9, and -10, which allows

for detection of intracellular RNA and DNA viruses resulting in IRF3 dependent production of type I IFNs. They also contribute to Th1 responses through production of IL-12. Due to the prominent IRF4 expression in cDC2, they are more efficient in presenting antigen to CD4<sup>+</sup> T cells (40). They express TLR-2, -4, -6, -8 and -9 and correspondingly produce a wide range of soluble factors in response to TLR stimulation such as TNF- $\alpha$ , IL-1, IL-6, IL-8, IL-12, and IL-18, and chemokines such as CCL3, CCL4, and CXCL8. The non-resident DCs migrate to the lymph node in steady-state and inflammatory conditions, facilitated by their chemokine receptor CCR7 which binds CCL21 in the lymphatics. Migration has also been reported for lymph node resident DCs, especially during infection (41). They migrate from the T cells zones to afferent lymph vessels for rapid uptake of antigens and activation of T cells.

Other groups of non-classical DCs that have been described include inflammatory DCs and Langerhans cells (42). Inflammatory or monocyte-derived DCs (moDC) arise from monocytes during inflammation (43). They have been described in both lymphoid and non-lymphoid organs of mice and humans (44). During inflammation, they present antigen to naive T cells and, depending on the environmental milieu, can polarise CD4<sup>+</sup> T cells to Th1, Th2 or Th17 biased responses (44–46). The nature of the stimuli influences the phenotype of inflammatory DCs. When exposed to LPS they express ZBTB46 and accumulate in the lymph node. However, when infected with *Listeria*, they produce a large amount of TNF- $\alpha$  (iNOS DC) but lack expression of ZBTB46 (47–49). Inflammatory DCs express features of both DCs and macrophages. Their genetic profile, as well as expression of macrophage surface markers CD64 and MAR1, delineates their monocytic origin (43,50). However, their expression of the unique DC transcription factor ZBTB46, as well as their functional specialisation, affirms their DC status (48). Other forms of inflammatory DCs include inflammatory dendritic epidermal cells (iDECs) and slanDCs found in atopic dermatitis and psoriasis, respectively (51,52). How these various forms of inflammatory DCs are related to each other is not clear (53). Additionally, the fate of inflammatory DC upon resolution of the insult is not known. Do they revert to monocytes, or do they remain as DC? This requires further investigation.

Langerhans cells (LCs), on the other hand, are a group of Langerin and Birbeck granule bearing cells found in the epidermis (54). They arise from foetal liver-derived monocytes (55). Unlike classical DCs, they self-renew in tissue and are not dependent on the specific DC growth factor, FLT3 ligand (56). Rather, they require keratinocyte-derived IL-34 and inflammatory neutrophil-derived factor (CSF-1) signalling through CSF1R for their development, homeostasis, and regeneration during inflammation (57). Other growth factors and cytokines

implicated in their development and maintenance in tissue include TGF- $\beta$ , AXL, BMP7, RUNX3, PU.1 (SPI1), and ID2. LCs are capable of most DC functions and have been shown in a skin infection model to polarise CD4<sup>+</sup> T cells to the Th17 phenotype upon exposure to *Candida albicans* (58). In humans, they are capable of presenting lipid antigens to T cells via the MHC-related molecules CD1a, b and c (59). Recent studies have also implicated LCs in the induction of peripheral tolerance. In the lymph node, LCs mediate deletion of auto-reactive CD4<sup>+</sup> and CD8<sup>+</sup> T cells. They induce development of regulatory T cells (Treg) and production of the immunosuppressive cytokine IL-10. However, their genetic and transcriptomic profiles seem more closely related to tissue macrophages than to classical DCs (60). LCs remain the only immune cells with dual identity (61). They express both macrophage (MAFB) and DC (ZBTB46) transcription factors. It will be interesting to see if heterogeneity also exists within the LC family.

Finally, worthy of mention are the follicular dendritic cells, named as such due to their morphology. They differ from normal DCs in terms of ontogeny (they are not haemopoetic), transcription factor expression and gene expression profile. Their primary function is to maintain the germinal centre and to retain antigen for B cell maturation and memory cell formation (62).

### **1.1.1.2 Macrophages as Phagocytes and Professional APCs**

Macrophages are the second major subtype of APCs after DCs. They are known for their phagocytic role, the basis for their identification by Elie Metchnikoff(63,64). Macrophages are a heterogeneous group of cells, widely distributed in tissues, with highly plastic phenotypes and have several roles in the immune system ranging from pathogen defence, tissue homeostasis, and wound repair (65). Similar to DCs, they are classified based on their ontogeny, anatomical location, phenotype and functional specialisation. Ontologically, it is now known that tissue-resident macrophages have a dual origin. They are either from yolk sac and fetal liver progenitors during embryonic development or from bone marrow-derived monocytes (66). Hettinger et al. (2013), using quantitative proteomics, identified the bone marrow committed progenitor that gives rise to the monocyte-macrophage lineage alone (67). This committed progenitor was called the common monocyte progenitor (cMoP) and differs from the progenitor cells (MDP), which give rise to both macrophages and DCs, by the absence of expression of CD135.

In terms of their anatomical location, there are several specialised macrophages in various tissues of the body. For example, osteoclasts are found in bones, microglia in the brain, Kupffer cells in the liver, and alveolar macrophages in the lungs. These tissue-resident macrophages vary in ontogeny and functional specialisation, and this is influenced by their tissue microenvironment (68). Osteoclasts are important for bone remodelling, while alveolar macrophages are endowed with high expression of PRR because of the direct exposure of the lung to environmental antigens.

Gut macrophages are anti-inflammatory in order to maintain tolerance to gut microbial flora and food micronutrients. Comparison of the gene profile of peritoneal macrophages with microglia showed that as many as 2000 mRNAs are differentially expressed between the two cell types and these variations are also associated with functional specialization (69). Moreover, this study also demonstrates the plasticity of tissue-resident macrophages. The authors showed that transfer of peritoneal macrophages to alveolar air spaces in the lungs results in reprogramming of their gene profile to an alveolar macrophage-like pattern and that microglia and peritoneal macrophages lose their specific expressed gene set upon transfer to an *in vitro* environment. This also confirmed the fact that signals from tissue microenvironments determine the functional and gene expression profile of resident macrophages. The identity of these signals in tissues is yet to be unravelled. However, a plausible assumption is that these are classical signalling molecules that bind to specific receptors which in turn regulate gene expression (70). For example, retinoic acid regulates peritoneal macrophage phenotypes by inducing expression of GATA6 (71). TGF $\beta$  regulates the activities of SMAD proteins which are involved in maintaining the microglial specific phenotype (72). Dissecting the full complement of signals that modulate and maintain tissue-resident macrophage gene expression will help in unravelling their roles in most diseases. Also, it will be interesting to know if this plasticity of resident macrophages affects their functional specialisation.

Further classification of macrophages is based on their activation status. Two major groups of macrophages have been identified; first classically activated (M1), and second, alternatively activated (M2) and/or regulatory macrophages. The M1 macrophages promote inflammation, suppress tumour growth and mediate defence against pathogens while M2 and/or regulatory macrophages counteract the M1 macrophages by suppressing inflammation, mediate tissue regeneration and wound repair, and promote tolerance to tumours (73). However, this classification may be too simplistic because macrophage activation most likely reflects a spectrum of responses depending on the cue received rather than a division of two cell lineages

(74).

In addition to tissue macrophages, blood monocytes also contribute to the tissue macrophage pool especially during inflammation. They are classified based on their phenotype. In mice, they are classified based on the expression of Ly6C and CCR2 into Ly6C<sup>hi</sup> (CD62L<sup>+</sup>CD43<sup>low</sup>CCR2<sup>+</sup>CX3CR1<sup>mid</sup>) and Ly6C<sup>low</sup> (CD62L<sup>-</sup>CD43<sup>hi</sup>CCR2<sup>-</sup>CX3CR1<sup>hi</sup>) while in humans they are classified based on expression of CD14 into CD14 high or low monocytes (75). Using gene expression profiling techniques, the two monocyte subsets in mice and the humans have been aligned together. Ly6C<sup>lo</sup> cells in mice are equivalent to CD14<sup>lo</sup> cells in humans, and Ly6C<sup>hi</sup> equate to CD14<sup>hi</sup> (76). While the Ly6C<sup>hi</sup> group and their human counterpart maintain the macrophage/DC population in tissues during inflammation, the Ly6C<sup>lo</sup> group and their human counterpart maintain the integrity of the endothelial wall.

### 1.1.2 APCs and Viral Infections

Viruses are obligate intra-cellular parasites that cannot propagate on their own. They depend on various host cell functions to complete their life cycle. The process of replication results in a series of interactions between the parasite and the host. While the host immune system works towards the elimination of the virus, the virus devises various evasion mechanisms to allow replication and production of progeny. At the centre of this interaction is APC. Various APCs by virtue of their location, function, and phenotype are primary targets of many viruses (77). DCs and macrophages are found at mucosal surfaces where most viruses gain access to the body and also in the blood. They possess numerous surface receptors that bind viruses, and their function in antigen presentation initiates and modulates adaptive immune responses to the virus. In addition, APCs have a unique membrane-transport pathway that facilitates uptake of pathogens. DCs constitutively take-up extracellular fluid by macropinocytosis and, similarly to macrophages, may engulf antigens and whole pathogens by endocytosis and phagocytosis. For example, DCs can capture human immunodeficiency virus (HIV) via binding by Fc receptors and C-type lectins such as DC-SIGN (78). This, in turn, induces maturation of APCs causing up-regulation of MHC, co-stimulatory molecules and other signals that activate naive T cells resulting in the subsequent elimination of the pathogen (79). The importance of APCs in resolving viral infections has been shown for several viruses including human respiratory syncytial virus, influenza virus, Arenaviruses and filoviruses(80–83). The interaction of APCs with viruses has two sides: recognition and induction of immunity versus replication of the

virus where it may evade restriction factors and use the cell to disseminate.

### **1.1.2.1 Recognition and Induction: APCs as Innate Immune System**

#### **Sensors of RNA Virus Infection**

APCs are endowed with various surface and intracellular PRRs. These receptors detect viruses by binding to unique molecular patterns on or within the viruses called PAMPs. This detection results in uptake and processing of the virus for outright killing or presentation to the cells of the adaptive immune system. The PRRs include members of the TLR family, the card helicase proteins (retinoic acid-inducible gene I (RIG-I)-like receptors, RLRs) and nucleotide-binding oligomerisation domain containing leucine-rich repeats (NOD-LLR)-like proteins (NLR) (84,85).

The TLR family is the most characterised of the PRR, and there are approximately 13 of them, numbered 1-13 in mammals (eg mice, although only TLR-1 to -10 are found in humans). They are membrane bound, found mainly on the cell surface or intracellularly on endosomes. The RLRs are cytosolic proteins that sense viral nucleic acids, usually RNA. They include the proteins, retinoic acid-inducible gene I (RIG-I), melanoma differentiation factor-5 (MDA5), and laboratory of genetics and physiology-2 (LGP-2). Another cytoplasmic sensor that detects DNA is DNA-dependent activator of IRFs (DAI) (86–88). Similarly, the NLR proteins are also found in the cytosol and sense mainly PAMPs from bacterial pathogens, although they have also been implicated in both direct and indirect detection of viral PAMPs (84,89). Professional APCs express PRRs at different levels. When activated via the PRRs, they also use different downstream signalling molecules to initiate immune responses, which has been used to delineate their functional specialization (90). For example, pDCs express TLR-1, -3, -6, -7, -9 and -12, cDC1 express TLR-3, -10 and -11 and lack TLR-4 to -7 or express them at very low levels whereas cDC2, moDC, and monocytes express TLRs such as TLR-1, -2, -4 and -6 that detect bacterial components (90–92). Based on PRR expression, Dalod et al. (2014) suggested that pDCs and cDC1s are useful in sensing intracellular pathogens while moDC and cDC2 are effective against extracellular pathogens (90). However, this classification may be too simplistic because of our limited understanding of DC biology and functional specialisation as well as the functional overlaps, redundancy and crosstalk that exist among various subsets in different animals. Several excellent reviews have been written on the role of PRRs in microbial and danger signal sensing, some of which are referenced here (85,89,90,93). For my work, I will

limit my discussion to only the PRRs involved in RNA virus sensing by APC. These PRRs include members of the TLR family, TLR-2, -3, -4, -7 and -8, and the cytosolic sensors, RIG-I, MDA5 and LGP-2.

### **1.1.2.2 Toll-like Receptors (TLR) in RNA Virus Sensing**

The TLRs (TLR-3, -7 and -8) implicated in RNA virus sensing by detecting RNA in DCs are mostly found on endosomes, with the exception of TLR-3 which is also found on the cell surface (84,85). TLR-7 recognises single-stranded RNA viruses like influenza virus and genomic or synthetic single-stranded RNA oligonucleotides containing U or GU repeats (94,95). It is preferentially expressed in pDCs in human and signals via the adaptor molecule MyD88 then IRF3 or IRF7 to initiate type I IFN anti-viral responses. In mice, TLR-7 is present not only in pDCs but also in cDC2s however, rather than use IRF3 or IRF7 to activate downstream signals, cDC2s signal via IRF1 (85). In addition, TLR-8, which is functionally similar to TLR-7, also senses single-stranded RNA viruses or synthetic forms of RNA (96) and have been implicated in HIV and other RNA virus detection. However, TLR-8 is only functional in humans; in mice, it is inactive or may perform a non-immune role (85). TLR-3, on the other hand, detects double-stranded RNA which forms the genome of some viruses and an intermediate product of all single-stranded RNA virus replication cycles. It is implicated in sensing of viruses such as reovirus, rotavirus, and West Nile virus (89). TLR-3 is preferentially expressed on cDCs and not on pDCs. Among the cDCs, it is constitutively expressed in CD8 $\alpha$ <sup>+</sup> DCs and aids in cross-presentation, which is a unique feature of this subset of DCs (84,97). Other TLRs involved in RNA virus sensing, such as TLR-2 and -4, recognise viral proteins rather than nucleic acid. Activation of TLR-2 results in the production of pro-inflammatory cytokines while TLR-4 is capable of inducing both pro-inflammatory and type I IFN production. TLR-2 has been shown to recognise the hemagglutinin protein of measles virus while TLR-4 is implicated in the detection of mouse mammary tumour virus and coxsackie B virus (98–100). Secreted and envelope GP protein of Ebola virus has also been shown to be detected by TLR-4 (101,102). However, TLR-4 engagement is considered to be an evasion strategy by the virus rather than viral recognition (84,85).

### 1.1.2.3 Cytosolic Sensors of RNA Viruses

Card helicase proteins are preferentially expressed in cDCs rather than pDCs because the latter employ TLRs in RNA virus sensing instead of RLRs (like cDC). However, Kato et al. (2005) have shown that RLRs are also active in pDC where they detect paramyxovirus which escapes the TLR pathway (103). Among cDC subsets, splenic CD11b<sup>-</sup> DCs express low amounts of RIG-I and MDA5, and this allows West Nile virus to replicate better in this cell type than other cDC subsets (104). RIG-I and MDA5 are similar in structure and function. They contain an RNA-binding helicase domain and two caspase activation and recruitment domains (CARDs). In terms of their functions, they both recognise dsRNA of varying lengths. While RIG-I senses short length dsRNA containing a 5' triphosphate, MDA5 recognises longer dsRNA of about 2 kb as well as large RNA aggregates in infected cells (105–107). They also differ in their interaction with dsRNA; RIG-I binds the end of the RNA while MDA5 wraps along the length of the RNA strands (108). RIG-I has been implicated in sensing of viruses from different families, including the agents of viral haemorrhagic fevers such as filoviruses, Arenaviruses, and orthomyxoviruses (89). For example, the VP35 protein of Ebola virus actively competes for dsRNA with RIG-I as a mechanism to evade recognition by the immune system (109). This phenomenon was shown to be effective in cDCs but not in pDCs, where TLRs are the preferred viral sensors (110). MDA5 by virtue of its ability to recognise long dsRNA is only active in infected cells and not in resting or uninfected cells. This is because long dsRNA is only seen following viral invasion and this positions MDA5 as an effective PRR in notifying the immune system of viral infection (89). MDA5 is activated upon infection with picornaviruses such as encephalomyelitis virus and Sendai virus. Other reports suggest that both receptors might cooperate in immune detection of some viruses like West Nile virus and rotavirus (89). LGP-2 is the third member of the card helicase family of cytosolic proteins implicated in RNA virus sensing. However, rather than viral detection, LGP-2 plays an immunomodulatory role as both a negative and positive regulator of RIG-I and MDA5 (111). This has been attributed to the lack of the card helicase domain that is used by the other RLRs to couple adaptor molecules and induce IFN responses. The exact physiological role of LGP-2 has not yet been ascertained, and the explanation for its varying immunomodulatory roles compared to other members of the card helicase family is also not well understood (112). In addition to the RNA sensors, DNA sensors can also sense the DNA products of RNA and DNA viruses, thereby activating the innate immune response. For example, DNA products of HIV reverse transcription are recognised by the cyclic GMP-AMP synthase (cGAS). This produces the atypical dicyclic

nucleotide cGAMP which activates the central innate signalling adaptor protein STING (113).

#### **1.1.2.4 Downstream Signalling of Pathogen Recognition Receptors for RNA Viruses**

Both the TLRs and RLRs utilise different adaptor molecules to couple downstream signalling molecules for activation of immune responses. MyD88 is commonly used by most TLRs, except TLR-3 which uses TRIF as the adaptor molecule. The RLRs use mitochondrial anti-viral signaling proteins (MAVS), also known as Inositol-3-phosphate synthase isozyme 1 (IPS-1), as an adaptor molecule to couple downstream signalling. Dixit et al. (2010) showed that the location of MAVS affects the outcome of activation of RLRs (114). Peroxisomal MAVS induced early and short-term IFN-independent responses, while mitochondrial MAVS produced late, long IFN dependent responses. Regardless of the adaptor molecule utilised following activation, both TLR and RLR signalling pathways converge at the level of the TANK-binding kinase 1/ I $\kappa$ B kinase (TBK1/IKK) complex to activate IRF gene products or IKK/NF $\kappa$ B (nuclear factor- $\kappa$ B) proteins. This results in activation of three major signalling pathways: mitogen-activated protein kinase (MAPK), NF- $\kappa$ B and IFN regulatory factors (IRFs) (84). These pathways dictate the functional outcome of DC activation that includes: maturation of DCs, activation and polarisation of T cells and initiation of appropriate immune responses. Activation of MAPK and NF $\kappa$ B signalling pathways results in the production of pro-inflammatory cytokines such as IL-12, IL-1, IL-6, IL-18, and TNF $\alpha$ . These cytokines play important roles in DC and macrophage activation and T cell polarisation. The IFN regulatory pathway acts via activation and phosphorylation of IRF3 or 7 resulting in the production of type I IFN and hence other IFN-stimulated genes (ISG) which are the major effectors involved in anti-viral immune responses (84,97).

#### **1.1.2.5 Interferon and RNA Viruses**

IFNs are a group of inducible cytokines that induce the anti-viral functions of innate immunity. They are classified into three classes: type I, II and III, based on their amino acid sequence, chromosomal location and receptor specificity (115). Type I and III are the major classes involved in the anti-viral response while type II can work in collaboration with type I and III to

neutralise the virus. The focus of this introduction will be on type I and III and less on type II IFN which is secreted by lymphocytes. Type I IFN is the largest IFN family consisting of IFN- $\alpha$ , IFN- $\beta$ , IFN- $\epsilon$ , IFN- $\kappa$  and IFN- $\omega$  (115,116). They were discovered in 1957 based on their activity against influenza virus. Most type I IFNs are encoded by single genes except IFN- $\alpha$  which has 13 genes (12 proteins) in humans, and 14 genes in mice. Other type I IFNs such as IFN- $\delta$ , IFN- $\tau$  and IFN- $\zeta$  (or limitin) have been identified in swine, ruminants and mice, respectively (117). IFN- $\alpha$  and - $\beta$  are the best studied of the type I IFNs and can be produced by all cells in the body, however pDC are the major producers of IFN- $\alpha$  and have been shown to produce as much as 3-10 pg/l of IFN- $\alpha$  in response to HSV infection (118).

IFN- $\alpha$  and - $\beta$  signal via a heterodimeric receptor, IFN $\alpha$ R1 and IFN $\alpha$ R2, where ligand binding to either subunit is necessary for dimerization. However, binding produces different downstream effects (119). For example, IFN- $\beta$  compared to IFN- $\alpha$  binds more strongly to IFN $\alpha$ R1 resulting in robust anti-proliferative and anti-viral effects. In fact, IFN- $\beta$  treatment hastens virus clearance in persistent LCMV infection compared to polyclonal IFN- $\alpha$  antibody (116). IFN- $\alpha$  may be more involved in immunomodulation (120).

Type III IFNs were discovered recently and they include IFN- $\lambda$ 1 (IL-29 in humans, a pseudogene in mice), IFN- $\lambda$ 2 (IL-28A), IFN- $\lambda$ 3 (IL-28B), and IFN- $\lambda$ 4 (not present in mice)(121). They signal via a heterodimeric receptor made up of IFN $\lambda$ R1 (IL-28R $\alpha$ ) and IL-10R $\beta$  subunits. While the IL-10R $\beta$  subunit is widely expressed in various cell types, IFN $\lambda$ R1 is predominantly expressed on epithelial tissues (122).

Despite using different receptors, both type I and III IFNs use similar downstream pathways to generate their anti-viral response (119,123). Interaction with their various ligands results in activation and phosphorylation of the receptor-associated tyrosine kinases JAK1 and tyrosine kinase 2 (TYK2). This, in turn, leads to phosphorylation and dimerization of the cytosolic proteins STAT1 and STAT2. The STAT1/STAT2 heterodimer associates with IRF9, forming IFN stimulated gene factor 3 (ISGF3). The ISGF3 complex then translocates into the nucleus and drive the transcription of interferon inducible genes first by binding to the IFN-stimulated response elements (ISREs) in promoter regions of the genes. The ISRES is important because it makes the transcription by ISGF3 specific. (124,125). The type I IFN can act in an autocrine or paracrine manner to limit replication and spread of the virus. The direct anti-viral effect by type I IFN results from the production of many IFN-stimulated genes such as the ds-RNA-

activated enzymes, (2'-5')-oligoadenylate synthetase and ds-RNA-dependent PKR (126). These ISGs inhibit protein synthesis in infected cells and thus limit the production of progeny viral particles.

Numerous ISGs have been studied in relation to their anti-viral functions. Some have broad responses while others are specific to certain viruses (127,128). They also act at different stages of the virus life cycle to execute their anti-viral functions. For example, PKR, 2'-5'-oligoadenylate synthetase (OAS)/RNaseL, IFIT1, ZAP (zinc finger antiviral protein), SLFN1 (Schlafen 1), and Mx (Myxovirus resistance) have all been shown to inhibit virus replication in cells (129). IFITM and tetherin impair viral entry and release from cells (130). Viperin has multiple inhibitory effects against virus replication and release and is more effective against mucosal viruses such as reovirus (131,132). An emerging role for ISGs in anti-viral immunity involves modulation of cellular metabolic pathways such as the synthesis of cholesterol, polyamines and tryptophan (70). Cholesterol-25-hydroxylase (CH25H), an ISG mostly expressed in APCs, executes its anti-viral function by converting cholesterol to the soluble oxysterol, 25-hydroxycholesterol (25-HC) (133). In cell culture, CH25H has been shown to inhibit many enveloped viruses including HCV, HIV, Ebola virus, West Nile virus and the recent SARS-CoV-2 (134,135). Previous studies held that CH25H has no antiviral role against non-enveloped viruses. However, Civra et al. (2014) disputed this and demonstrated antiviral activity of CH25H against three pathogenic non enveloped viruses - human papillomavirus-16 (HPV-16), human rotavirus (HRoV), and human rhinovirus (HRhV)(136). Note, that many of these studies are in invitro system and not much information is available on the *in vivo* role of CH25H in anti-viral immunity.

There is a division of labour with regards to the role of type I and III IFN responses (137). This functional specialization is mediated by the differences in expression of their receptors in various cells and tissues in the body as well as the kinetics of induction. Type I IFN induces robust ISG responses in many tissues including liver, spleen, and kidney, whereas the type III IFN response is most prominent in organs with mucosal surfaces such as the lungs and intestines (138). In the gut mucosa, intestinal epithelial cells (IECs) have high expression levels of IFN $\lambda$ R with low levels of IFN $\alpha$ R1 and IFN $\alpha$ R2 and *vice versa* in the cells of the lamina propria (mostly immune cells) with low levels of IFN $\lambda$ R and high levels of IFN $\alpha$ R (139,140). Moreover, IFN- $\alpha$  induces rapid but transient ISG expression, while the effects of IFN- $\lambda$  are delayed and last longer (141). These variations in response have been shown to affect the tropism of some viruses (119). For example, type I IFN is enough to prevent acute murine

norovirus (MNV) infection whose tropism is mainly for DCs and macrophages, but it can only limit the systemic spread of a persistent MNV strain whose tropism is for intestinal epithelial cells (IEC). A similar response has also been shown for intestinal rotavirus. It is not known whether the restriction of virus spread is an intrinsic property of the cells or due to differential IFN induction by the viruses. More work is needed to understand the mechanism by which IFNs affects tissue tropism of specific viruses.

The timing of induction of IFN has also been shown to affect the outcome of virus infection, especially in persistent infections (22). Exogenous administration of IFN $\alpha$ 2a early in simian immunodeficiency virus (SIV) infection augments the expression of anti-viral genes and prevents systemic infection; however, sustained IFN $\alpha$ 2a treatment induces type I IFN desensitization, decreases anti-viral gene expression, increases viral load and accelerates CD4<sup>+</sup> T cell loss (142). Similarly, early administration of exogenous type I IFN prevents chronic LCMV infection while clearance of virus is not successful if it is administered late. In fact, blockade of type I IFN signalling during chronic LCMV infection improves T cell function and diminishes viral persistence (143). Other functions of IFNs include immunomodulatory and anti-cancer functions such as activation and maturation of APC, activation of T cells, NK cells, innate lymphoid cells, and regulation of chemokines involved in activation of adaptive immune responses. They promote apoptosis in tumour cells and negatively regulate proliferation and differentiation of T regulatory cells and myeloid suppressor cells. The anti-neoplastic activity of many chemotherapeutic agents has been shown to be dependent on type I IFN (22,123,144). Additionally, the use of LCMV infection induced tumour regression in viral therapeutics is dependent on induction of type I IFN (145). Apart from the beneficial anti-pathogenic response, type I IFN responses can also be detrimental to the host. This is seen in breakdown of immune tolerance following recognition of self-nucleic acid. This abnormal IFN response results in various auto-inflammatory and autoimmune diseases collectively called type I interferonopathies (123,146).

### **1.1.2.6 Migration and Dissemination**

Some APCs are mobile, such as migratory DCs, macrophages and monocytes. They migrate in response to environmental cues (usually inflammatory cytokine or activation via PAMP/PRR interaction) and chemokines from the mucosal surfaces to the lymphoid tissues to initiate adaptive immune responses. Many viruses exploit this migratory capacity of APCs to gain

access to different parts of the body in order to replicate and maintain their survival. DCs express CC-chemokine receptor (CCR7) chemokine that binds CC-chemokine ligand 21 (CCL21), enabling their migration to and within the lymph node. Macrophages use the CCR2-CXCL20 interaction to home to the lymph node. DCs disseminate HIV by either direct infection (cis-infection) or by transporting virus bound to the DC-specific lectin DC-SIGN to HIV-specific T cells in lymph nodes (trans-infection) (78). Though this is yet to be demonstrated *in vivo*, it has been observed in hepatitis C virus (HCV) infection (147). Immature moDCs can capture and transmit HIV-1 particles to T cells. It is not clear if this occurs via the receptor proteins SIGLEC-1 and DC-SIGN (148). There are discrepancies in the role of DCs in capture and transmission of HIV-1 particles (149,150). Hence, the migratory capacity of APCs inadvertently aids in virus spread to different tissues in the body.

### **1.1.2.7 Restriction Factors and Evasion Mechanisms**

The core function of APCs is to detect and process pathogens' antigens for presentation to cells of the adaptive immune system for elimination from the host. Therefore, APCs are endowed with several anti-viral factors that interfere with entry and replication of most viruses. An example is the anti-retroviral protein APOBEC3G, which has been shown to interfere with HIV replication. Expression levels of APOBEC3G have been shown to correlate with resistance of moDCs to HIV-1 infection. In addition, APOBEC3G upregulation by IFN- $\alpha$  has been shown to restrict HIV-1 infection in pDCs (77). Furthermore, one of the downstream results of the interaction of PRRs on/in APCs and virus products is the production of IFNs and ISGs, which are the major innate anti-viral effectors.

On the other hand, viruses have developed some evolutionary counter-measures to prevent detection and killing by APCs and the adaptive immune system. In some cases, this enables the virus to establish a persistent infection. For example, some viruses, such as those of the Herpesviridae family, generate a latent/ reactivating infection in which the virus lies dormant within host cells to escape immune surveillance. Infection with these viruses is characterized by long periods of viral inactivity interspersed by periods of reactivation when viral replication re-occurs but is quickly controlled by the immune system. However, this close, long term association with their hosts has allowed herpesviruses to evolve or acquire many different, active immune evasion mechanisms such as interference with antigen processing and presentation, antibody and cytokine responses. Other viral infections such as HIV, hepatitis B

virus (HBV), HCV, and the prototypic Arenavirus LCMV possess virus-encoded evasion strategies and thus are able to maintain sustained viremia (147). ICP47 of herpes simplex virus 1 and US6 of human herpesvirus 5 are known to inhibit the loading of antigenic peptides onto MHC-I molecules, impairing the ability of infected DCs to prime naïve T cells efficiently. *In vitro* studies have also shown that HCV envelope glycoprotein E2, as well as sera from HCV-infected patients, inhibit the migration of DCs towards CCL21 (77). Hepatitis B virus envelope protein HBsAg and HIV-1 envelope protein gp120 have been shown to impair TLR-9-mediated IFN- $\alpha$  production through binding to a C-type lectin, blood DC antigen 2 (BDCA2, also known as CLEC4C). Other viruses such as measles virus, LCMV and respiratory syncytial virus proteins also subvert the type I IFN responses and interfere with DC development and function (126). Interaction of APCs with viruses may therefore inadvertently help propagate viruses by providing access to more cells in other parts of the body.

### **1.1.2.7 *In vitro* Assays as Tools for Studying APC Biology and Function**

Much of our knowledge of DC biology has come from *in vitro* culture systems. Following isolation of DC from mouse spleen by Steinman in the 1970s, a culture system purifying DC from splenocytes based on their adherence to a plastic plate was developed (151). The non-adherent cells were called DC, while adherent cells like macrophages were removed by erythrocyte agglutination (EA) rosetting. Because of the paucity of APCs in tissue, a new method was developed in the 1990s to improve on the limitations of the previous methods. This method involves culturing bone marrow haematopoietic stem cells with growth factors which are involved in the development and homeostasis of mononuclear phagocytes: such as GM-CSF, M-CSF, and FLT3-L for several days and harvesting the differentiated cells (152). These comprise a heterogeneous mix of granulocytes, dendritic cells and macrophages. DCs are harvested as non-adherent CD11c<sup>+</sup> and MHC-II high expressing cells while macrophages are the adherent cells. M-CSF mainly generates macrophage-like cells, while FLT3-L gives rise to both cDC and pDCs. These culture systems have been useful tools in research into DC biology and function due to the generation of large numbers of cells. Recently, they have also been used in DC-based cancer immunotherapy (153). Despite the enormous usefulness of bone marrow derived dendritic cell (BMDC) *in vitro* culture, there is still little or no information on how they fit into the DC lineage network. They align with moDC as well as migratory DC. Helft et al. (2015) showed that CD11c<sup>+</sup> and MHC-II<sup>hi</sup> cells from GM-CSF culture are not homogeneous

but rather a heterogeneous mixture of DCs and macrophages which differ in terms of their phenotype, morphology, function and transcriptomic profile (154). This heterogeneity was shown amongst adherent, loosely adherent and non-adherent BMDC.

### **1.1.2.8 APC Biology and Future Studies: Single Cell Transcriptomic Technology**

Since their discovery, DC phenotypic plasticity has impeded full understanding of their biology and function despite their fundamental role in immune responses. Single cell transcriptomic technology has revolutionised the field of APC studies and provided insight into the origin, functional specialisation and discovery of rare APC populations. For example, we now know the progenitor cells that give rise to the cDC1 subset of DCs and the interplay of transcription factors involved in their development. Using single cell transcriptomics, Villani et al. (2017) isolated a pure culture of pDC that is unable to perform antigen presentation but produced type I IFN (30). This resolved a long-held debate about whether subsets of pDC could perform antigen presentation instead of their known type I IFN production function. Despite the advancement in these technologies, there is still much we do not know. For example, though the broad classification of DC into cDC1 and cDC2 has now been accepted, this is still simplistic as there are variations in phenotype and functional specialisation of these cells within and across tissues in different species. How these various subsets relate to each other within and across tissues is unclear. Are these subsets distinct from each other with specific progenitors or are they just developmental intermediates that vary because of local signals from the tissue microenvironment or functional demands? I favour the intermediate hypothesis proposed by Sichen et al. (2007) where the variation in DC within and across tissues is based on local signals from the microenvironment and functional demands of the body (31). There are cDC1 and cDC2 intermediates in the blood. These two groups possess the capacity to express different surface markers and functional specialisation based on the signal they received from the tissues they enter. This has been demonstrated in macrophage and monocyte biology, but the role of the microenvironment in DC development and function has yet to be established. Furthermore, this model sheds light on the plasticity of DCs. A good analogy for the progenitor - intermediate hypothesis can be seen in times of need such as war: there is high demand for different services such as military personnel, medical professionals etc. Many civilians can be co-opted into the military to fight, while some soldiers due to shortage of medical professionals, instead of

fighting, acquire basic medical training such as first aid just to provide emergency medical support during the war. The main aim of the country is to win the war and successfully defend the country. After the war, these civilians turned soldiers can go on being soldiers, or they can return to their normal lives as civilians. Similarly, the soldiers can continue with their primary assignment, which is being a soldier. It will be interesting to know, for example, what happens to inflammatory DC after the insult has been eliminated. Do they remain as DC until they are removed or do they return to their monocyte origin? This can be answered using single-cell RNA technology to assess the gene profile of moDC pre- and post-inflammation. With the recent advancement in single cell transcriptomics and multiplex cytometry, interesting development lie ahead in APC biology and function research.

## **1.2 Arenavirus Overview**

### **1.2.1 Classification and Virus Replication**

Mammarenaviruses are single-stranded ambi-sense RNA viruses that are endemic in different rodent species across various geographical areas. Some are capable of zoonotic spillover to humans, frequently causing fatal viral hemorrhagic fever. They are divided into Old World and New World viruses based on their phylogenetic, serological, and geographical differences (155,156). The Old World Arenaviridae include Lassa virus (LASV), Lujó virus (LUJV), Okahandja, Wenzhou, Lunk, Gairo, Mariental, Mobala, Ippy, Mopeia (MOPV), Merino Walk, Menekre, Gbagroube, Morogoro, Kodoko, Luna, and the ubiquitous LCMV. LASV and LUJV virus are endemic in Africa whereas LCMV is widely distributed. LCMV mainly causes clinical disease in immunocompromised humans such as transplant patients and pregnant women that can be quite serious, resulting in spontaneous abortion, neurological dysfunction and even death (157). Because only the serious LCMV infections in immunocompromised people are reported, it is difficult to estimate the true incidence of LCMV infection, which most times goes unnoticed.

The New World Arenaviruses, on the other hand, are composed of 18 species of viruses divided into four lineages: clades A, B, C, and D based on their host, geographical location, antigenic cross-reactivity, and amino acid sequence differences (i.e. at least 12 % divergence in the nucleoprotein (NP) amino acid sequence) (158). The New World lineage A includes five South American viruses which do not normally infect humans: Flexal virus (Brazil), Pichinde virus

(Colombia), Paran´a virus (Paraguay), Allpahuayo virus (Peru), and Pirital virus (Venezuela). Lineage B comprises agents of viral haemorrhagic fever (VHF) such as Junin virus (Argentina); Chapare and Machupo viruses (Bolivia); Sabi´a, and Guanarito virus (Venezuela) and non-VHF causing viruses: Cupixi, and Amapari viruses (Brazil); and Tacaribe virus (Trinidad). Lineage C New World Arenaviruses are the smallest clade with only two viruses: Latino virus (Bolivia) and Oliveros virus (Argentina) which are non-pathogenic to humans. Lineage D comprises Bear Canyon, Tamiami, and Whitewater Arroyo viruses in the United State which have been implicated in three fatalities associated with VHF in California in the 1990s (159).

**1: Table 1.1: Summary of Viral Agents of Haemorrhagic Fevers**

<b>Virus family</b>	<b>Representative virus</b>	<b>Genome</b>	<b>PRR</b>	<b>Immunopathology</b>	<b>Immune evasion</b>	<b>Reservoir host</b>
<b>Filoviruses:</b> Marburg, Ebola virus	Zaire Ebola virus (EBOV)	- ssRNA	hMGL, DC-SIGN, ASGPR-1, L-selectin, DC-SIGNR, NPC-1, RIG-I	<p>Proinflammatory cytokines (TNF<math>\alpha</math>, IL-8, IL-1) disrupts endothelial barrier function resulting in increased vascular permeability, hypovolemia, and shock</p> <p>Tissue factor from macrophages contributes to DIC,</p> <p>TNF<math>\alpha</math>, TRAIL induces bystander apoptosis of lymphocytes</p> <p>Aberrant DC activation impairs T cell activation and lack of adaptive immune response</p>	<p>VP35: inhibits activation and phosphorylation of IRF3, TBKI, PKR, sumoylation of IRF7</p> <p>VP24: prevents nuclear translocation of STAT1</p> <p>GP protein sequesters tetherin/BST-2</p>	Fruit bats ( <i>Hypsignathus monstrosus</i> , <i>Epomops franqueti</i> , <i>Myonycteris torquata</i> )
<b>Arenavirus:</b> Old World Arenavirus - Lassa virus, Lujo virus  New World: Junin virus, Machupo virus, Sabia virus, Guanarito virus,	Lassa virus	- ssRNA	$\alpha$ -dystroglycan ( $\alpha$ -DG), DC-SIGN, L-selectin, Axl, Tyro3, LAMP1, RIG-I	Lack of DC and macrophage activation results in immunosuppression and ineffective adaptive immune response	<p>Nucleoprotein (NP) degrades dsRNA and inhibits activation of NF<math>\kappa</math>B, phosphorylation of IKK<math>\epsilon</math> and IRF3</p> <p>Z protein disrupts interaction of RLRs and MAVS, inhibits activation of macrophages</p>	<i>Mastomys natalensis</i> (multimammate rat)

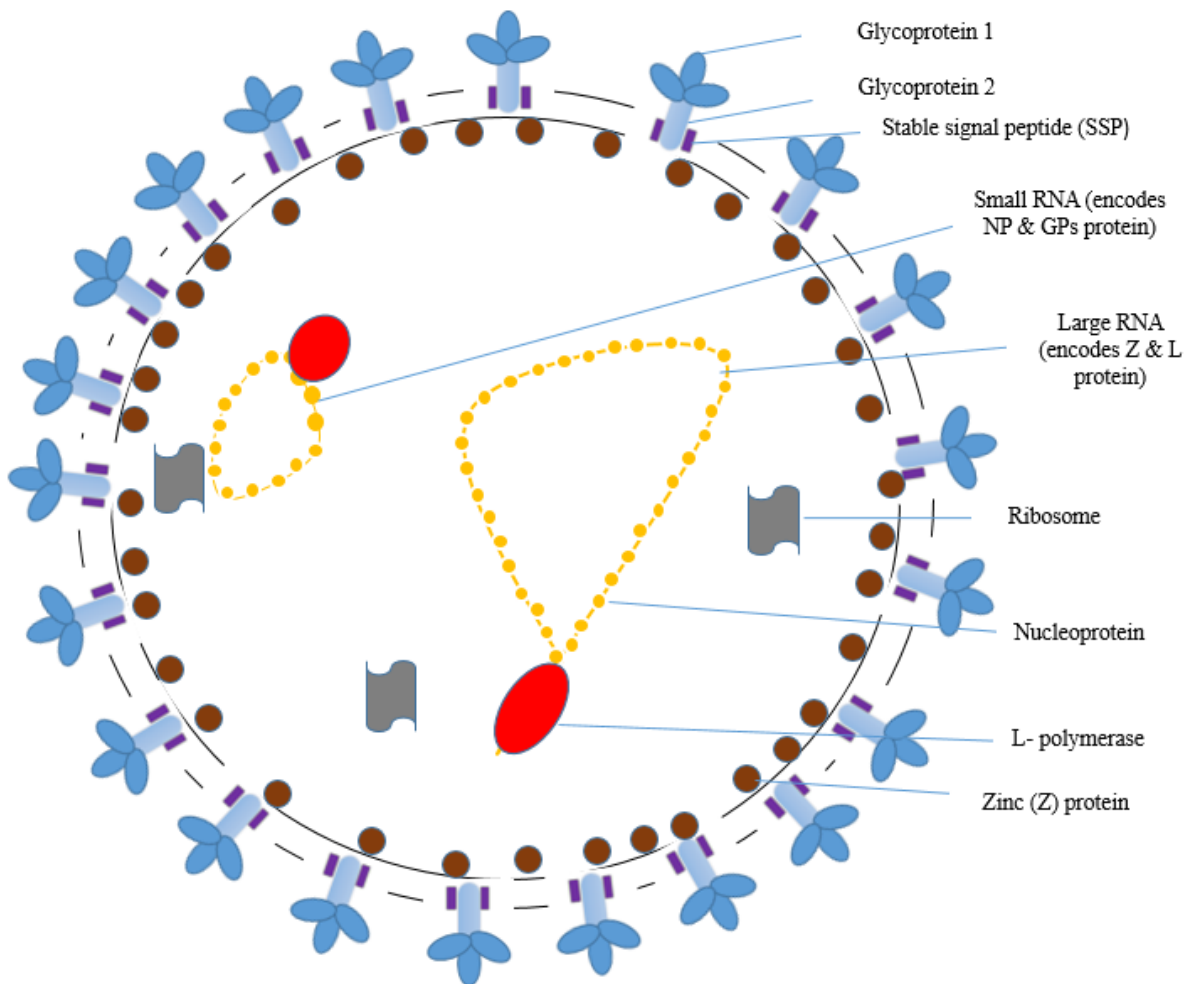
Chapare virus	Junin virus	- ssRNA	Human transferrin receptor 1(TFR1), DC-SIGN, L-selectin, TLR-2, RIG-I	Vasoactive mediators from infected endothelial cells causes increased vascular permeability and shock syndrome  High IFN- $\alpha$ production disrupts platelets and endothelial cell functions	Same as above	<i>Calomys musculinus</i> (drylands vesper mouse)
<b>Bunyavirus:</b> Crimean Congo hemorrhagic fever virus, Rift valley fever viruses, Hanta virus etc	Hanta virus	- ssRNA	$\alpha v\beta 3$ integrins	Immune complex induced renal damage and hemorrhagic disease	N-protein blocks TNF $\alpha$ -directed endothelial cell responses  Gn protein (Gn-tail) inhibits RIG-I and TBK 1	Rodents, shrews, and bats
<b>Flavivirus:</b> Yellow fever virus, Dengue viruses, Omsk hemorrhagic fever virus, Kyasanur Forest disease virus, Alkhumra virus	Yellow fever virus	+ ssRNA	Heparan sulfate, TYRO3, AXL and MER	Proinflammatory cytokines cause endothelial damage, DIC and circulatory shock  TGF- $\beta$ induces tissue damage  Apoptosis of infected hepatocytes by cytotoxic T cells and cytokine decreases hepatic synthesis of clotting factors (bleeding)	NS4B blocks activation of STAT1	African primates

Table 1.1 shows a summary of four virus families implicated in viral haemorrhagic fever. The filovirus (Zaire Ebola virus), Arenavirus (Old World - Lassa virus and New World - Junin virus), flavivirus (yellow fever virus) and Bunyavirus (Hanta virus). Also, their reservoir hosts, genome type, viral entry receptors, immunopathology, and immune evasion mechanism.

It is important to note that this classification, especially the New World Arenaviruses, is not 100 % clear cut. For example, the genetic distance observed between Pampa virus and its closest relative, Oliveros virus, both found in Argentina, suggests that Pampa virus should be considered as a genotype of Oliveros virus rather than as a new viral entity. This was corroborated by its geographic distribution and mammalian host (*Bolomys spp.*), which are identical to those of Oliveros virus (160). However, both viruses are classified differently; Oliveros virus in clade C and Pampa virus in clade A. Because of the specificity of the rodent host of most Arenaviruses, previous studies showed that Arenaviruses could prevent co-infection by another virus by a mechanism called superinfection interference. Therefore, it was believed to be a good model for virus-host co-divergence whereby a particular host co-evolved with a particular virus such that the virus is unable to infect another already infected animal host. However, recent studies dispute this and show that especially the reptArenaviruses are capable of co-infection, which can result in recombination and host switching (161,162). Cells infected with Junin virus do not prevent infection with a second virus (163) suggesting that Arenaviruses have the capability to exchange genetic material and acquire new hosts.

The genome of mammaryarenavirus consist of two ambisense segments - the Large and the Small segment. The large RNA segment (L) encodes the RNA polymerase (L) and a small zinc-binding protein (Z) which is the equivalent of the matrix protein in other RNA viruses (164). The small RNA segment (S) encodes the nucleoprotein (NP) and the envelope glycoprotein precursor, GPC. Both polypeptides from each RNA segment are separated by an intergenic (IGR) non-coding region that forms a stable loop (hairpin) (165). The IGR functions in structure dependent transcription termination. The nucleoprotein is the major structural protein of Arenavirus (see Figure 1.1). It is arranged in bead-like structures along the viral genome. It is a multi-functional protein playing essential roles in the replication and transcription of viral RNA as well as virion assembly (166). The glycoprotein (GPC) is the viral envelope protein that mediates viral attachment and entry into the cell. The L-protein (LP) is the viral polymerase that functions in transcription and replication (Figure 1.1). It has three parts: the N-terminal region, the central RdRp region and the C-terminal region similar to the influenza virus polymerase subunits (PA,PB-1, and PB-2 respectively) (167). The Z protein is a small polypeptide of less than 100 amino acid. It is also made up of three domains: the N-terminal domain, the Central domain and the C-terminal domain. The N-terminal domain contains a myristoylation site that allows for protein-lipid interaction thereby anchors the Z

protein to the plasma membrane. The central domain contains the Really Interesting New Gene (RING) which chelates zinc and interacts with the LP protein to halt the polymerase reaction. The C-terminal domain contains proline rich motifs which interacts with the endosomal sorting complexes required for transport (ESCRT) machinery and aids viral budding (168). It also harbours the late domain (169). The Z protein late domain differs among Old and New World Arenaviruses. For example, the Old World Arenaviruses contain a PTAP and PPPY amino acid domains whereas the New World viruses generally contain a PT/SAP amino acid domain (170). The production of defective interfering particles (defective virions) during LCMV replication, an Old World Arenavirus, has been shown to be due to the PPPY late domain which is absent in the New World Arenaviruses (171).



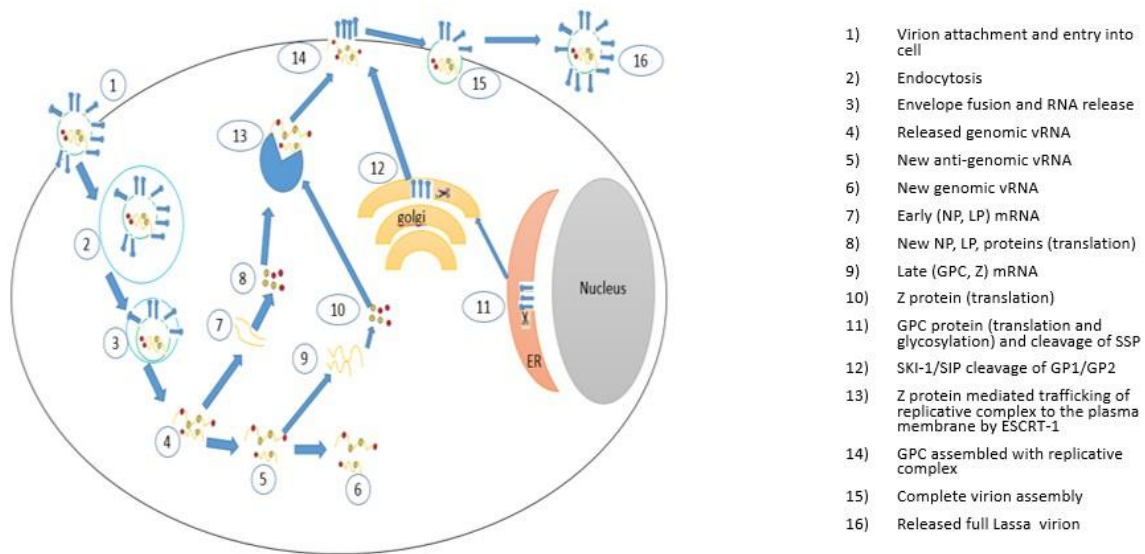
### 3: Figure 1.3: Arenavirus Structure

Structure of Lassa virus, a prototype Old World Arenavirus showing different parts of the virion: the glycoprotein (blue) mediates viral attachment and entry into the cell; the L protein, polymerase (red), functions in transcription and replication; the Nucleoprotein (NP, orange)

forms the bead-like structural protein of the virus; and other proteins in the virions such as the Z protein, or packaged ribosome (172).

Because mammarenaviruses are bisegmented negative stranded RNA viruses, their proteins cannot be translated directly from their genomic RNA. Once released inside the cell, the N-terminal domain of LP alongside the NP snatches the 5' caps of host mRNA to initiate transcription of the positive strands. This early transcription is terminated by the IGR region between them. The LP and the NP are the earliest gene products to be translated from these viral mRNAs. The new NP will then bind the viral mRNA and allow continued transcription of the late gene products and assembly of the progeny virus. The transition from the early gene products to the late gene products requires the polymerase to read through the IGR hair pins and make a complimentary copy of the genomic RNA. This anti-genomic RNA will form the template for the transcription of the late gene product mRNA; to allow production of the Z protein and GPC (170). This is the unique feature of Arenavirus referred to as ambisense structure.

The GPC protein is translated in the endoplasmic reticulum. It is proteolytically processed by host cell subtilase SKI-1/S1P into a heterotrimer consisting of receptor-binding GP1 domain, a GP2 class I membrane fusion protein, and a retained myristoylated stable signal peptide (SSP). The heterotrimer forms the glycoprotein spike in the lipid bilayer of the mature virion (173). When the progeny virion is ready, the central domain of the Z protein interacts with the LP to stop the polymerase reaction. The mechanism is not clear but Peng et al. (2020) suggested that the Z protein blocks the nucleoside triphosphate (NTP) entrance thereby preventing RNA synthesis (167). The NP then interacts with Z protein to facilitate the transport of the replication complex to the cell membrane. Viral budding is initiated by the interaction of the late domain of the Z protein with the Tumour Susceptibility Gene 101 (TSG101) of the ESCRT machinery (174). A new virion is produced by budding, which seeks another cell, often an APC, for continuous propagation. The replication of an Old World Arenavirus is shown in figure 1.2.



**4: Figure 1.4: Arenavirus replication cycle**

Arenavirus replication from attachment and entry into the cell (1) to release of a full virion (172).

### 1.2.2 Arenavirus infection: The Role of APC

APCs are central to the pathogenesis of Arenavirus disease. They are early cellular targets, their migration inadvertently spreads the virus in the host and allows the virus access to various organs and tissues in the body (175). Virus replication in DCs and macrophages is associated with disruption of cellular function in terms of antigen presentation and the induction of an adaptive immune response. Thus, infection of these cell types initiates the immune dysregulation that is observed in patients. Previous studies have shown that the interaction of APC with Arenaviruses varies between the Old World and New World viruses and affects the outcome of infection (155). In contrast to the generalised immunosuppression seen in LASV infection, Junin virus infection is characterised by a severe inflammatory response referred to as a cytokine storm. LASV is capable of productive infection of DCs and macrophages but fails to activate or induce IFN or the production of inflammatory cytokines. Junin virus, on the other hand, productively infects both macrophages and DCs and induces a strong IFN response from DCs as well as lung epithelial cells. This variation in the immune response is further attributed to the differences in their viral entry receptors (42). The Old World viruses mainly use  $\alpha$ -dystroglycan for cellular entry while the New World viruses utilise the human transferrin

receptor 1 (hTfR1). In addition to using the cell surface receptor  $\alpha$ -dystroglycan, LASV virus also uses LAMP1 in the acidic phagosomal compartment to trigger virus entry into the cytoplasm; however, no such molecule has yet been identified for New World Arenavirus infection (176). Furthermore, variation is also seen in the disease pathology between the two groups of Arenaviruses. While hepatitis and acute kidney disease are common in many severe Lassa fever cases, they are uncommon or mild in Junin infected patients. In contrast, haemorrhage, neurological changes, leukopenia and thrombocytopenia are much more common in Junin-infected patients than in LASV-infected patients (177).

### **1.2.3 Arenaviruses and Viral Haemorrhagic Fever Syndrome**

Viral haemorrhagic fever (VHF) is a term used to describe a syndrome caused by a group of RNA viruses which is characterised by febrile illness and vascular compromise that usually ends up in 'shock' and death. The term was coined by a group of Soviet Union scientists investigating an outbreak of haemorrhagic fever with renal syndrome caused by hantavirus, one of the causative VHF agents (165). About 23 RNA viruses belonging to four diverse viral families (Flaviviridae, Filoviridae, Arenaviridae, and Bunyaviridae) have been implicated in VHF. These viruses vary in their geographic distribution, reservoir hosts, immune response and pathology but end up producing a similar clinical syndrome, hemorrhagic fever (178).

The endemicity of VHF seems to be related to the presence of habitat for their natural host (179). Junin virus, the cause of Argentinean hemorrhagic fever is common in South America due to the widespread distribution of the Dryland vesper mouse, which is the natural host. Lassa fever is endemic in most parts of West Africa where the giant rat (*Mastomys natalensis*), the reservoir host, is common. LCMV is ubiquitous because the reservoir host *Mus musculus* is widely distributed across the world. However, this is rapidly changing with increasing incidence of these viruses in areas where they have not been reported previously. The 2013-2016 Ebola outbreak in West Africa is not only the first with large-scale human to human transmission in that region, but the virus was also carried to other continents including America and Europe, previously foreign to these infections (180). This change in distribution has been attributed to the increase in international travel, climate change and migration of natural hosts due to human encroachment and loss of habitat. VHF is currently seen as a serious global health threat that requires research for future prevention. This is not just because of the burden of disease in endemic areas but also the potential of the agents to be used as weapons of bioterrorism and the

fact that there are limited or no vaccines and drugs for management of infections. The 2013-2016 West Africa Ebola epidemic killed over 11000 people, the 2016 yellow fever virus outbreak in Angola caused more than 3700 infections and 364 deaths, in 2018 Lassa virus affected about 500 people in Nigeria with 95 deaths and an estimated annual burden of 100,000 to 300,000 people in Africa (181–183).

Despite the variation in aetiological agents, geographical location, and clinical outcomes, a working model for most VHF infections suggested by Basler (2017) involves viral contact with the skin or mucous membrane: exposure of mucous membranes or breaks in the skin to infectious virus increases the risk of infection with Ebola virus; exposure to excreta from infected rodents is seen in LASV; or the bite by an infected insect breaking the skin allows Yellow fever virus (YFV) to infect (184). After introduction to the body, myeloid cells especially macrophages and DCs are the first targets of infection. Macrophages and DCs support productive replication of the virus and promote systemic dissemination by migrating to the lymph nodes to activate the adaptive immune response. From the lymph node, the virus can gain access to various organs and tissues of the body resulting in the pathological process that manifests as VHF. For example, liver damage may depress production of clotting factors, which may result in haemorrhage. Infection and activation of macrophages will result in the production of excessive amounts of inflammatory cytokines, commonly referred to as a cytokine storm. This promotes vascular damage that may lead to disseminated intravascular coagulation. Additionally, bystander lymphocyte apoptosis commonly seen in Ebola virus disease, may be due to the effect of these cytokines.

Infection of DCs, on the other hand, leads to a dysregulated phenotype characterised by lack of inflammatory and IFN responses. There is impaired maturation of DC and lack of antigen presentation to T cells. This causes immune impairment and failure of activation of T cells, leading to T cell apoptosis. The culmination of these processes with systemic vascular damage is referred to as VHF. In most cases, it results in the death of the patient, but some cases do survive. Notably, there is debate about the relevance of the term VHF to the diagnosis, clinical presentation and management of the disease (184,185). This is because many different RNA viruses are implicated in the syndrome, and haemorrhage and fever (the hallmark of VHF) are not seen in most clinical cases except in severe forms. For example, Ebola virus-induced VHF is now reclassified as Ebola virus disease to reflect this. For the sake of clarity, I will continue to use VHF. A summary of the agents of VHF, their genome, reservoir host, immune evasion and immunopathological mechanisms as well as their innate PAMPs is presented in Table 1.1.

My work will focus on a prototypic Old World Arenavirus called LCMV.

LCMV does not cause VHF. However, LCMV is a well-studied virus with a wealth of information available in the literature. It is easily accessible and does not require a BSL-4 high containment facility like its sister virus, LASV that causes VHF. LASV is a major VHF agent endemic in West Africa. Therefore, LCMV presents an excellent model to study the biology and interaction of Arenavirus with the host.

#### **1.2.4 LCMV as a Model of Virus Persistence in APCs**

A virus persists by causing little or no damage to the cell as well as by inhibiting the host immune response that can eliminate the virus (186). The Old World Arenavirus LCMV presents an important model to study virus persistence. Since its isolation from cerebrospinal fluid of people with aseptic meningitis, LCMV has been an important tool in the field of virology and immunology (187). Many immunological discoveries and Nobel prizes have resulted from the study of LCMV. According to Michael Oldstone, LCMV remains the best model for studying virus persistence, immunological tolerance, and immunopathogenesis (188). LCMV has prototypic acute and persistent strains. The parental virus, Armstrong 53b (ARM), causes an acute infection characterised by profound CD8<sup>+</sup> T cell expansion and type 1 IFN production with infection resolving within two weeks. The persistent strain, clone 13, which is derived from ARM causes an infection that lasts for over 100 days and is characterised by immunosuppression and impairment of adaptive immune responses (189,190). The initial immune response is similar against both the acute and persistent strains of virus. Interestingly, the collapse of the adaptive immune response occurs after one week of infection with clone 13. The reason for the immunosuppression is not fully understood, but type I IFN has been implicated (191). Sequence comparison of the two strains show that they differ by 5 nucleotides which cause two amino acid substitutions, one each in the viral glycoprotein and polymerase protein. LCMV ARM has phenylalanine (F) at position of 260 of GP-1 while Clone 13 has leucine (L). The other amino acid substitution is seen at position 1079 of LP; ARM has Lysine (K) while Clone 13 has glutamine (Q). The variation in the GP protein allows clone 13 to bind with high affinity to the major Old World Arenavirus cellular receptor  $\alpha$ -Dystroglycan, a protein expressed at high concentrations on the surface of DCs. This was implicated in the persistent capability of clone 13 compared to the ARM strain (192). Similar to other Arenaviruses, LCMV preferentially infects and replicates in DC and macrophages. Previous studies showed that

clone 13 preferentially infects CD11c<sup>+</sup> and DEC-205<sup>+</sup> (>75 %) DCs in the marginal zone of the spleen whereas the ARM strain infects F4/80 expressing cells mainly in the red pulp (193). Other differences between the two strains are shown in Table 1.2.

The availability of an enormous data set in the literature and two distinct strains with different clinical outcomes makes LCMV one of the best models to understand the mechanism of Arenavirus persistence. Before the discovery of HIV, LCMV infection of in-bred laboratory mice was and still is the best model for studying immunological mechanisms involved in chronic RNA virus infections (194). Much of the data generated from LCMV has provided the foundation for our understanding of many immunological processes. Previous studies have focused on genetics and cellular tropism to explain LCMV persistence with very few studies focusing on understanding the contribution of immune cells especially APC. Recent work by Tejiro et al. (2013) showed that the persistence of LCMV clone 13 is due to immunosuppressive cytokines from DC, and this is type I IFN dependent (143). In light of recent advances in technology, there is the need for revision of some of the data generated from LCMV studies. For example, previous work showed preferential infection of DEC-205 expressing DC by LCMV clone 13 and F4/80 expressing cells by LCMV ARM. Recent work has suggested the plasticity of APC where F4/80 is expressed in both macrophages and DC. Also, the role of moDC and monocytes recruited during infection is not known. Elucidating the mechanism of LCMV persistence will aid our understanding and management of other persistent viruses such as LASV.

**2: Table 1.2: Comparison Between the Acute Strain (LCMV Armstrong) and the Persistent Strain (LCMV clone13) of LCMV**

LCMV Armstrong	LCMV clone 13
Causes acute infection that clears within 7-10 days	Persistent infection that can last for about 60 days
Predilection for F4/80 <sup>+</sup> macrophages in the red pulp	Predilection for CD11c <sup>+</sup> DEC205 <sup>+</sup> DC in the marginal zone and white pulp of the spleen
Carries phenylalanine at position 260 of GP1 protein and Lysine at position 1079 of L protein	Carries Leucine at position 260 of GP1 protein and Glutamine at position 1079 of L protein
Binds weakly to $\alpha$ -DG and easily displaced by ECM laminin	Binds strongly to $\alpha$ -dystroglycan (DG)
Does not interfere with DC development, maturation, and function	Inhibits development of DC from progenitors, and functional maturation and this has been shown to be interferon dependent (IRF9/STAT2 dependent, STAT1 independent)

Table 1.2 shows a summary of the differences between the acute (LCMV Armstrong) and persistent (LCMV clone 13) strain of LCMV.

#### **1.2.4.1 LCMV as a Useful Model for Studying Lassa Fever Virus**

Both LCMV and LASV belong to the Old World Arenaviruses, sharing about 60 % genetic homology (195). Similar to LASV, LCMV infects APC and shares some of the clinical picture associated with Lassa virus disease such as vascular compromise and CNS complications. Both viruses are yet to adapt to human to human transmission, the reason for this bottleneck is unknown. They both can cause immunosuppression thereby inhibiting the adaptive immune response. Parental LCMV strain ARM causes an acute infection, thus providing a comparable model for LASV. Finally, LASV can only be handled at biosafety containment level (BCL) 4, which is not readily available, making it difficult and expensive to study. On the other hand, LCMV can be studied at lower containment facilities (BCL2 and BCL3) as it is considered less dangerous than LASV. These facilities are readily available and less expensive to run than BCL4. Thus, LCMV presents a good and accessible model to understand the mechanism of persistence in LASV infection.

### **1.3 Hypothesis and Aims**

#### **1.3.1 Hypotheses:**

BM derived cells comprises subsets of dendritic cells and macrophages and the interaction with LCMV varies between these different subtypes of BM derived cells.

APCs modulate the outcome of LCMV infection and persistence at the single cell level.

Persistent LCMV infection affects subsequent responses to a secondary infection.

#### **1.3.2 Aims and Objectives:**

The aim of the project was to investigate, using the new model of BM derived APC and new

single cell sequencing technology, the interaction of LCMV and APC.

Objective 1: Which cell subtypes from BM derived APC are infected by LCMV

Objective 2: How does LCMV infection affect specific APC subtype functions

Objective 3: To understand the biological consequence of persistent LCMV infection to the response to a secondary infection.

# Chapter 2

## General Materials and Methods

### 2.1 Cell Lines

BV-2 cell (a mouse microglial cell line), a kind gift from Prof. Ian Goodfellow (Pathology Department, University of Cambridge), was derived from primary microglial cell cultures from C57BL/6 mice immortalised by infection with a v-raf/v-myc oncogene carrying retrovirus. This cell line was found to share the antigen profile, phagocytic and antimicrobial properties of activated macrophages.

RAW 264.7 (a mouse monocyte-macrophage cell line), was originally established from an ascites of a tumour induced in a male mouse by intraperitoneal injection of Abelson Leukaemia Virus (A-MuLV) (HPA Culture Collections 91062702).

BHK-21 clone 13 cells (Hamster kidney fibroblast cell line) and Vero African green monkey kidney epithelial (ATCC CCL-81), were kind gifts from Prof. Juan Carlos de la Torre (The Scripps Research Institute, La Jolla, CA). BHK-21 clone 13 is a subclone of a parental line derived from the kidneys of five unsexed, 1-day-old hamsters. Both cell lines are useful for passage and growth of many RNA viruses including LCMV.

These cells were maintained by growing in Dulbecco's modified Eagle's medium (DMEM) supplemented with 10 % foetal calf serum (FCS), 2 mM L-glutamine, 100 U penicillin/ml and 0.1 mg streptomycin/ml (10%DMEM). The cells were seeded (at  $2-5 \times 10^4$  cells per  $\text{cm}^2$ ) in tissue culture flasks and incubated at 37 ° C, 5 %  $\text{CO}_2$ . Every 3-4 days the cells were split (approximately 1:10).

T cell hybridomas 5A1 (epitope mapping the I-Ah-binding peptide PI3 consists of amino acids 61-80 of the LCMV-GP) and CTL-2 (IL-2 sensitive) cells were provided by Prof. Annette Oxenius (Institute for Microbiology ETH Zurich Valdimir-PrelogWeg 4 8093 Zurich Switzerland)(196)

T cell hybridoma 5A1 cells was maintained by growing in RPMI-1640 supplemented with 10 % FCS, 2mM L-glutamine, 100 U penicillin/ml and 0.1 mg streptomycin/ml (10%RPMI). The cells were seeded (at  $2-5 \times 10^4$  cells per  $\text{cm}^2$ ) in tissue culture flasks and incubated at 37 ° C, 5

% CO<sub>2</sub>. Every 3-4 days the cells were split (approximately 1:10). CTLL-2 was maintained in a similar way with the addition of human recombinant IL-2 (1 ng/ml).

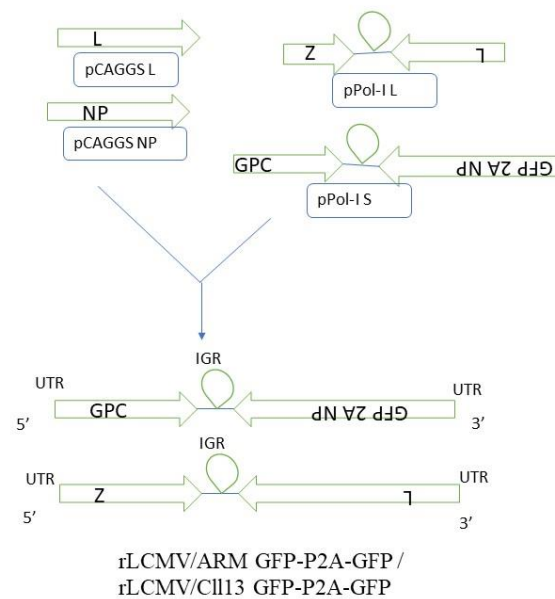
## 2.2 Mice

Adult (C57BL/6 wild-type) and C57BL/6J (Rosa26floxedSTOPtdTomato) mice, age range between 6 to 14 weeks, were used in the study(197). Adult (C57BL/6 wild-type) were used for *in vitro* experiments while C57BL/6J (Rosa26floxedSTOPtdTomato) mice were used for *in vivo* experiments. The former was a kind donation from Prof W.H Colledge at the Department of Physiology, Development and Neuroscience, while the latter were a kind donation from Prof CJ Watson at the Gurdon Institute, both at the University of Cambridge. C57BL/6 wild type mice were used as a source of bone marrow from the tibia and femur for *in vitro* experiments. The C57BL/6J (Rosa26floxedSTOPtdTomato) mice used for the *in vivo* experiments were housed on hardwood chip bedding under specific- pathogen-free conditions at the BSL 3 unit of the Animal Breeding Centre of the Cambridge Biomedical Centre (CBS). They were held in individually ventilated cages and lights were on a 12-h light/dark cycle. Rodent chow and water were given *ad libitum* throughout the experiment. All the experimental procedures took place in compliance with the University ethical review process and Animals (Scientific Procedures) Act 1986.

## 2.3 Viruses

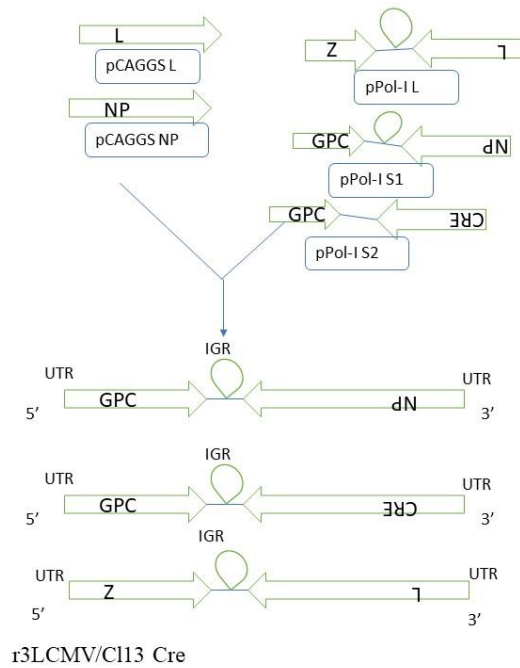
rLCMV/ARM GFP-P2A-GFP ( $1.0 \times 10^6$  genome copies/ml), rLCMV/C113 GFP-P2A-GFP ( $3.0 \times 10^6$  genome copies/ml), r3LCMV/C113 Cre ( $3.4 \times 10^6$  genome copies/ml) were provided by Professor Juan Carlos de la Torre (The Scripps Research Institute)(198,199). These recombinant viruses were made by reverse genetics. In the rLCMV/ARM GFP-P2A-GFP and rLCMV/C113 GFP-P2A-GFP, the NP ORF in the pPol-I S plasmid was replaced by the bicistronic ORF GFP-P2A-GFP, which contained the ORF of green fluorescent protein (GFP) tagged to the N terminus of NP and separated by the 2A peptide (P2A) sequence derived from the porcine teschovirus (PTV1). The P2A sequence allows for production of both GFP and NP proteins from the same mRNA transcribed from the NP locus of the S genome segments. The r3LCMV/C113 Cre on the other hand, involved one pPol-I L segment, and two pPol-I S segments. The NP ORF in one of the segments is replaced by Cre recombinase (pPol-I S1 NP/Cre) see figure 2.1 and 2.2 for the virus constructs.

Once generated, these stocks were passaged twice through BHK-21 cells to generate P3 stocks used for infection assays. These recombinant viruses are stable and have been shown to exhibit the same growth characteristics as wild type viruses(200). Also, because they are carrying reporter gene (GFP and Cre) infected cells can easily be evaluated and separated from uninfected and bystander cells by their fluorescence expression.



### 5: Figure 2.1: Recombinant LCMV Arm and Clone 13 construct (with GFP)

Recombinant LCMV expressing green fluorescent protein (GFP) was generated by reverse genetics. The NP ORF in the pPol-I S plasmid was replaced by two GFP ORF separated by the 2A peptide (P2A) sequence derived from the porcine teschovirus (PTV1).



**6: Figure 2.2: Trisegmented recombinant LCMV Clone 13 construct (with Cre recombinase)**

The trisegmented recombinant LCMV (r3LCMV/C113 Cre) was generated by replacing the NP ORF in one of the S segments with a Cre recombinase. It is trisegmented because it contains one pPol-I L segment, and two pPol-I S segments.

### 2.3.1 Generation and Quantitation of High-Titre Virus Stocks

LCMV virus stocks (P0) were grown in BHK-21 cells in 10%DMEM. BHK-21 cells were cultured overnight in tissue culture flasks with a surface area of 25 cm<sup>2</sup>. Infection was carried out the next day when flasks were around 70 % confluent at a multiplicity of 0.01 FFU/ml. The flask was incubated at 37 ° C for 3 h with gentle agitation applied every 30 min. After this incubation, a further 3 ml of media was added to each flask (5 ml total) and the cells were incubated at 37 ° C, 5 % CO<sub>2</sub> for 48 h. The supernatant was decanted to sterile tubes and centrifuged (5 min, 1500 x rpm). The resulting clarified supernatant, which contained the virus, was aliquoted (1 ml/tube) into 2 ml cryotubes and stored at -150 ° C.

For quantification of virus, Vero cells were seeded in 96 well plates overnight (3 x 10<sup>4</sup> cells/well) in 10%DMEM. The cells were infected with a serial dilution of the LCMV virus stocks and incubated at 37 ° C, 5 % CO<sub>2</sub> for 48 hours. The cells were harvested with trypsin

and fixed with 4 % formaldehyde. GFP expression was measured by flow cytometry. This was used to calculate the FFU/ml for each virus stock.

## **2.4 *In vitro* Infection of Bone Marrow Derived Cells**

### **2.4.1 Generation of Bone marrow (BM) Derived Cells**

Bone marrow was extracted from the femurs and tibias of mice (C57BL/6 wild-type) by flushing with Iscove's modified Dulbecco's medium (IMDM) supplemented with 10 % FCS, 100 U penicillin/ml, 0.1 mg streptomycin/ml and 50  $\mu$ M 2-mercaptoethanol (10% IMDM) using a syringe and 25G needle into a petri dish. The bone marrow was forced through a 70  $\mu$ m cell strainer and centrifuged for 5 min at 400 x g and 4 ° C. Pelleted cells were plated in 10 ml petri dishes at a density of  $2 \times 10^6$  cells in 10% IMDM supplemented with various growth factors: GM-CSF (20 ng/ml) alone or GM-CSF (20 ng/ml) with IL-4 (10 ng/ml), M-CSF (20 ng/ml) and FMS-like tyrosine kinase 3 ligand (FLT3-L) (200 ng/ml) (all from PeproTech) and incubated for six or eight days (37 ° C, 5 % CO<sub>2</sub>) depending on the assay. After incubation, the dish containing the cells was placed on ice for at least 30 min. The cells were harvested by scraping adherent cells into suspension, then pelleting all cells (5 min, 400 x g, 15 ° C) before resuspension in 10%IMDM at the required cell density for use in various assays, such as surface marker staining (8 days incubation) or infection and functional studies (6 days incubation).

### **2.4.2 LCMV Infection of BM Derived Cells**

Sorted CD11c<sup>+</sup> MHC class II<sup>+</sup> BM derived cells were seeded into individual wells of 24-well plates, at a density of  $1 \times 10^5$  cells per well in 200 ul of 10%IMDM. Cells were allowed to settle overnight in an incubator at 37 ° C, 5 % CO<sub>2</sub>. The next day, the medium was carefully removed and replaced with the virus inoculum diluted to the stated MOI (usually 10 FFU/cell) in 2%IMDM or replaced with 2%IMDM alone (mock infection). Both mock and infected cells were incubated for 1 h, 37 ° C, 5 % CO<sub>2</sub>, with gentle agitation every 15 min. After this 1 h infection period, the inoculum was carefully removed, and cells were washed with PBS and medium replaced with fresh 10%IMDM. The plate was returned to the incubator until the

corresponding time points for the required assay such as flow cytometry, RT-qPCR, ELISA assay, and single-cell RNA sequencing.

### **2.4.3 Infection Assays on RAW and BV-2 Cells**

Cells were harvested from flasks during logarithmic phase and seeded into individual wells of 24-well plates, at a density of  $1 \times 10^5$  cells per well respectively, unless described otherwise. Cells were allowed to adhere to the plates overnight at 37 ° C, 5 % CO<sub>2</sub>. The next day, the medium was removed and replaced with the virus inoculum diluted to the stated MOI in 10%DMEM or replaced with 10%DMEM alone (mock infection). Infected cells were incubated for 1 h, 37 ° C, 5 % CO<sub>2</sub>, with gentle agitation every 15 min. After this 1 h infection period, the inoculum was removed and cells were washed with PBS and replaced with fresh 10% DMEM. The plate was returned to the incubator until the corresponding time points for the required assay; such as flow cytometry, RT-qPCR or ELISA assay.

### **2.4.4 Treatment of BM Derived Cells with Poly(I:C)**

Sorted CD11c<sup>+</sup>, MHC class II<sup>+</sup> BM derived cells were seeded into plates as described in Section 3.2.4. After overnight incubation, the medium was removed from the wells and replaced with 10%IMDM supplemented with 100 µg poly (I:C)/ml (Sigma Aldrich, P1530). Cells corresponding to the baseline time point were processed at this stage, by removal of the supernatant for ELISA analysis (Section 3.2.8), and lysis of the cells for RNA extraction (Section 2.7), reverse transcription and gene expression analysis (Section 2.8). Otherwise, cells were returned to the incubator (37 ° C, 5 % CO<sub>2</sub>) until the required time points (0, 3, 6, 9, 12 and 24 h P.I.) for similar processing.

## **2.5 *In vivo* Infection of Mice**

### **2.5.1 Intraperitoneal Infection with r3LCMV/Cl13 Cre or Stimulation with Poly (I:C)**

r3LCMV/ Cl 13 Cre virus stock was diluted in PBS to the required infectious titre ( $2 \times 10^6$  pfu per mouse). Mice were gently restrained without anaesthesia and injected with 100 µl of

virus inoculum and/or poly I:C (20 µg/50 µg) in PBS (Sigma-Aldrich, P1530) administered from a 1 ml syringe and 27 gauge hypodermic syringe. Uninfected mice were injected with 100 µl of PBS.

## **2.5.2 Isolation of Mouse Splenic Mononuclear Cells**

The spleen was placed in 1mg collagenase D/ml (Roche, 11088882001) solution for 30 min to breakdown connective tissues and ease the release of cells. Single cell suspensions in PBS were generated by grinding the organs through 70 µm cell strainers. Mononuclear cells were isolated from the suspension using histopaque (Sigma-Aldrich, 1077) according to the manufacturer's instructions. The cell suspension was overlaid onto histopaque at a ratio of 2:1 in a 15 ml tube. The tube was centrifuged at 400 x *g* for 30 min at room temperature in a swinging-bucket rotor with no break. The top clear layer was removed, and the buffy coat interface was collected, washed twice with PBS-EDTA (10 mM), and centrifuged for 10 min at 250 x *g* with the brake on. The pelleted cells were suspended in red blood cell lysis buffer (1 mM KHCO<sub>3</sub>, 0.15 M NH<sub>4</sub>Cl, 0.1 mM EDTA, HCl pH 7.2 to 7.4) at room temperature for 5 min. The cells were washed again with PBS-EDTA, centrifuged at 250 x *g* for 10 min at 4 ° C and resuspended in appropriate medium for further assay (surface antibody staining and cell sorting).

## **2.6 Flow Cytometry**

### **2.6.1 Surface Staining of BM Derived and Splenic DCs and Macrophages**

Cells were resuspended in FACS buffer (1 % FCS, 0.05 % sodium azide in PBS) containing 20 µg 2.4G2/ml to block Fc receptors (BD Biosciences) for 10 min at 4-8 ° C. Antibody cocktails prepared in FACS buffer at the concentrations shown (see Table 2.2) were added to the cells and incubated in the dark at 4 ° C, for 30 min. Cells were washed and resuspended with FACS buffer (2 x 10<sup>6</sup> cells in 200 ul) for sorting. Those for phenotypic assays (surface marker expression) were washed in PBS and the pelleted cells fixed with 4 % paraformaldehyde in PBS at 4 ° C, for 30 min. After fixing, the cells were washed in PBS and resuspended in an appropriate volume of FACS buffer for detection of cell surface markers by flow cytometry

## 2.6.2 Detection of Cell surface Markers by Flow Cytometry

Antibody stained and unstained cells in FACS buffer were acquired using an Accuri C6 flow cytometer (BD Biosciences, CA) and expression of cell surface markers was analysed using AccuriC6 software. Relevant isotype control antibodies were used to exclude non-specific binding, and these did not display increased fluorescence compared with the unstained controls. Spectral overlap between fluorescence channels was compensated electronically using isotype negative and single positive stained cells to set compensation values. After exclusion of debris and doublets, single cells were characterised based on the expression of CD11c, MHC class II and CD11b into three populations. The expression of various surface markers was analysed for each population of cells.

## 2.6.3 Sorting of BM Derived and Splenic DCs and Macrophages

Cells were sorted using an Aria III flow cytometer (BD Biosciences, CA) into various subsets of DCs and macrophages (see table 2.1 for Aria III configuration and set up). The sorted cells were collected into 5 ml polypropylene tubes (Falcon 352063) containing 1 ml of 10% IMDM at 4 ° C to reduce adherence to the plastic (see each chapter for specific for flow cytometer set up and staining plate map). The cells were counted and used for further assays.

**3: Table 2.1 Aria III Configuration and Set up**

Laser	Filter			
407	450/50, 510/50, 610/20, 660/20, 710/50, 780/60			
488	FSC, SSC (488/10), 530/30, 695/40,			
561	582/15, 610/20, 670/14, 710/50, 780/60			
633 nm	660/20, 730/45, 780/60			
Laser	Filter	Filter (Long Pass -LP)	Filter (Band Pass- BP)	Dyes (Fluorophore)
407 nm	A	735LP	780/60	Qdot800

	B	685LP	710/50	Qdot705
	C	630LP	660/20	Qdot655
	D	600LP	610/20	Qdot605
	E	502LP	510/50	AmCyan/HorizonV500
	F		450/50	DAPI/HorizonV450/Pacific Blue
488 nm	A	655LP	695/40	PerCP-Cy5.5 (PE-Cy-5.5)
	A	570 LP	585/15	PE
	B	502LP	530/30	FITC
	B	495 LP	509/21	GFP
	C		488/10	SSC
561 nm	A	735LP	780/60	PE-Cy7
	B	685LP	710/50	PE-Cy5.5/PE AlexaFluor700
	C	630LP	670/14	PE-Cy5
	D	600LP	610/20	PE-TxRed/mCherry/PI
	E		582/15	PE
633 nm	A	755LP	780/60	APC-Cy7/APC-H7
	B	690LP	730/45	AlexaFluor700
	C		660/20	APC

Diva v8 need 32 bit Windows 7 with at least 4 MB RAM (8 better) Java JDK/JRE 1.6.0\_29

## 2.6.4 Antibodies

Cells were stained with cocktails containing various antibodies with different conjugates obtained from BD Biosciences, USA or from Biolegend, USA (Table 2.2).

**4: Table 2.2 List of Antibodies**

<b>Marker</b>	<b>Fluorophore</b>	<b>Clone</b>	<b>Isotype</b>	<b>Catalogue No.</b>	<b>Amount / Volume Used *</b>
anti-mouse CD8 $\alpha$	APC-Cy7	53-6.7	rat IgG2a, $\kappa$	Biolegend 100714	0.2ug/100ul
anti-mouse CD11c	FITC	N418	Armenian hamster IgG1	Biolegend 117306	0.2ug/100ul
anti-mouse CD11c	APC	N418	Armenian hamster IgG1	Biolegend 117310	0.2ug/100ul
anti-mouse I-A/I-E	PE	M5/114.15.2	rat IgG2b, $\kappa$	Biolegend 107607	0.1ug/100ul
anti-mouse I-A/I-E	PE-Cy7	M5/114.15.2	rat IgG2b, $\kappa$	Biolegend 107630	0.1ug/100ul
anti- mouse/human CD11b	PerCP-Cy5.5	M1/70	rat IgG2b, $\kappa$	Biolegend 101227	0.2ug/100ul
Anti-mouse CD205	AlexaFluor 647	NLDC145	rat IgG2a, $\kappa$	Biolegend 138203	0.2ug/100ul
anti-mouse CD115	APC	AFS98	rat IgG2a, $\kappa$	Biolegend 135510	0.2ug/100ul
anti-mouse CD135	APC	A2F10	rat IgG2a, $\kappa$	Biologend 135310	0.2ug/100ul
anti-mouse CD117	AlexaFluor 647	2B8	rat IgG2b, $\kappa$	Biolegend 105818	0.2ug/100ul

anti-mouse CD273 (PD- L2)	APC	TY25	rat IgG2a, κ	Biolegend 107210	0.2ug/100ul
anti-mouse CD197 (CCR7)	APC	4B12	rat IgG2a, κ	Biolegend 120108	0.2ug/100ul
anti-mouse F4/80	APC	BM8	rat IgG2a, κ	Biolegend 123116	0.2ug/100ul
anti-mouse CD14	APC	Sa14-2	Rat IgG2a, κ	Biolegend 123312	0.2ug/100ul
anti-mouse CD64	APC	X54-5/7.1	Mouse IgG1, κ	Biolegend 139306	0.2ug/100ul
anti-mouse CD86	AlexaFluor 647	GL-1	Rat IgG2a, κ	Biolegend 105012	0.2ug/100ul
anti-mouse CD40	AlexaFluor 647	3S23	Rat IgG2a, κ	Biolegend 124614	0.2ug/100ul
anti-mouse CD80	AlexaFluor 647	1.1610A1	Armenian Hamster IgG	Biolegend 104718	0.2ug/100ul
anti-mouse CD24	AlexaFluor 647	M1/69	rat IgG2b, κ	Biolegend 101818	0.2ug/100ul
anti-mouse Ly-6C	Brilliant Violet 711	HK1.4	rat IgG2c, κ	Biolegend 128037	0.2ug/100ul
anti-mouse CD3	Brilliant Violet 605	17A2	rat IgG2b, κ	Biolegend 100237	0.2ug/100ul
anti-mouse NK-1.1	Brilliant Violet 605	PK136	Rat IgG2a, κ	Biolegend 108753	0.2ug/100ul

anti-mouse CD19	Brilliant Violet 605	6D5	Rat IgG2a, κ	Biolegend 115540	0.2ug/100ul
anti-mouse Ly-6G	Brilliant Violet 605	1A8	Rat IgG2a, κ	Biolegend 127639	0.2ug/100ul
anti- mouse/human CD45R/B220	Brilliant Violet 605	RA3-6B2	Rat IgG2a, κ	Biolegend 103244	0.2ug/100ul
Anti-Mouse Siglec-F	Brilliant Violet 605	E50-2440	Rat IgG2a, κ	BD Bioscience 740388	0.2ug/100ul
anti-mouse CD45 and MHC class I Hashtag 1 Antibody	TotalSeq™- A0301	M1/42; 30- F11	rat IgG2a, κ	Biologend 155801	0.2ug/100ul
anti-mouse CD45 and MHC class I Hashtag 2 Antibody	TotalSeq™- A0302	M1/42; 30- F11	rat IgG2a, κ	Biologend 155803	0.2ug/100ul
anti-mouse CD45 and MHC class I Hashtag 3 Antibody	TotalSeq™- A0303	M1/42; 30- F11	rat IgG2a, κ	Biologend 155805	0.2ug/100ul
anti-mouse CD45 and MHC class I Hashtag 4 Antibody	TotalSeq™- A0304	M1/42; 30- F11	rat IgG2a, κ	Biologend 155807	0.2ug/100ul

anti-mouse CD45 and MHC class I Hashtag 5 Antibody	TotalSeq™- A0305	M1/42; 30- F11	rat IgG2a, κ	Biologend 155809	0.2ug/100ul
anti-mouse CD45 and MHC class I Hashtag 6 Antibody	TotalSeq™- A0306	M1/42; 30- F11	rat IgG2a, κ	Biologend 155811	0.2ug/100ul
anti-mouse CD45 and MHC class I Hashtag 7 Antibody	TotalSeq™- A0307	M1/42; 30- F11	rat IgG2a, κ	Biologend 155813	0.2ug/100ul
anti-mouse CD45 and MHC class I Hashtag 8 Antibody	TotalSeq™- A0308	M1/42; 30- F11	rat IgG2a, κ	Biologend 155815	0.2ug/100ul
anti-mouse CD45 and MHC class I Hashtag 9 Antibody	TotalSeq™- A0309	M1/42; 30- F11	rat IgG2a, κ	Biologend 155817	0.2ug/100ul
anti-mouse CD45 and MHC class I Hashtag 10 Antibody	TotalSeq™- A0310	M1/42; 30- F11	rat IgG2a, κ	Biologend 155819	0.2ug/100ul
anti-mouse CD45 and MHC class I	TotalSeq™- A0311	M1/42; 30- F11	rat IgG2a, κ	Biologend 155821	0.2ug/100ul

Hashtag 11 Antibody					
anti-mouse CD45 and MHC class I Hashtag 12 Antibody	TotalSeq™- A0312	M1/42; 30- F11	Rat IgG2a, κ	Biolegend 155823	0.2ug/100ul
anti-mouse CD45 and MHC class I Hashtag 13 Antibody	TotalSeq™- A0313	M1/42; 30- F11	rat IgG2a, κ	Biolegend 155825	0.2ug/100ul
anti-mouse CD45 and MHC class I Hashtag 14 Antibody	TotalSeq™- A0314	M1/42; 30- F11	Rat IgG2a, κ	Biolegend 155827	0.2ug/100ul
anti-mouse CD45 and MHC class I Hashtag 15 Antibody	TotalSeq™- A0315	M1/42; 30- F11	Rat IgG2a, κ	Biolegend 155829	0.2ug/100ul

\*Amount and volume used for 1 million cells

## 2.7 RNA Extraction

All RNA extractions were performed using the Mammalian GenElute Total RNA Miniprep Kit (Sigma-Aldrich, RTN350), according to the manufacturer's protocol. All protocols were identical once the sample was added to the RNA lysis buffer (containing 1% 2-mercaptoethanol). Briefly, up to 200 µl RNA lysis buffer containing the sample RNA was added to a filtration column and centrifuged to remove the cellular debris and shear genomic

DNA. An equal volume equivalent of 70 % ethanol was added to each sample and the resulting mixture was centrifuged through a GenElute Binding column. Washes of the columns were performed with the provided solutions, and subsequently the RNA was eluted from the column in 40 µl of the provided elution buffer. Processing of different samples into RNA lysis buffer was performed as below.

### **2.7.1 Cells in Culture**

Except where otherwise stated, RNA was extracted from cells after removal of the supernatant (usually retained for ELISA or other assays). Cell culture plates were centrifuged at 400 x *g*, 10 min and the supernatant removed. 200 µl of RNA lysis buffer was added to each well and RNA extraction performed as previously described.

## **2.8 Reverse Transcription and Gene Expression Assays**

### **2.8.1 Reverse Transcription**

Reverse transcription of extracted RNA to generate cDNA was performed using the QuantiTect reverse transcription kit (Qiagen, 205313), according to the manufacturer's protocol, with the exception that reactions were scaled down from a total volume of 20 µl to a total volume of 12 µl.

### **2.8.2 Gene Expression Analysis**

Gene expression levels in individual cDNA samples were quantified using a RotorGene SYBR green PCR kit and Quantitect primer assays (Qiagen) (see Table 3.3 for list of primers). Reactions were set up using a QIAgility automated pipetting robot (Qiagen) according to the manufacturer's recommendations except that reactions were scaled down to 15 µl. The PCR was performed in a RotorGene6000 with the following parameters: DNA polymerase activation (5 min, 95°C); 40 cycles of denaturation (5 s, 95°C), annealing and extension (10 s, 60°C); followed by a melt curve, ramping from 60°C (1 s) to 95°C (5 s), to check the specificity of the PCR product. Fluorescence data were collected at the end of each extension phase.

Data were analysed using the RotorGene6000 series software v1.7, and the threshold cycle (Ct) values were assigned from a set threshold value. For each cDNA sample, PCRs for two

reference genes (*Rpl38*, *Eef2*) were performed, and the mean Ct value of these genes was used to define the “Reference Ct” for that sample. Fold expression levels of genes of interest (GOI) were expressed as  $2^{-\Delta\Delta Ct}$  (201). This was calculated by subtracting the mean Ct value of the house keeping genes from the test samples and negative control ( $\Delta Ct$ ) and then further subtracting the mean  $\Delta Ct$  of the negative control from the test sample.

Fold gene expression =  $2^{-\Delta\Delta Ct} = 2^{-(\text{test sample [Ct GOI - Ct ref]} - (\text{negative control [Ct GOI - Ct ref]})}$

## 2.9 Statistical Analysis

Statistical analysis and generation of graphs was performed using GraphPad Prism 6 (GraphPad Prism Software, CA) or Microsoft Excel (Microsoft, WA).

# Chapter 3

## Infection of *in vitro* Bone Marrow Derived APC with LCMV Virus

### 3.1 Background

Specialised antigen presenting cells (APC) such as dendritic cells (DC) and macrophages, despite their essential role in immune responses are rare in tissues and sometimes difficult to isolate for study into their biology and function (202). In the 1970s, Steinman developed a purification system for DC from splenocytes based on their lack of adherence to plastic (151). Non-adherent cells were called DC, while adherent cells were macrophages. The adherent macrophages were removed by erythrocyte agglutination (EA)-IgG resetting to allow for a pure DC culture. However, the number of cells recovered was small. In the 1990s, another method was developed to produce increased numbers of cells for study, which involved culturing bone marrow (BM) haematopoietic stem cells with growth factors such as granulocyte-monocyte colony stimulating factor (GM-CSF) for several days and harvesting the differentiated cells (152). The BM culture system is based on the principle that haematopoietic stem cells can differentiate into primary cells in an appropriate environment supplemented with the growth factor GM-CSF. GM-CSF is involved in the development and homeostasis of mononuclear phagocytes *in vivo*. The differentiated cells were called bone marrow derived cells and comprised of a heterogeneous mix of granulocytes, dendritic cells and macrophage. DCs are purified from this mix as non-adherent, MHC class II high expressing cells after removal of granulocytes and B-cells. This system provides quick access to a large number of DC for study into their biology and function. Recently, they have also been used in DC-based cancer immunotherapy(153). *In vitro* DC culture has also been developed for studies in veterinary species such as dogs, cats, cow, sheep and chicken (202–205). Despite the enormous spectrum of cells derived from BM *in vitro* culture, there is still little or no information on how they fit into the DC lineage network. In 2015, Helft et al. (2015) (154) showed that CD11c<sup>+</sup> and MHC class II<sup>hi</sup> BM derived cells from the GM-CSF culture system comprise a heterogeneous mixture

of DC- and macrophage-like cells. This is in contrast to previous data showing that CD11c<sup>+</sup> and MHC class II<sup>hi</sup> expressing cells from culture are all bonafide DC. Helft et al. (2015) (154) demonstrated this heterogeneity in terms of the cells' origin, phenotype, morphology, functional and transcriptomic profile. This heterogeneity was shown amongst adherent, loosely adherent and non-adherent BM derived cells. Several other studies have validated the heterogeneity of DC culture systems in the mouse and have extended this to veterinary species specifically dog, sheep, and chicken (202,204,206–208) Therefore, it is imperative to apply caution in interpreting results from BM culture systems.

Lymphocytic choriomeningitis virus (LCMV) is a well-studied virus that has contributed immensely to our knowledge of anti-viral immunity (209). There are two established strains of LCMV: the acute strain, Armstrong (ARM), and the persistent strain, clone 13, and they both infect and replicate in APC. Previous studies have shown that clone 13 preferentially infects CD11c<sup>+</sup>, DEC-205<sup>+</sup> DCs in the marginal zone of the spleen while the ARM strain infects F4/80 expressing cells, mainly in the red pulp (20). Furthermore, in the spleen, LCMV clone 13 preferentially induced and sustained the expression of immunosuppressive receptors including PD-L1 in CD8 $\alpha$ <sup>-</sup> DC but not in CD8 $\alpha$ <sup>+</sup> DC. Most immunological studies using LCMV and BMDC culture systems have not considered differentiated CD11c<sup>+</sup> and MHC class II<sup>hi</sup> expressing cells as a heterogeneous mix. Therefore, in this chapter, I aimed to validate the heterogeneity of CD11c<sup>+</sup> and MHC class II<sup>hi</sup> expressing APC generated from in vitro BM culture systems and show how this heterogeneity affects the cellular response to LCMV infection and dsRNA stimulation. I also described a third group of BM derived cells; the double negative cells which neither expressed CD11c nor MHC class II. All my experiments involving LCMV virus, I used both Armstrong and clone 13 LCVM strains expressing green fluorescent protein for easy tracking of infected cells.

## **3.2 Materials and Methods**

### **3.2.1 Generation of Bone-marrow (BM) Derived Cells**

Bone marrow was extracted from the femurs and tibias of mice (C57BL/6 wild-type) by flushing with Iscove's modified Dulbecco's medium (IMDM) supplemented with 10 % foetal calf serum (FCS), 100 U penicillin/ml, 0.1 mg streptomycin/ml and 50  $\mu$ M 2-mercaptoethanol (10% IMDM) using a syringe and 25G needle into a petri dish. The bone marrow was forced through a 70  $\mu$ m cell strainer and centrifuged for 5 min at 400 x g and 4 ° C. Pelleted cells were

plated in 10 ml petri dishes at a density of  $2 \times 10^6$  cells in 10% IMDM supplemented with various growth factors: GM-CSF (20 ng/ml) alone or GM-CSF (20 ng/ml) with IL-4 (10 ng/ml), M-CSF (20 ng/ml) and FMS-like tyrosine kinase 3 ligand (FLT3-L) (200 ng/ml) (all from PeproTech) and incubated for six or eight days (37°C, 5 % CO<sub>2</sub>) depending on the assay. After incubation, the dish containing the cells was placed on ice for at least 30 min. The cells were then harvested by scraping adherent cells into suspension, then pelleting all cells (5 min, 400 x g 15°C) before resuspension in 10% IMDM at the required cell density for use in various assays such as surface marker staining (8 days incubation) or infection and functional studies (6 days incubation).

### **3.2.2 Flow Cytometry Analysis**

#### **3.2.2.1 Surface Marker Staining of Bone Marrow Derived Cells by Flow Cytometry**

Cells were resuspended in FACS buffer (1 % FCS, 0.05 % sodium azide in PBS) containing 20 µg 2.4G2/ml to block Fc receptors (BD Biosciences) for 10 min at 4-8 ° C. Antibody cocktails prepared in FACS buffer at the concentrations shown (see Table 2.2) were added to the cells and incubated in the dark at 4 ° C, for 30 min. Cells were washed and resuspended with FACS buffer ( $2 \times 10^6$  cells in 200 ul) for sorting. Those for phenotypic assays (surface marker expression) were washed in PBS and the pelleted cells fixed with 4 % paraformaldehyde in PBS at 4 ° C, for 30 min. After fixing, the cells were washed in PBS and resuspended in an appropriate volume of FACS buffer for detection of cell surface markers by flow cytometry

#### **3.2.2.2 Detection of Cell Surface Markers by Flow Cytometry**

Antibody stained and unstained cells in FACS buffer were acquired using an Accuri C6 flow cytometer (BD Biosciences, CA) and expression of cell surface markers was analysed using the Accuri C6 software. Relevant isotype control antibodies were used to exclude non-specific binding and these did not display increased fluorescence compared with the unstained controls. Spectral overlap between fluorescence channels was compensated electronically using isotype negative and single positive stained cells to set compensation values. After exclusion of debris and doublets, single cells were characterised based on the expression of CD11c, MHC class II and CD11b into three populations. The expression of various surface markers was analysed for each population of cells (Table 3.1).

**5: Table 3.1 Experimental Procedure for Bone Marrow Derived Cell Phenotyping (Plate Map)**

Channel	(M1)	(M2)	M3	M4	M5	M6	M7
FL1 - FITC	Ham IgG FITC	CD11c - FITC (Ham IgG)	CD11c - FITC				
FL2 PE	IgG2b PE	IE/IA-PE (IgG2b)	IE/IA-PE (IgG2b)	IE/IA-PE (IgG2b)	IE/IA-PE (IgG2b)	IE/IA-PE (IgG2b)	IE/IA-PE (IgG2b)
FL3 PE-Cy5.5	IgG2b PE-Cy5.5	ITC IgG2b PE-Cy5.5	CD11b-PE-Cy5.5 (IgG2b)				
FL4 APC/Alexa647	IgG2b Ax647	ITC APC (IgG2a)	ITC Ax647 (IgG2a)	DEC205 Ax647 (IgG2a)	CD273 APC (IgG2a)	CD135-APC (IgG2a)	CD197-APC (IgG2a)
M8	M9	M10	M11	M12	M13	M14	M15
CD11c - FITC	CD11c - FITC	CD11c - FITC	CD11c - FITC	CD11c - FITC	CD11c - FITC	CD11c - FITC	CD11c - FITC

IE/IA-PE (IgG2b)	IE/IA-PE (igG2b)	IE/IA-PE (igG2b)	IE/IA-PE (igG2b)	IE/IA-PE (igG2b)	IE/IA-PE (igG2b)	IE/IA-PE (igG2b)	IE/IA-PE (igG2b)
CD11b- PE- Cy5.5 (IgG2b)	CD11b- PE- Cy5.5 (IgG2b)	CD11b- PE-Cy5.5 (IgG2b)	CD11b- PE-Cy5.5	CD11b- PE-Cy5.5 (IgG2b)	CD11b-PE- Cy5.5 (IgG2b)	CD11b-PE- Cy5.5 (IgG2b)	CD11b-PE- Cy5.5 (IgG2b)
F4/80 APC (IgG2a)	CD14- APC (igG2a)	CD64- APC (igG1k)	CD115- APC (igG2a)	CD80 Ax647 (IgG2a)	CD86- Ax647 (IgG2a)	CD40- Ax647 (IgG2a)	CD24- Ax647 (IgG2b)

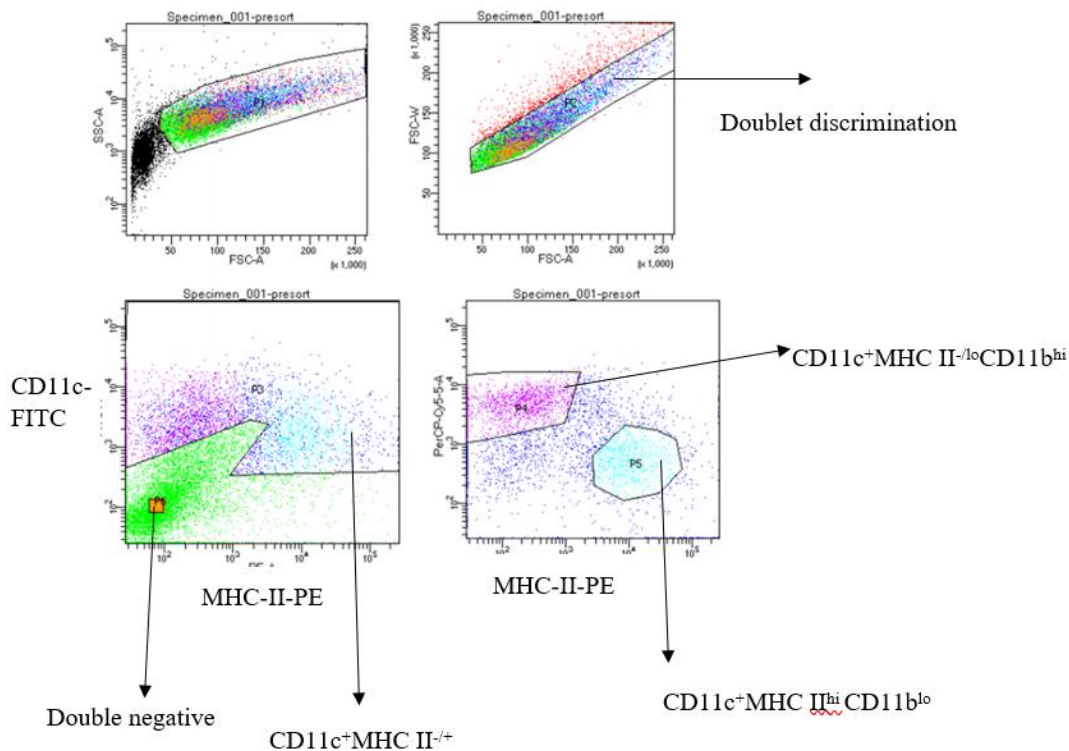
### 3.2.2.3 Sorting of BM Derived Cells by Flow Cytometry

Cells were sorted using an Aria III flow cytometer (BD Biosciences, CA) into three subsets of bone marrow derived cells based on expression of CD11c (FITC), MHC class II (PE) and CD11b (PerCP-Cy5.5) as was done by Helft et al. (2015) (154). The sorted cells were collected into 5 ml polypropylene tubes (Falcon 352063) containing 1 ml of 10% IMDM at 4°C to reduce adherence to the plastic (see Table 3.2 and Figure 3.1 for flow cytometer set up and staining plate map). The cells were counted, and an appropriate number used for LCMV infection or poly (I:C) stimulation.

**6: Table 3.2 Bone Marrow Derived Cell Sorting Procedure**

Channel	M1	M2
	Isotype control	Fully stained cells
FITC	Ham IgG-FITC	Anti-CD11c-FITC (Ham IgG)
PE	Rat IgG2b-PE	I-A/I-E-PE (rat IgG2b)

PerCP-Cy5.5	Rat IgG2b- PerCP-Cy5.5	CD11b-PerCP-Cy5.5 (rat IgG2b)
-------------	---------------------------	----------------------------------



### 7: Figure 3.1 Bone Marrow Derived Cell Sorting Procedure

The three subsets of BM derived cells generated with different growth factors were sorted using Aria III flow cytometer (BD Biosciences, CA). Cells were selected by the size (FSC-A) and molecular granularity (SSC-A). After removal of debris, and doublet cells, CD11C and MHC-II expressing cells were selected and sorted into CD11c<sup>+</sup>MHC II<sup>hi</sup> CD11b<sup>lo</sup>, and CD11c<sup>+</sup>MHC II<sup>-/lo</sup>CD11b<sup>hi</sup>. Non CD11c and MHC-II expressing cells were selected as double negative cells.

### 3.2.3 BM derived cell morphology by light microscope

Sorted CD11c<sup>+</sup> MHC class II<sup>+</sup> BM derived populations were observed under the light microscope (x20) objective lens. Each group was classified based on their morphology.

### **3.2.4 LCMV infection of BM derived cells**

Sorted CD11c<sup>+</sup> MHC class II<sup>+</sup> BM derived cells were seeded into individual wells of 24-well plates, at a density of  $1 \times 10^5$  cells per well in 200  $\mu$ l of 10% IMDM. Cells were allowed to settle overnight in an incubator at 37°C, 5 % CO<sub>2</sub>. The next day, the medium was carefully removed and replaced with the virus inoculum diluted to the stated MOI (usually 10 FFU/cell) in 2% IMDM or replaced with 2% IMDM alone (mock infection). Both mock and infected cells were incubated for 1 h, 37°C, 5 % CO<sub>2</sub>, with gentle agitation every 15 min. After this 1 h infection period, the inoculum was carefully removed, and cells were washed with PBS and medium replaced with fresh 10% IMDM. The plate was returned to the incubator until the corresponding time points for the required assay such as flow cytometry, RT-qPCR, ELISA assay, and single-cell RNA sequencing.

### **3.2.5 Quantification of LCMV-GFP infectious units in Vero cell**

Vero cells were seeded overnight in 24-well plates, at a density of  $1 \times 10^5$  cells per well in 200  $\mu$ l of 10%IMDM. The cells were infected with 100  $\mu$ l of the supernatant from infected and uninfected cultures of the three groups of BM derived cells and incubated at 37 ° C, 5 % CO<sub>2</sub> for 48 h. The cells were harvested with trypsin and fixed with 4% formaldehyde. GFP expression was measured by flow cytometry and used to demonstrate that the BM derived cells support productive LCMV infection.

### **3.2.6 Treatment of BM derived cells with poly (I:C)**

Sorted CD11c<sup>+</sup>, MHC class II<sup>+</sup> bone marrow derived cells were seeded into plates as described in Section 3.2.4. After overnight incubation, the medium was removed from the wells and replaced with 10%IMDM supplemented with 100  $\mu$ g poly (I:C)/ml (Sigma Aldrich, P1530). Cells corresponding to the baseline time point were processed at this stage, by removal of the supernatant for ELISA analysis (Section 3.2.8), and lysis of the cells for RNA extraction (Section 3.2.7), reverse transcription and gene expression analysis (Section 2.0.6). Otherwise, cells were returned to the incubator (37 ° C, 5 % CO<sub>2</sub>) until the required time points (0, 3, 6, 9, 12 and 24 h P.I.) for similar processing.

### **3.2.7 Gene expression analysis**

Gene expression levels in individual cDNA samples were quantified using a RotorGene SYBR green PCR kit and Quantitect primer assays (Qiagen) (Table 3.3). Reactions were set up using a QIAgility automated pipetting robot (Qiagen) according to the manufacturer's recommendations except that reactions were scaled down to 15  $\mu$ l. The PCR was performed in a RotorGene6000 with the following parameters: DNA polymerase activation (5 min, 95°C); 40 cycles of denaturation (5 s, 95°C), annealing and extension (10 s, 60°C); followed by a melt curve, ramping from 60°C (1 s) to 95°C (5 s), to check the specificity of the PCR product. Fluorescence data were collected at the end of each extension phase.

Data were analysed using the RotorGene6000 series software v1.7, and the threshold cycle (Ct) values were assigned from a set threshold value. For each cDNA sample, PCRs for two reference genes (*Rpl38*, *Eef2*) were performed, and the mean Ct value of these genes was used to define the "Reference Ct" for that sample. Fold expression levels of genes of interest (GOI) were expressed as  $2^{-\Delta\Delta Ct}$  (201). This was calculated by subtracting the mean Ct value of the house keeping genes from the test samples and negative control ( $\Delta Ct$ ) and then further subtracting the mean  $\Delta Ct$  of the negative control from the test sample.

$$\text{Fold gene expression} = 2^{-\Delta\Delta Ct} = 2^{-\text{(test sample [Ct GOI - Ct ref])} - \text{(negative control [Ct GOI - Ct ref])}}$$

**7: Table 3.3 Quantitect Primer Assays (Qiagen) used for Gene Expression Analysis**

<b>Gene symbol</b>	<b>Catalogue number</b>
<i>Rpl38</i>	QT00145726
<i>Eef2</i>	QT00167293
<i>Ifnb1</i>	QT00249662
<i>Tnfr1</i>	QT00104006
<i>Mxl1</i>	QT01064231
<i>Isg15</i>	QT00322749
<i>Zbtb46</i>	QT00168056
<i>Mertk</i>	QT00148561

### **3.2.8 IFN- $\beta$ Enzyme-Linked Immunosorbent Assay (ELISA)**

The concentration of IFN- $\beta$  in supernatants collected from individual wells of the poly (I:C) treated cell cultures (See subsection 3.2.6) was quantified by ELISA. The mouse IFN- $\beta$  ELISA Kit (Biolegend, 439407) was used according to the manufacturer's protocol.

### **3.2.9 Single cell RNA sequencing of LCMV infected bone marrow derived cells**

Sorted CD11c<sup>+</sup>, MHC class II<sup>+</sup> bone marrow derived cell populations (dendritic cells [BM-DC], macrophages [BM-M], double negative cells [DN]) were infected with LCMV clone 13 (GFP) as previously described for 12 h and 48 h and single cells (from the 12 h culture) were sorted into customised BD WTA single cell encoding plates for RNA extraction and reverse transcription (primary infection) according to manufacturer's instructions (PN 910000014 Rev. 03). Furthermore, a set of infected cells (from the 48 h culture) were stimulated with 100  $\mu$ g poly (I:C)/ml (as in section 3.2.5) and incubated for another 6 h before single cell sorting as above. Libraries of the cellular RNA were made using the BD WTA single cell kit and sequenced using MiSeq V2 from Illumina (BM-DC, BM-M, DN). Sequence data were analysed using the Seven Bridges Genomics bioinformatics platform (BD: Precise Whole Transcriptome Assay Analysis Pipeline v2.0). A cell was considered to be infected if there was at least one GFP sequence read count. This information was then used to define the groups to compare in EdgeR. Differential gene expression was measured between infected and uninfected cells in each subset (Adjusted p-value less than 0.05).

### **3.2.9 Antigen presentation assays**

#### **3.2.9.1 BM derived cell co-culture with T cell hybridoma 5A1 cells**

BM derived cell populations (BM-DC, BM-M, DN) generated by the method detailed in Subsubsection 3.2.1 were infected with LCMV-GFP as previously described in subsection 3.2.4. Infected (GFP positive) and uninfected cells were co-cultured with the T cell hybridoma 5A1 at a ratio of 1:1 in 96-well tissue culture plates (flat-bottomed) containing 200  $\mu$ l of 10%IMDM for 24 hours (196). The cells were harvested and stained with anti-CD25-PE

conjugated antibody for 30 min. CD25 expression (activation) was measured by flow cytometry using an Accuri C6 flow cytometer (BD Biosciences, CA).

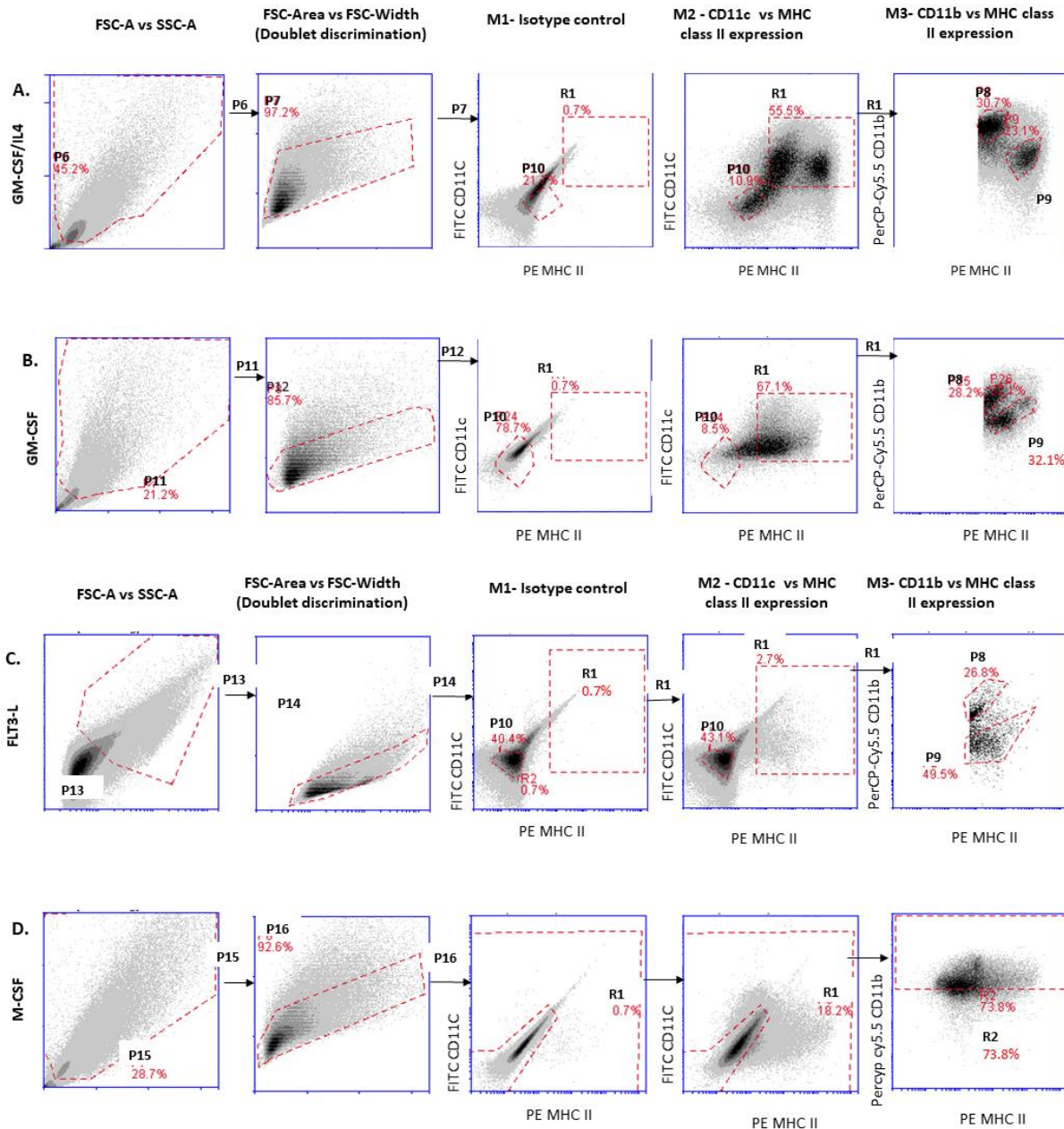
### **3.2.9.2 BM derived cell activation phenotype**

Infected and uninfected BM derived populations (BM-DC, BM-M, DN) were harvested and stained with antibodies to measure the expression of co-stimulatory receptors (CD80, CD86, CD40) using the Accuri C6 flow cytometer (BD Biosciences, CA). The infection, staining, data acquisition and analysis of BM derived cell subsets for the expression of co-stimulatory receptors were as described in subsection 3.2.1.2 for the bone marrow derived cell phenotyping.

## **3.3 Results**

### **3.3.1 Description of *In vitro* Bone Marrow Derived Cell Heterogeneity**

Published work has shown that CD11c<sup>+</sup> MHC class II<sup>hi</sup> bone marrow derived cells generated with GM-CSF *in vitro* are a heterogeneous mixture of dendritic cells and macrophages based on their ontogeny, phenotype, transcriptional and functional profile (154). However, we do not know whether this heterogeneity exists in cells derived using other growth factors such as FLT3-L and GM-CSF with IL-4. To validate this heterogeneity across other BM derived culture systems, I cultured haematopoietic progenitor cells from the BM of C57BL/6 mice for eight days with different growth factors and then stained for surface marker expression. Based on CD11c, MHC class II and CD11b expression, three subsets of cells were identified: CD11c<sup>+</sup> MHC class II<sup>lo</sup> or <sup>hi</sup> CD11b<sup>lo</sup> (thought to be BM-DC); CD11c<sup>+</sup> MHC class II<sup>lo</sup> CD11b<sup>hi</sup> (thought to be BM-M); and CD11c<sup>-</sup> MHC class II<sup>-</sup> (double negative, DN) (see figure 3.2). These three subsets were seen after culture with all the growth factors used (GM-CSF, GM-CSF/IL-4, and FLT3-L) except M-CSF. Cells differentiated in the presence of M-CSF were a homogeneous culture of CD11b<sup>hi</sup> macrophage-like cells (BM-M).



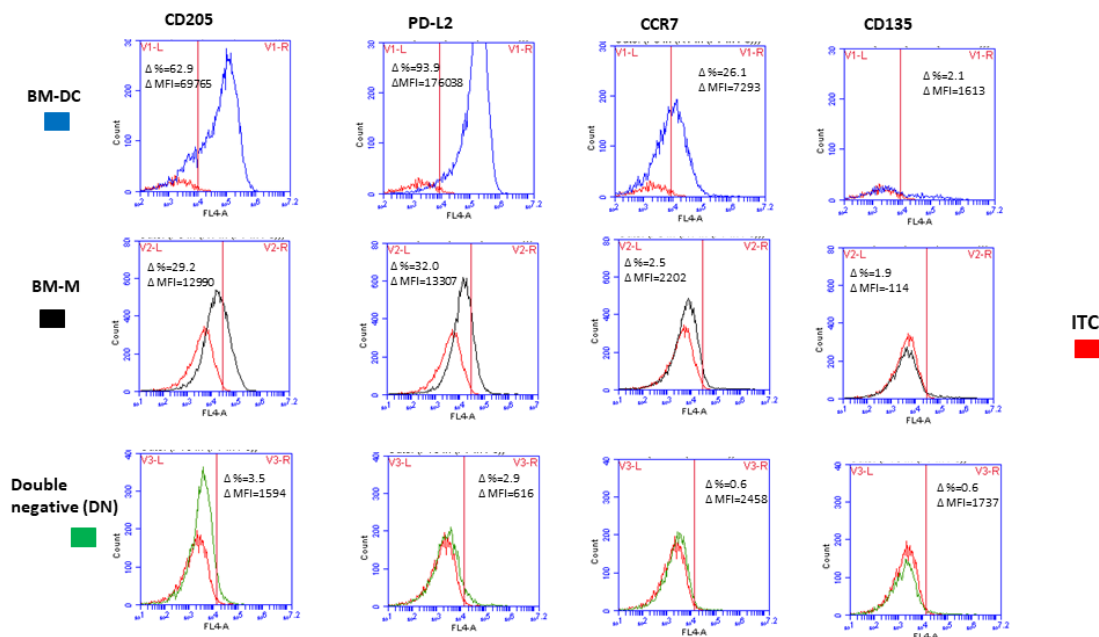
**8: Figure 3.2 CD11b+ Expression on CD11c+MHC class II+ Bone Marrow Derived Cells Differentiated with Various Growth Factors**

Identification of bone marrow derived cells differentiated with various growth factors (A. GM-CSF/IL-4; B. GM-CSF; C. FLT3-L; D. M-CSF) using CD11c, MHC class II and CD11b expression by flow cytometry.

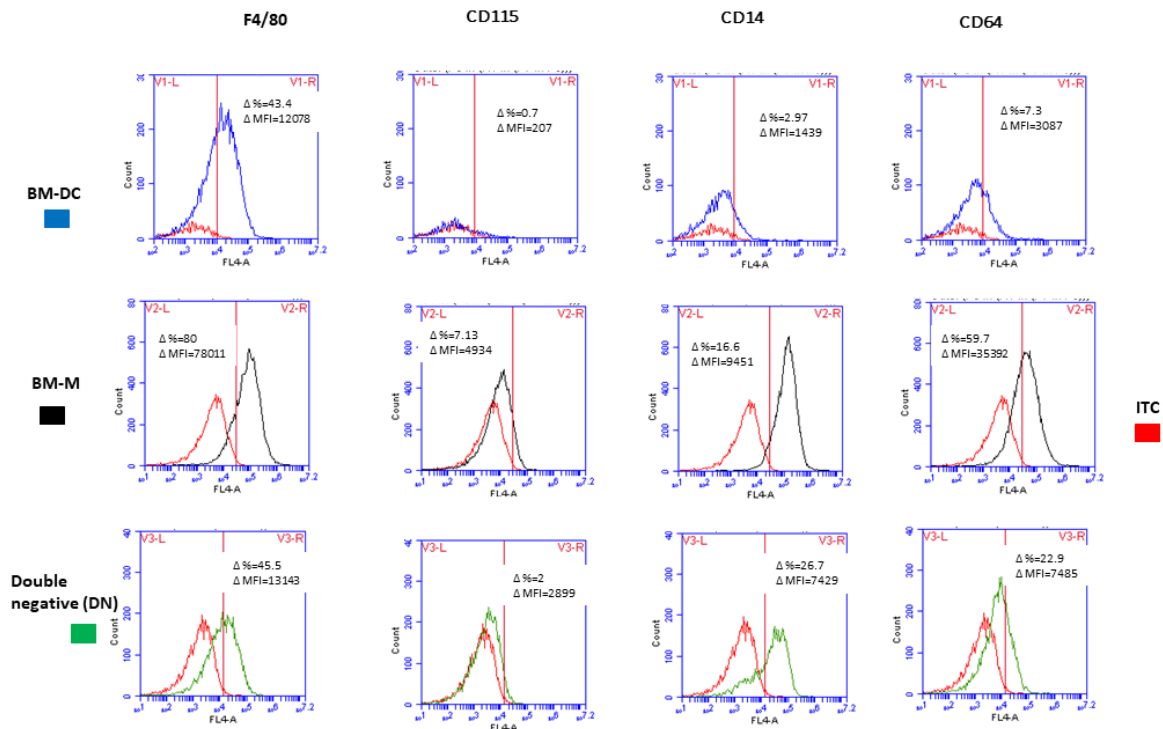
After removal of debris, and doublet cells, single cells were first characterised by their expression of CD11c and MHC class II (R1). These cells were then sorted into three populations of bone marrow derived cells (BM-DC (P9), BM-M (P8), DN (P10)) based on the expression of CD11c, MHC class II and CD11b.

Red dotted boxes depict gates and numbers correspond to percentage of cells in each gate.

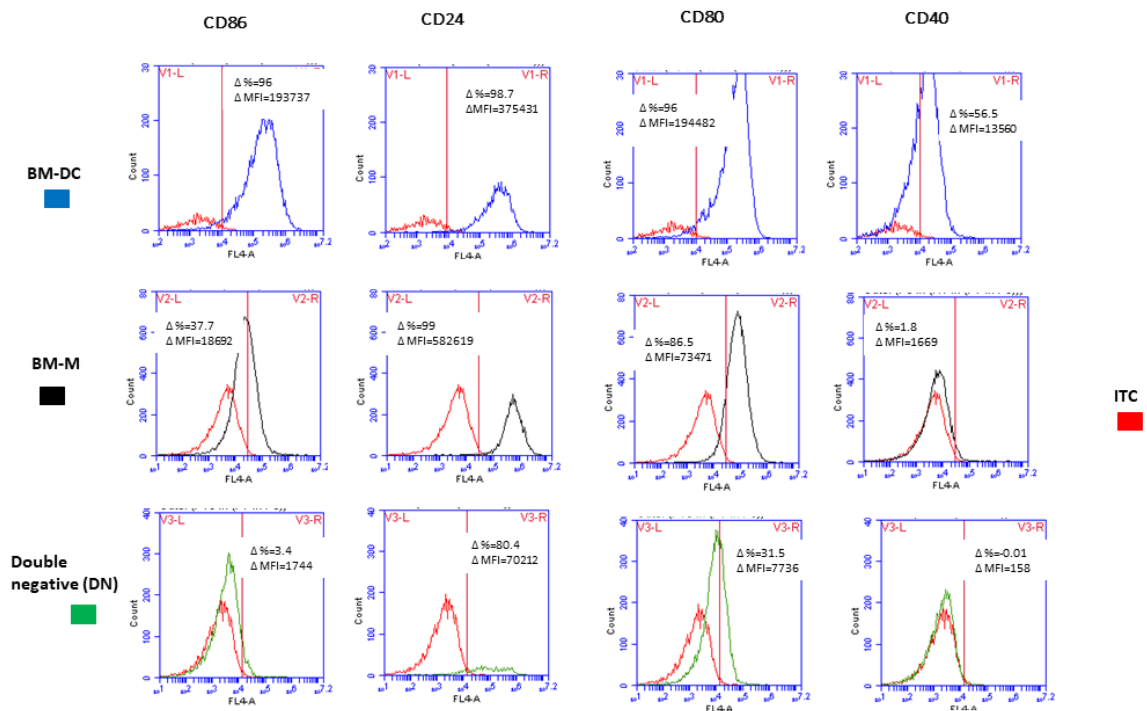
Next, I investigated the surface marker expression differences between the three subsets of BM derived cells. I grouped the various surface markers assayed: dendritic cell associated, macrophage associated and co-stimulatory receptors, and compared the expression between the three cell subsets (see figure 3.3 A-C). The BM-DC showed higher expression levels of DC markers and co-stimulatory receptors (CD205/DEC-205, PD-L2, CCR7, CD86 and CD40) compared to BM-M. The BM-M subset expressed more of the macrophage associated markers (F4/80, CD14, CD64, and CD115) compared to BM-DC. Overall the double negative group looked more similar to the BM-M than the BM-DC subset. They did not express the DC associated markers but rather expressed some of the macrophage associated markers like CD14, CD64. They also had the least expression of co-stimulatory receptors like CD86 and CD80. CD135 and CD115 were not detected on any of the subsets even after testing with a different batch of antibody.



9: Figure 3.3A Dendritic Cell Associated Receptor



10: Figure 3.3B Macrophage Associated Receptors

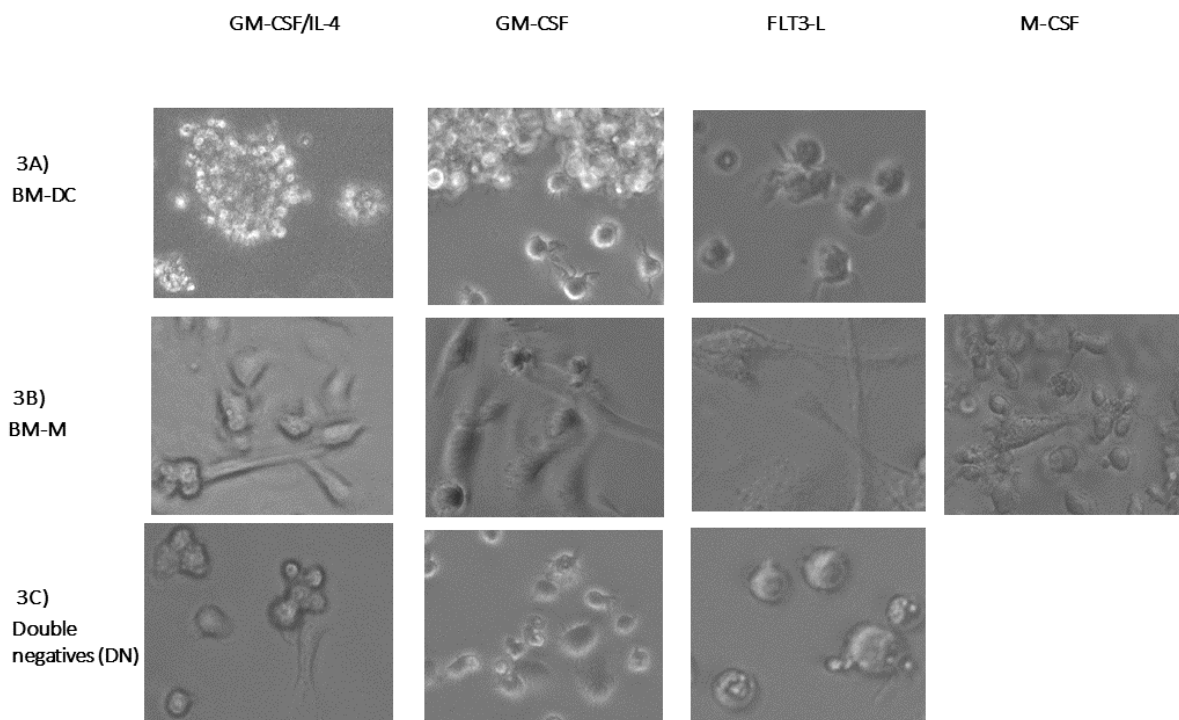


11: Figure 3.3C Costimulatory Receptors

Figure 3.3. Surface Marker Expression on the Three Groups of Bone Marrow Derived Cells Differentiated with GM-CSF/IL-4

Histograms show the surface expression of the indicated markers by BM-DC (blue), BM-M (black) and DN (green) cells. Red histograms represent isotype-matched irrelevant specificity controls. Histograms were taken from cells differentiated with GM-CSF/IL-4, although similar trends were seen across all the other growth factors except M-CSF that yielded only BM-M cells. **A.** Dendritic cell associated receptors; **B.** Macrophage associated receptors; **C.** Co-stimulatory receptors. The data are representative of 4 replicate experiments.

Furthermore, I examined the morphology of the three subsets by phase contrast microscopy. Similar to DC and macrophages as seen by Helft et al. (2015)(154), BM-DC were round with dendrites, loosely adherent to plastic, but cell to cell adherent to form balls of cells. BM-M were stellate, more plastic adherent, and contained numerous granules (see figure 3.4). DN cells appeared to be a mix of cells with features of both BM-DC and BM-M but fewer surface dendrites. The homogenous cells from the M-CSF culture looked similar to the BM-M group.



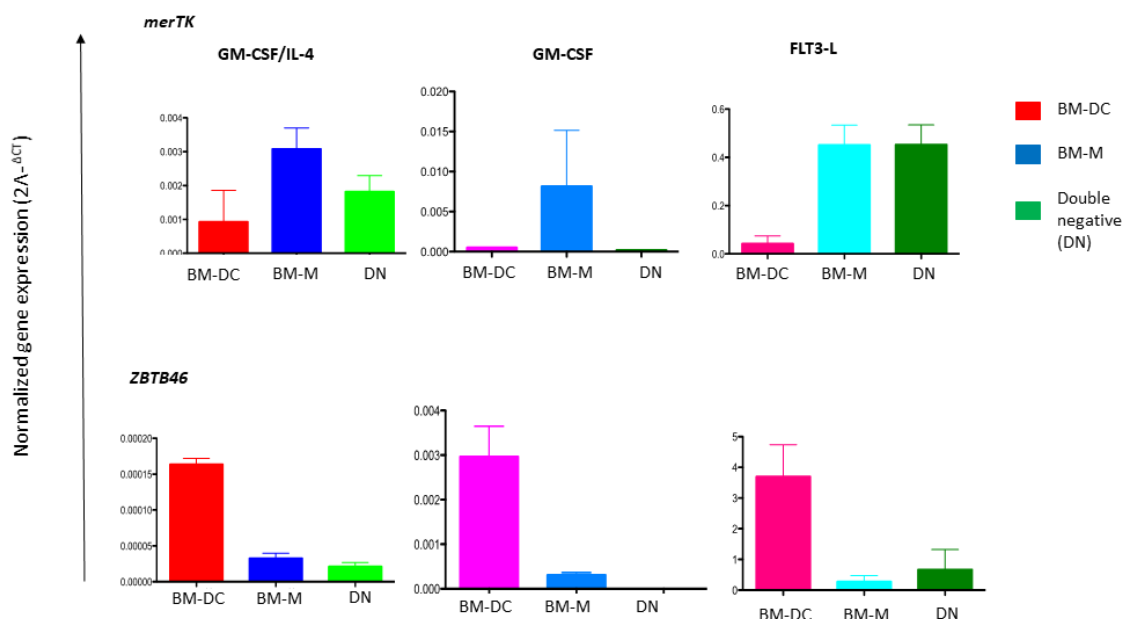
**12: Figure 3.4. Morphology of the Three Groups of Bone Marrow Derived Cells Differentiated with Different Growth Factors**

Bone marrow derived cells were sorted into three subsets after 8 days of culture supplemented with different growth factors. Each subset of bone marrow derived cells was

analysed by phase contrast light microscopy (A. BM-DC, B. BM-M and C. DN). The images were taken after 8 days of culture at 20x magnification.

Note that differentiation in M-CSF yielded a homogeneous cell type with a similar shape as the BM-M group

At the mRNA level, BM-DC had higher levels of expression of DC associated transcription factor, *ZBTB46* (Figure 3.5). BM-M, on the other hand, expressed macrophage transcription factor *merTK* (Figure 3.5). Thus, my finding validated the heterogeneity of CD11c<sup>+</sup> and MHC II<sup>+</sup> expressing cells from BM derived cell culture systems. I identified similar cells to those described previously by Helft et al. (2015) (154) and then showed that this heterogeneity is seen across commonly used growth factors for derivation of BM-DC except M-CSF.



**13:Figure 3.5 Transcription Factor Expression of Three Groups of CD11c<sup>+</sup> MHC class II<sup>+</sup> and/or CD11b<sup>+</sup> Bone Marrow Derived Cells Differentiated with Various Growth Factors**

Quantitative RT-PCR for *MerTK* and *ZBTB46* transcripts in cDNA from sorted BM-DC (red), BM-M (blue) and DN (green) subsets. Data represent mean ± SD of triplicate wells from three representative experiments.

Note: cells from M-CSF culture not shown

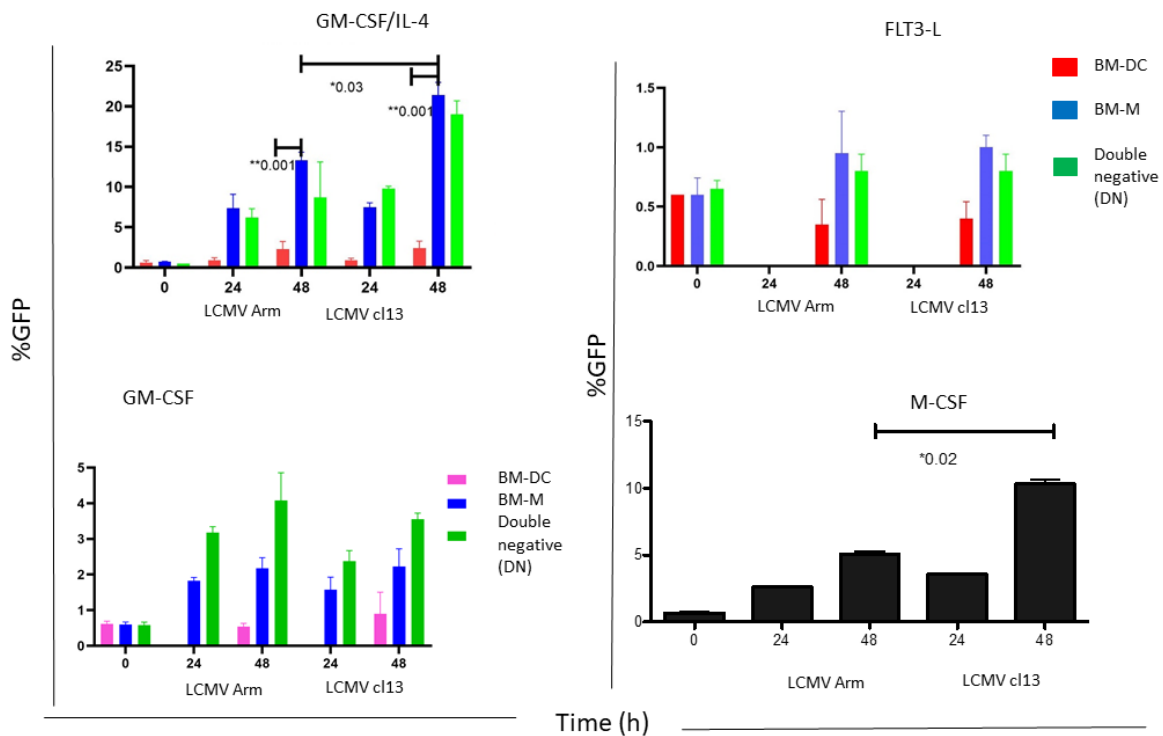
### **3.3.2 Susceptibility of BM derived cells to LCMV infection**

Here, I used both strains of LCMV expressing GFP proteins to measure the susceptibility to virus infection of the three populations of BM derived cells. I also checked the ability of the three groups of BM derived cells to support growth of the virus.

I harvested cells from BM culture and sorted them into the three populations (BM-DC, BM-M and DN) as described previously (see subsection 3.2.1). The cells in each population were infected with GFP expressing LCMV ARM or clone 13 for 24 and 48 h. I determined the proportion of cells expressing GFP from harvested and fixed cells by flow cytometry. To measure if the infection of the BM derived cells was productive, I collected supernatants from the infected cultures and used them to infect Vero cells for 48 h. I then determined the frequency of GFP positive Vero cells by flow cytometry.

My results showed that there was a difference in the susceptibility to both strains of LCMV in the BM derived sub-populations in cells derived with all the three growth factor conditions (GM-CSF, GM-CSF/IL-4, and FLT3-L). All three populations of BM derived cells were infected by both strains of the virus as seen by GFP expression. Although the proportion of cells infected was low in all three sub-populations, the highest frequency of infected cells was seen in the BM-M populations, both with LCMV ARM and clone 13 infections, followed by the DN group and the lowest proportion of positive cells was seen in the BM-DC populations. The exception to this was seen in the GM-CSF differentiated culture where the DN group had slightly higher number of GFP positive cells than the BM-M group.

BM-M and DN subsets showed greater than 10% GFP positive (LCMV infected) cells (both strains) while BM-DC showed less than 5% GFP positive cells in the cells differentiated with GM-CSF/IL4 and the difference was statistically significant. Also, LCMV clone 13 was more infectious than Armstrong both in BM-M and DN groups as well as the M-CSF differentiated group and the difference was also statistically significant (Figure 3.6).



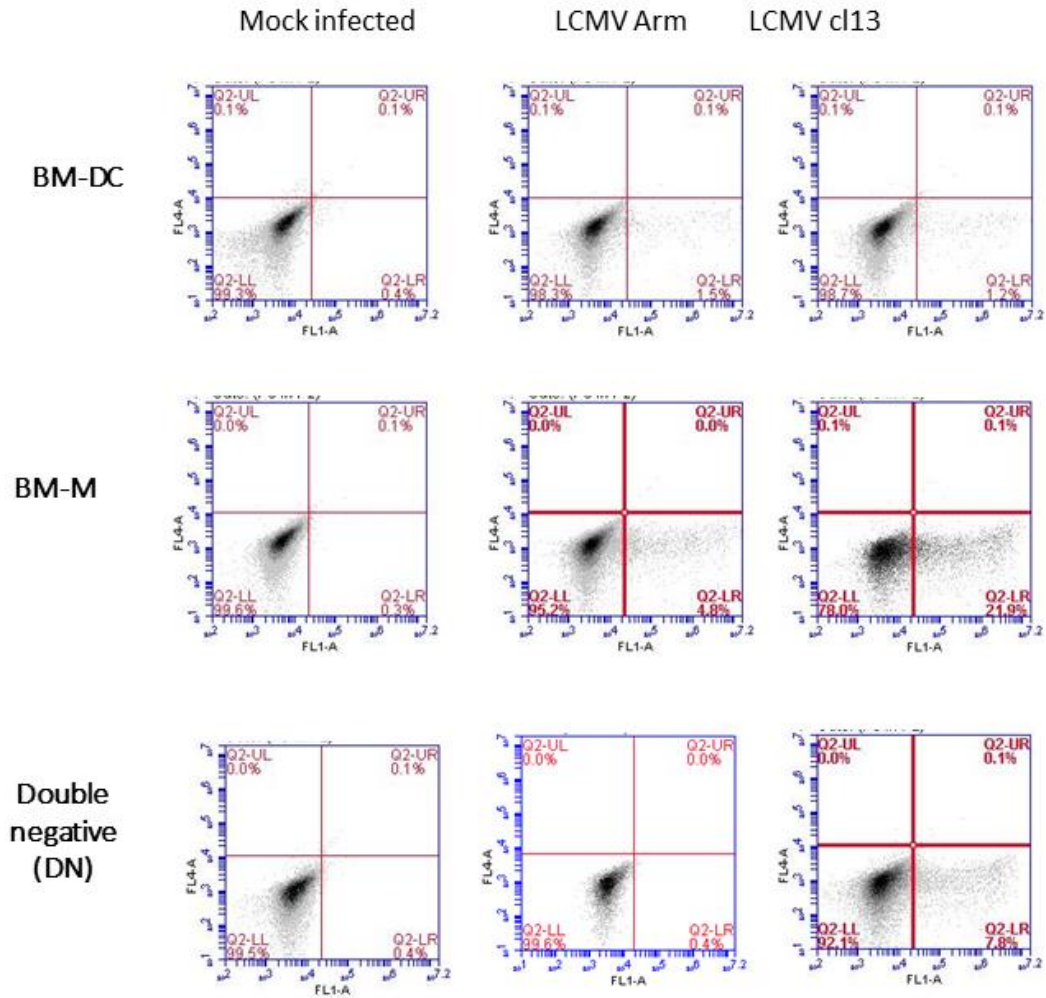
#### 14: Figure 3.6 LCMV (Armstrong and clone 13) Infection of BM Derived Cells

The three BM derived cell groups differentiated with various growth factors were infected with LCMV Armstrong and clone 13 expressing GFP (MOI 10) for 48 h. Cellular GFP expression was analysed by flow cytometry.

Statistical significance was calculated by Mann-Whitney test and p values are indicated. (capped line with \* indicate significance).

Note: zero (0) time is the negative control (uninfected group).

Furthermore, the supernatant from GM-CSF/IL-4 differentiated BM derived sub-populations successfully infected Vero cells. The GFP expression from Vero cells correlated to that from infection of the three groups of BM derived cells with both strains of LCMV (Figure 3.7). My results show that both strains of LCMV infected the three sub-populations of BM derived cells, and that this infection was productive.



15: Figure 3.7 Productive Infection of BM Derived Cells by LCMV (ARM and clone 13)

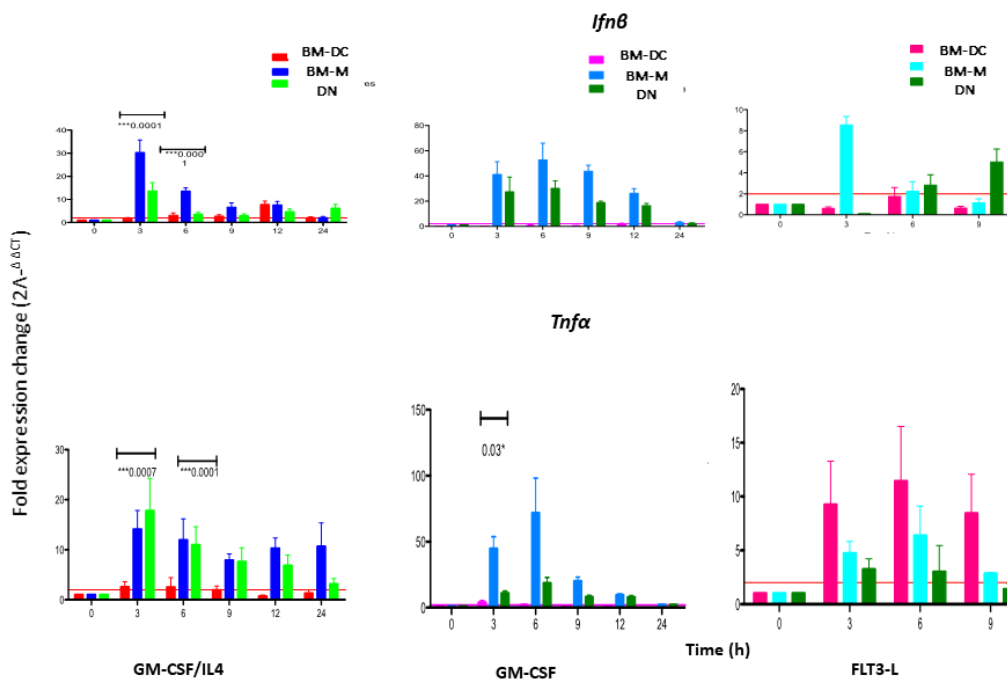
Supernatant from infected (48 h post infection) BM derived cell subsets (using GM-CSF/IL-4) was used to infect Vero cells for 48 h. GFP expression (FL1 – x-axis) in fixed Vero cells was measured by flow cytometry.

### 3.3.3 LCMV impairs cytokine production and antigen presentation in *in vitro* BM derived cells

Both strains of LCMV virus expressing GFP as well as synthetic dsRNA virus mimic Poly (I:C) were used to investigate the variation in cytokine response and antigen presentation capability of the three subsets of BM derived cells. Previous reports have shown that LCMV impairs maturation and cytokine production in APCs (143). This, in turn, results in failure of antigen presentation and activation of immunosuppressive T cells. Poly (I:C) on the other hand,

is a dsRNA mimic that can induce a potent type I IFN response which could help to overcome this defect.

I infected the three groups of BM derived cells with both strains of LCMV-GFP and/or stimulated them with poly (I:C). At different time points, I harvested RNA and performed RT-qPCR for gene expression analysis. My results showed that the three groups produced variable amounts of antiviral cytokines following stimulation with poly (I:C) (Figure 3.8, 3.9, 3.10). Both *Ifnb* and interferon inducible genes (*Mx1* and *Isg15*) were mostly produced in the BM-M group and to a lesser extent in the DN group. The BM-DC group had the least response (figure 3.8, 3.9). A similar response was also seen for *Tnfa* (Figure 3.8). These differences in cytokine response were seen across the three growth factors used for differentiating BM derived cells. Peak cytokine production (*Ifnb*, *Mx1* and *Isg15* and *Tnfa*) was seen between 3-6 hours post induction across the three growth factors and the differences between the BM-M, DN and BM-DC group for most of the cytokines at the peak production were significant.

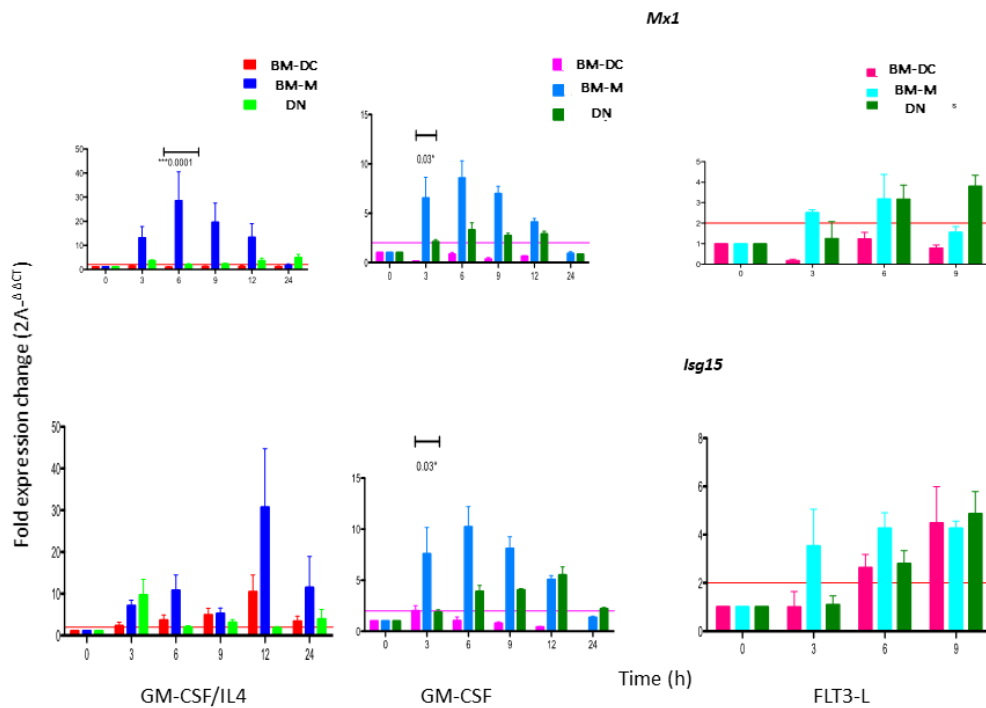


**16: Figure 3.8. *Ifnb1* and *Tnfa* mRNA Expression in BM Derived Cells after Poly (I:C) Stimulation**

The three subsets of BM derived cells generated with different growth factors were treated with 100  $\mu$ g poly(I:C)/ml and at specific time points RNA was extracted from each well, reverse transcribed and analysed for the expression of genes *Ifnb1* and *Tnfa* by RT-qPCR.

Bars represent the induction levels compared to mock treated cells, which are shown as  $2^{(-\Delta\Delta Ct)}$ . All values were normalised to the mean of two housekeeping genes (*Rpl38*, *Eef2*). Red bars indicate limit of positive response.

Statistical significance was calculated by Mann-Whitney test (\*;  $P < 0.05$ ).

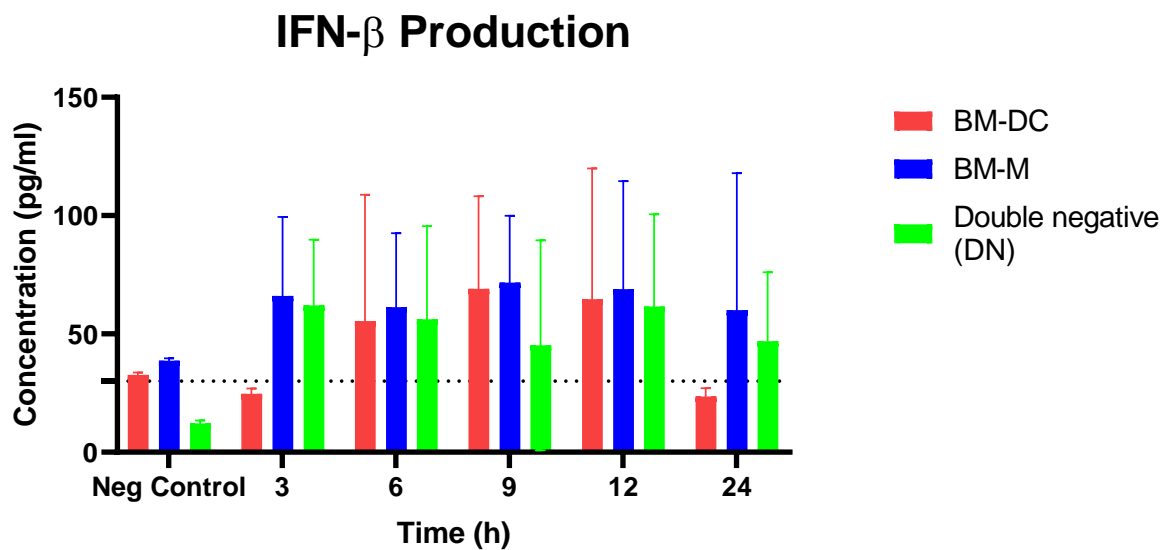


**17: Figure 3.9** *Mx1* and *Isg15* mRNA Expression in BM Derived Cells after Poly (I:C) Stimulation

The three subsets of BM derived cells generated with different growth factors were treated with 100  $\mu\text{g}$  poly (I:C)/ml and at specific time points RNA was extracted from each well, reverse transcribed and analysed for the expression of genes *Mx1* and *Isg15* by RT-qPCR.

Bars represent the induction levels compared to mock treated cells, which are shown as  $2^{(-\Delta\Delta Ct)}$ . All values were normalised to the mean of two housekeeping genes (*Rpl38*, *Eef2*). Red bars indicate limit of positive response.

Statistical significance was calculated by Mann-Whitney test (\*;  $P < 0.05$ ).



**18: Figure 3.10** ELISA for *IFN- $\beta$*  Production after Poly (I:C) Stimulation of BM Derived Cells

The three subsets of BM derived cells generated with different growth factors were treated with 100  $\mu\text{g}$  poly (I:C)/ml and at specific time points supernatant was removed and used in the ELISA.

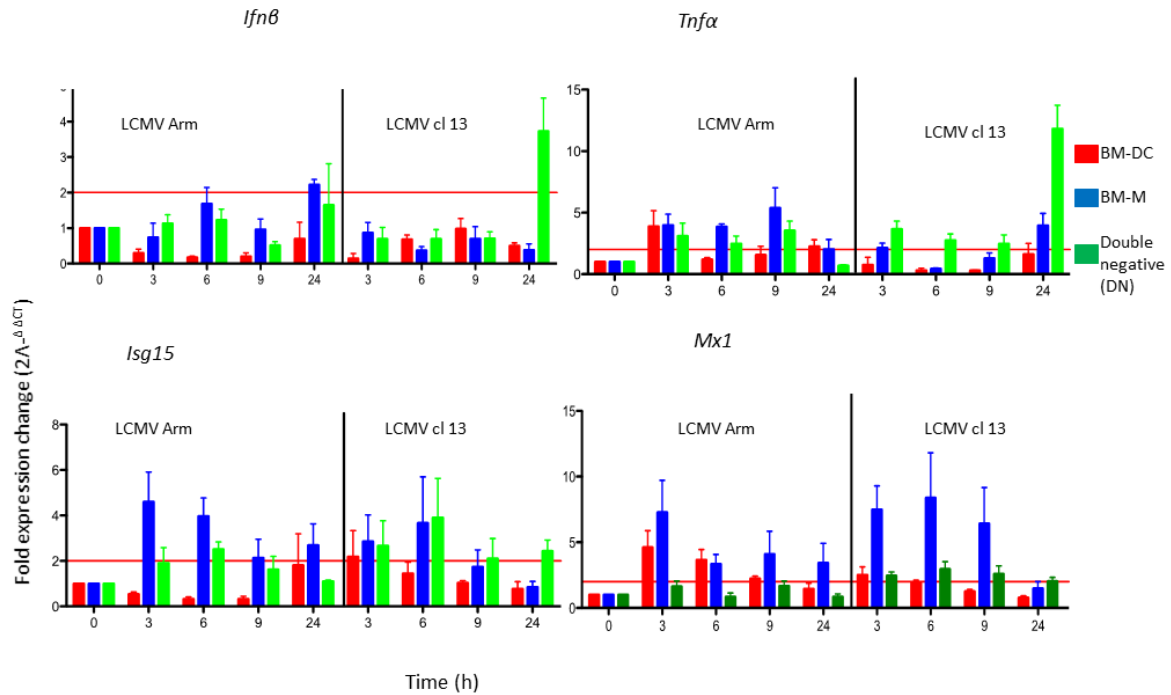
Dotted lines indicate limit of positive response (30 pg/ml)

Bars represent the mean of three technical replicates of a single sample, with error bars showing the range of these replicates.

The data shown were pooled from two independent experiments (n=2)

To validate that the interferon response was functional, I performed an ELISA to measure IFN- $\beta$  protein production from the GM-CSF/IL4 differentiated three groups of BM derived cells following poly (I:C) stimulation. The results correlated with the RT-qPCR data, BM-M had higher expression of IFN- $\beta$  than the BM-DC and DN groups. Peak expression was seen at 9 h post stimulation (see Figure 3.10). Thus, the three BM derived cell groups produced antiviral cytokines and responded to these cytokines when stimulated with a TLR-3 ligand, poly (I:C).

However, when these cells were infected with either strain of LCMV (GFP expressing) and cytokine gene expression was measured by RT-qPCR, there was little or no induction of cytokine or interferon stimulated gene expression from the three subsets of BM derived cells (figure 3.11). This result was seen with all the different growth factors used for generating BM derived cells (data not show). This may be due to low susceptibility of BM derived cells to LCMV infection *in vitro* as shown above. It may also be due to the ability of the LCMV virus to impair cytokine production as has been previously reported (190,210). To rule out that the impaired cytokine production is due to low susceptibility of the BM derived cells to LCMV virus, I did single-cell RNA sequencing to look at the antiviral cytokine RNA expression profile of infected and uninfected cells across the three sub-populations. I infected BM derived cells with LCMV clone 13 (GFP expressing) for 12 hours and sorted infected and uninfected cells singly into customised BD plates for library prep and sequencing. Infected cells were selected by their expression of GFP protein and compared against uninfected cells. The cytokine RNA expression profile from infected cells from the two sub-populations of BM derived cells (BMD-M and DN; BM-DC could not be analysed because there were not enough reads and the library did not pass quality control) correlated with the RT-qPCR results showing limited cytokine expression induction by LCMV infection (figure 3.12A and B). Thus, suggesting that the lack of cytokine induction had nothing to do with the susceptibility of the cells to the virus because the gene profile was measured at the single cell level.



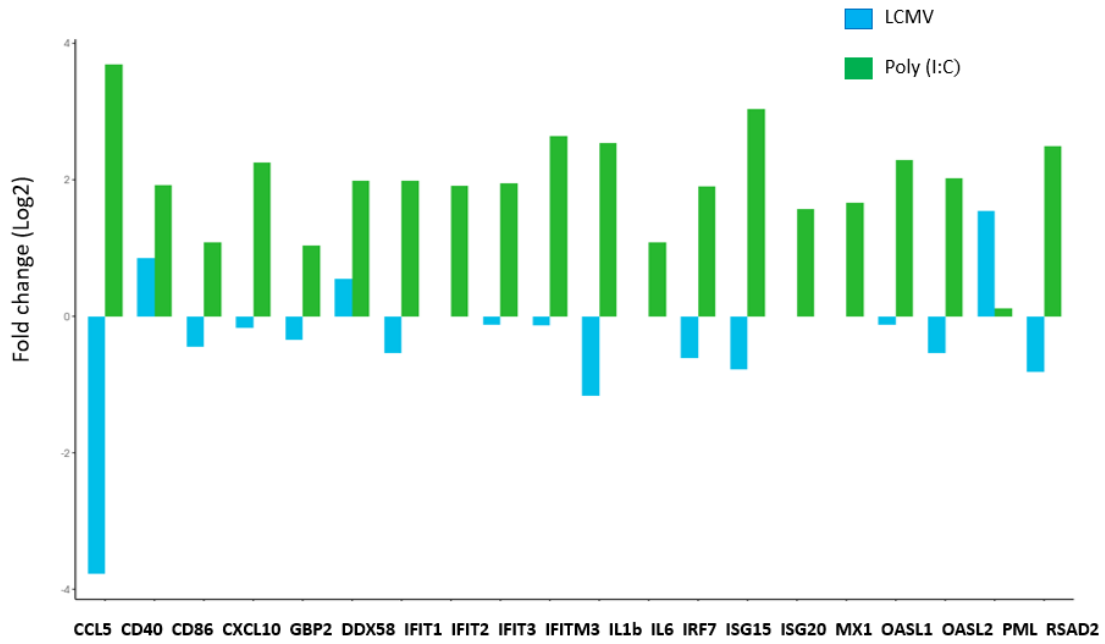
**19: Figure 3.11 RT-qPCR-based Gene Expression Analysis of BM Derived Cells Following LCMV Infection**

The three subsets of BM derived cells generated with GM-CSF/IL-4 were infected with LCMV (MOI 10) and at specific time points RNA was extracted from each well, reverse transcribed and analysed for the expression of the genes *Ifnb1*, *Tnfa*, *Mx1* and *Isg15*.

Data points represent the induction levels, which are shown as  $2^{-(\Delta\Delta Ct)}$ , normalised to the mean of two housekeeping genes (*Rpl38*, *Eef2*).

Red bars indicate limit of positive

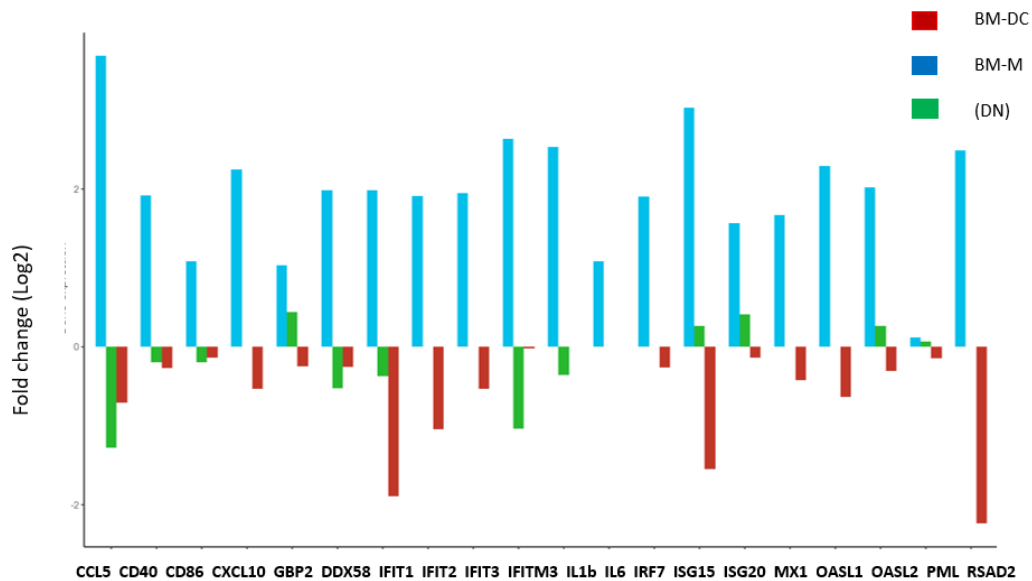
The data shown were pooled from two independent experiments.



20: Figure 3.12A BM-M: LCMV vs Poly (I:C)



21: Figure 3.12B DN: LCMV vs Poly (I:C)



## 22: Figure 3.12C LCMV clone 13 (GFP) infection then Poly (I:C) stimulation

### Figure 3.12. Single Cell RNA Sequencing and Antiviral Gene Expression Analysis of BM Derived Cells Infected with LCMV clone 13 (GFP) and then Stimulated with Poly (I:C)

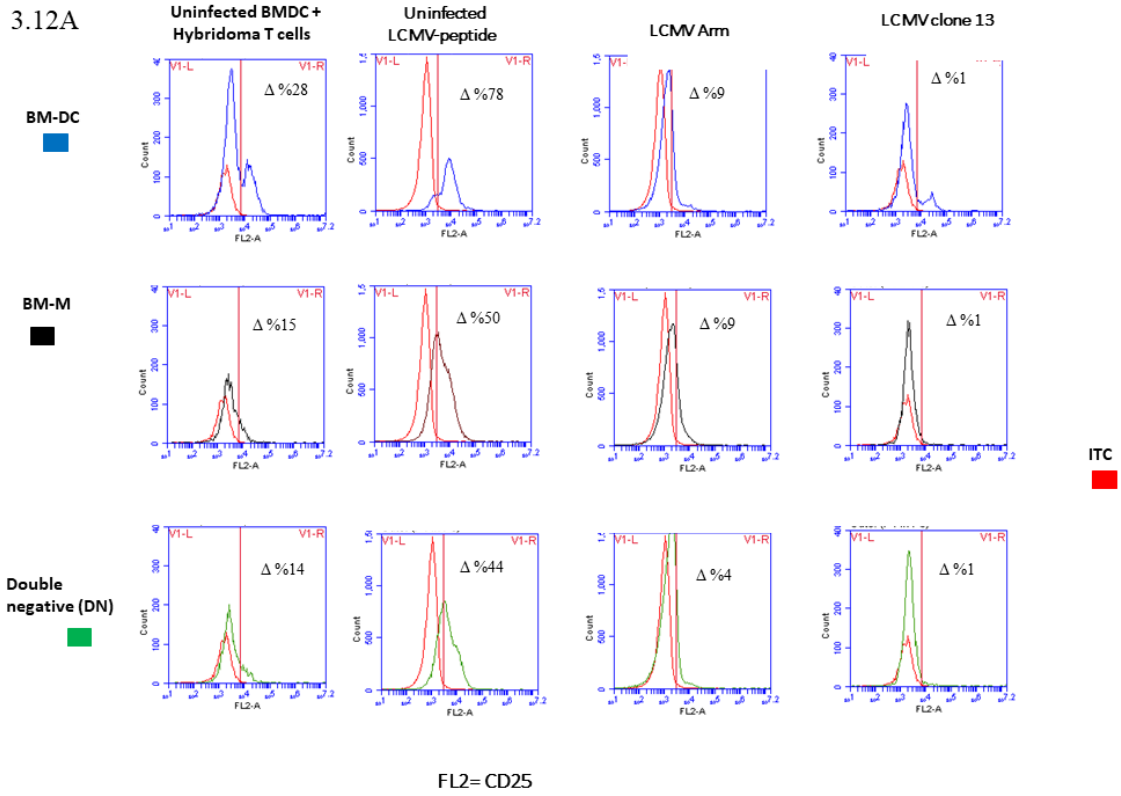
The three BM derived cell sub-populations were infected with LCMV clone 13 (GFP) (MOI 10) for 12 h and 48 h. RNA was harvested from sorted uninfected and infected cells from the 12 h culture for library prep and sequencing. Infected cells (GFP positive) from the 48 h culture were separated and subsequently stimulated with poly (I:C) for another 6 h. RNA was harvested for cDNA library preparation and sequencing. Expression of transcripts from the libraries (12 h and 48 h + poly (I:C) culture) generated using the BD RNA single cell sequencing methodology were analysed and expressed as log<sub>2</sub> difference in gene expression between infected and uninfected cells. Selected antiviral ISGs and other genes from a curated database ([http://www.informatics.jax.org/vocab/gene\\_ontology/GO:0002532](http://www.informatics.jax.org/vocab/gene_ontology/GO:0002532))

were compared between the three BM derived cells (*CCL5*, *CD40*, *CD86*, *CXCL10*, *DDX58*, *GBP2*, *IFIT1*, *IFIT2*, *IFIT3*, *IFITM3*, *IL1b*, *IL6*, *IRF7*, *ISG15*, *ISG20*, *MX1*, *OASL1*, *OASL2*, *PML*, *RSAD2*).

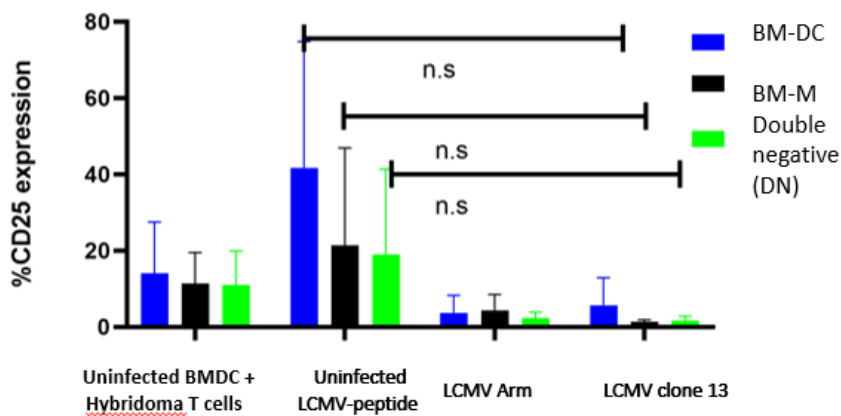
Note: LCMV clone 13 (GFP) infection (alone) of BM-DC was not analysed because there was not enough cDNA for sequencing. However, LCMV clone 13 infected then poly(I:C) stimulated BM-DC were analysed.

Furthermore, I investigated if the limited induction of cytokine expression by LCMV infected cells was permanent or temporary. Using similar methods described previously, I infected GM-CSF/IL-4 differentiated BM derived cells with LCMV clone 13 (GFP) for 48 hours. I separated infected cells from the three sub-populations (GFP positive cells) and stimulated them with poly (I:C) for 6 h and then harvested the cells for single-cell RNA sequencing. My results showed that infected BM-M and to some extent, the DN cells up-regulated antiviral ISG gene expression (*Isg15*, *Mx1*, *Ifitm3* etc.) upon stimulation with poly (I:C) while the ISGs were down-regulated in BM-DC despite the secondary stimulation with poly (I:C) (figure 3.12C). Thus, the limited induction of cytokine gene expression by infection is not due to low susceptibility to LCMV of *in vitro* BM derived cells and it is not permanent in BM-M because the cells could still induce antiviral cytokine and gene expression when reactivated with poly (I:C).

Furthermore, I wanted to see the effect of LCMV on the antigen presentation capabilities of the three sub-populations of BM derived cells. Previous studies have shown that both strains of LCMV impair antigen presentation by DC resulting in activation of immunosuppressive T cells (193,210). I co-cultured each sub-population of BM derived cells (using GM-CSF/IL-4) with LCMV specific T cell hybridoma and measured the expression of the T cell activation marker, CD25, by flow cytometry. BM derived cells were either fed LCMV peptide (as recognised by the T cells) or were infected and endogenous viral antigen used as a source of peptide. Successful presentation of antigen by BM derived cells will result in activation of the T cells and up-regulation of CD25. Thus, quantification of the CD25 expression can give a measure of the antigen-presenting capacity of the sub-populations of BM derived cells (211). All the three groups could present LCMV peptides to T cells as seen by expression of CD25 on the T cell hybridoma; however, BM-DC co-culture had an increased proportion of CD25 positive cells compared with BM-M and DN group though the difference was not statistically significant (figure 3.13B). When infected BM derived cells (both strains of LCMV) were co-cultured with the T cell hybridoma, the proportion of T cells expressing CD25 was reduced compared to cells with peptide in all the three BM derived cells though this was not statistically significant.



23: Figure 3.13A Antigen Presentation and T cell Activation by LCMV Infected BM Derived Cell Subsets



24: Figure 3.13B Percentage CD25 expression

Figure 3.13. Antigen Presentation and T cell Activation by LCMV Infected BM Derived Cell Subsets

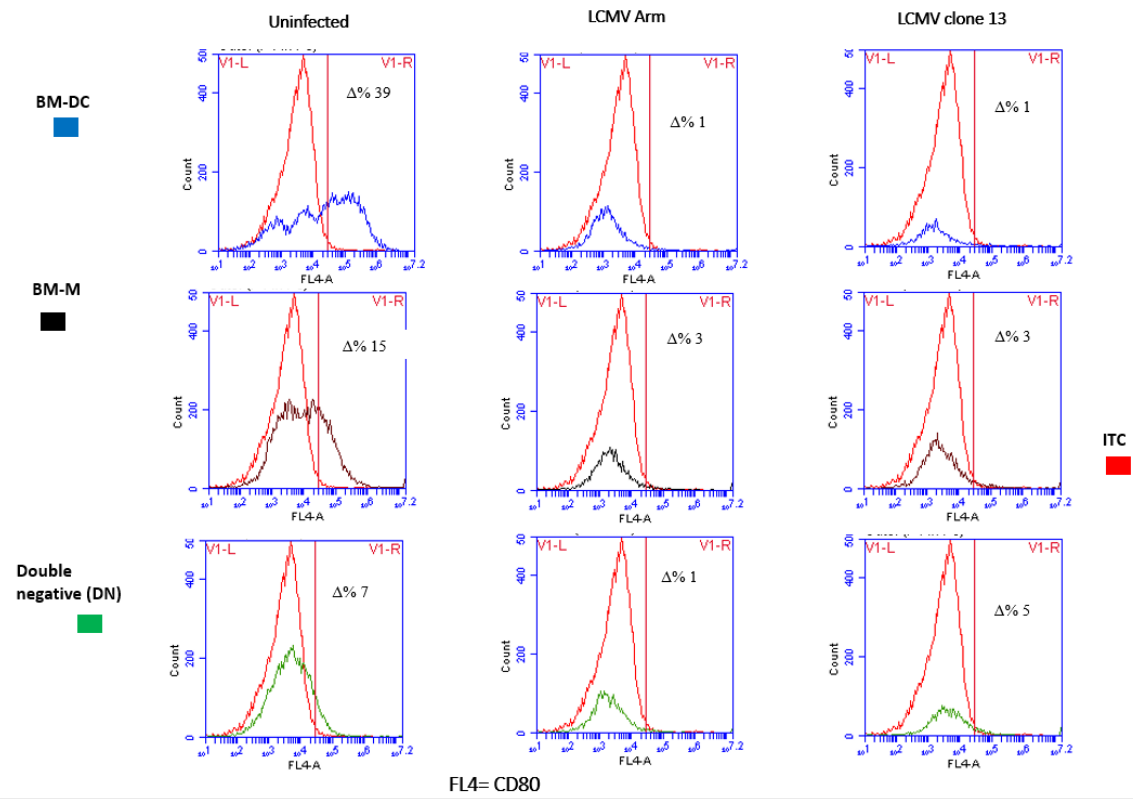
A. Uninfected or infected (LCMV Arm or clone 13) BM derived cell subsets (using GM-

CSF/IL-4) were co-cultured with LCMV specific hybridoma T cells  $\pm$  specific LCMV peptide for 24 hours. The expression of CD25 on T cells was measured by flow cytometry.

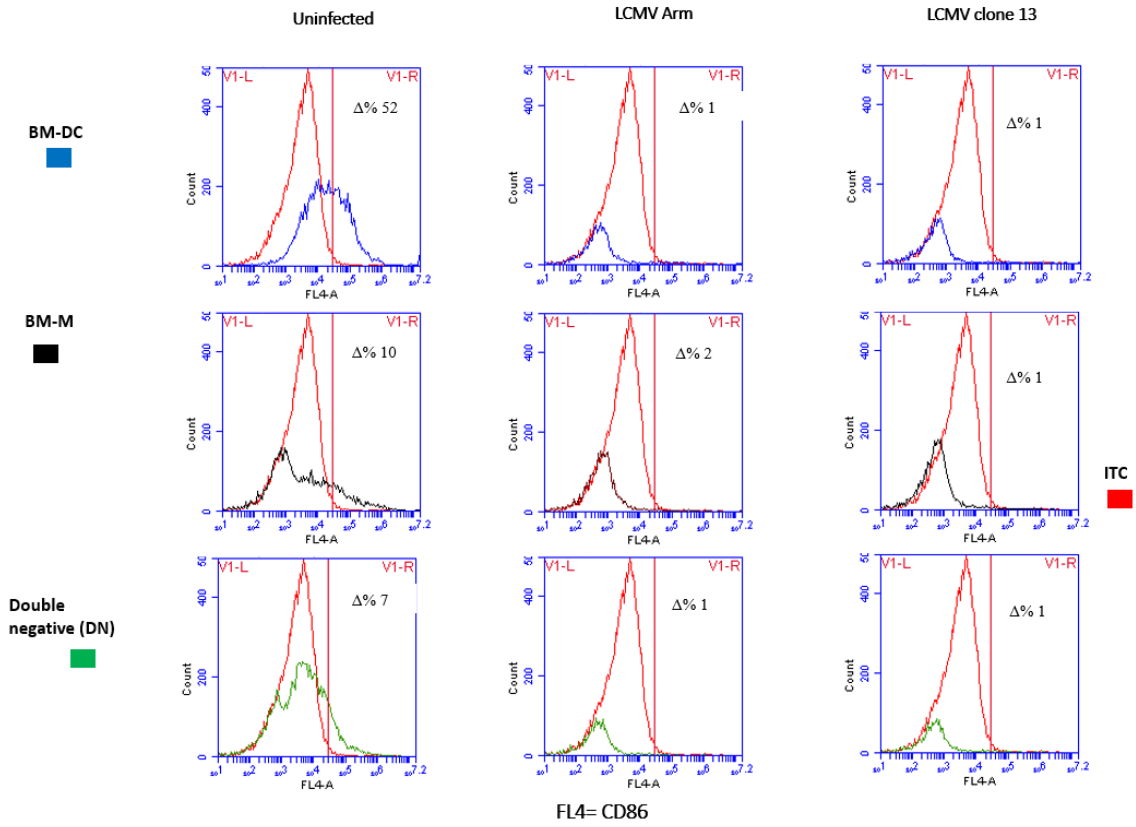
Histograms show surface expression of CD25 on T cells. Red histograms represent isotype-matched irrelevant specificity controls. Figures in the graphs show the mean percentage of cells expressing CD25 from 3 independent experiments.

B. Bar chart showing the three independent experiments. Statistical significance was calculated by Mann-Whitney test and p values are indicated (\*;  $P < 0.05$ ) (capped line with \* indicating significance, n.s – not significant).

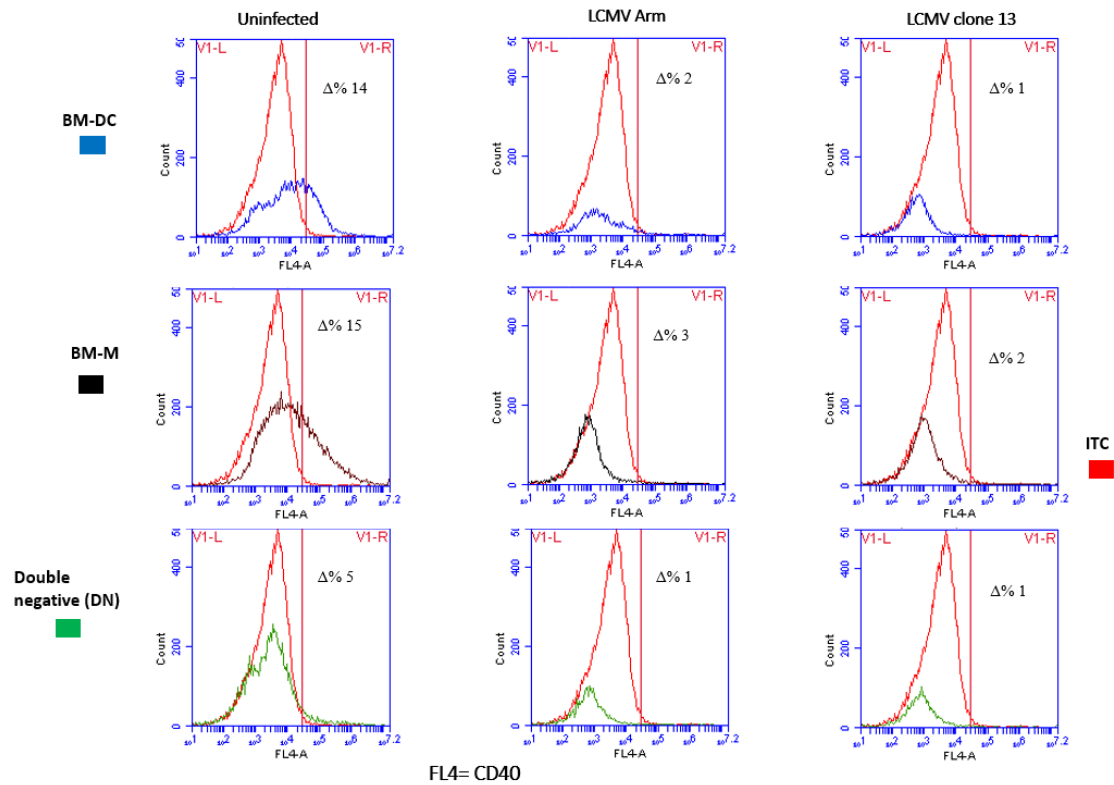
To understand the mechanism for the reduced antigen presentation by BM derived cells following infection with both strains of LCMV, I infected the three subsets of BM derived cells (from GM-CSF/IL-4 culture) with both strains of LCMV and measured expression of co-stimulatory receptors (CD80, CD86, CD40) at 48 h post infection. Though the differences were not statistically significant, in the uninfected cells, BM-DC had higher expression of co-stimulatory receptors (CD80, CD86, CD40) compared to both the BM-M and the DN group. For the infected cells, there was reduced expression of the co-stimulatory receptors in all the three groups of BM derived cells by both strains of LCMV (GFP) (figure 3.14).



25: Figure 3.14 A CD80 Expression



26: Figure 3.14 B CD86 Expression



## 27: Figure 3.14C CD40 Expression

### Figure 3.14. LCMV Infection and BM derived cell subset maturation states

The three subsets of BM derived cells generated with GM-CSF/IL-4 were infected with LCMV Armstrong and clone 13 (MOI 10) for 48 h. PBS was added to the uninfected BM derived cells as a mock infection control.

The expression of BM derived cell co-stimulatory receptors A: CD80; B: CD86; and C: CD40 was measured by flow cytometry.

Histograms show surface expression of the indicated marker by BM-DC (blue), BM-M (black) and DN (green). Red histograms represent isotype-matched irrelevant specificity controls.

Percentages in the figures show the mean percentage positive cells from three independent experiments.

In summary, similar to previously described DC, BM-DC were efficient at antigen presentation but poor at cytokine production, while BM-M, similar to previously described macrophage populations were good at cytokine production and poor at antigen presentation. However, both

strains of LCMV were capable of reducing or inhibiting cytokine production and antigen presentation by the three groups of BM derived cells.

### 3.4 Discussion

The work by Helft et al. (2015) and others (154,207) established the heterogeneity of CD11c<sup>+</sup> MHC class II<sup>hi</sup> expressing cells generated from mouse BM culture thereby challenging the previously held view that non-adherent cells expressing CD11c and MHC class II were bonafide DC.

In this chapter, I validated this BM derived cell heterogeneity in the mouse and showed that it was seen across all the growth factors I used in *in vitro* BM derived cell culture systems except M-CSF. I also used LCMV to investigate the functional profile of the groups of cells generated in BM derived cells culture.

Based on the morphology, phenotype, transcriptional and functional profile, I identified three groups of cells in BM derived cell cultures (BM-DC, BM-M, DN) across all the growth factors used except M-CSF. The first two subsets were similar to the ones identified by Helft et al. (2015) and other groups (154,207) thus validating the heterogeneity of CD11c<sup>+</sup> MHC class II<sup>+</sup> BM derived cells not just with GM-CSF but with other growth factor systems. The third subset, DN cells, did not express CD11c and MHC class II but expressed CD11b, hence the name double negative (DN). When DN cells were differentiated further in culture they gave rise to cells resembling BM-M more than BM-DC (data not shown) suggesting they could be immature BM-M. According to Helft et al. (2015) (154), CD115 and CD135 antibodies can be used to identify the two CD11c<sup>+</sup> MHC class II<sup>+</sup> BM derived cell subsets. Unfortunately, both markers were poorly expressed by the three groups of BM derived cells, as antibody reagents from different batches were unable to detect expression (data not shown). Expression of CD115 was only seen in the M-CSF culture showing that the antibody reagents against this marker were functioning correctly.

Furthermore, I investigated the susceptibility of the three subsets of BM derived cells to LCMV infection. LCMV is a well-studied Arenavirus that preferentially infects DC and macrophages (193). There is strain variation in the infectivity of DC by LCMV. A previous study has shown that DC are more susceptible to Clone 13 than Armstrong; about 75 % compared to 10 % infected cells (193). My findings correlated with this, all the three groups of BM derived cells

were more susceptible to the persistent strain of LCMV (clone 13) compared to the acute strain Armstrong. The reason for this is not known but may be due to the ability of the persistent strain to bind strongly to the major LCMV cellular receptor  $\alpha$ -dystroglycan (DG) compared to the weaker binding by the acute strain of the virus (212). The three subsets of cells supported the productive replication of both strains of LCMV as seen by onward infection in Vero cells.

Though LCMV can infect both DC and macrophages, previous *in vivo* data showed that clone 13 preferentially infected DEC205<sup>+</sup> DC, while Armstrong had a greater tropism for F4/80 positive macrophages in the red pulp of the spleen (193). For *in vitro* studies, most previous BM derived cell infections used bulk culture without separating the cells into DC and macrophages respectively, however, one of the studies showed that both strains of LCMV can infect GM-CSF and M-CSF differentiated BM cells with no preference (213). My findings did not correlate with previous *in vivo* and *in vitro* data. My data demonstrated preferential infection of BM-M compared to BM-DC by both strains of the virus. Because, the previous data did not separate BM derived cells into the different groups as seen in my culture, it will be difficult to ascertain if there was preferential infection in previous BM derived cell infections. Therefore, further studies using the new model of BM derived cells suggested by Helft et al. (2015) (154) and validated by my research should be investigated using other pathogens to determine if this preferential infection shown by LCMV in my study can be replicated.

LCMV infection of APCs has been shown to impair cytokine production, and maturation of antigen-presenting cells, thereby preventing T cell stimulation. In *in vitro* (193,212,214) BM culture, Alothaimen et al. (2020) and others (213,215) showed impaired production of pro-inflammatory cytokines by both strains of LCMV. My data agreed with this. Both strains of LCMV impaired cytokine production in the three groups of BM derived cells both in bulk culture and at the single cell level in my studies, thus validating the immunosuppressive nature of LCMV virus. To be sure the low level expression or absence of cytokine production in my infected BM derived cell cultures is not an inherent feature of the cells rather than induced by the virus, I used a known TLR-3 agonist (poly (I:C)) to stimulate the three groups of BM derived cells. Previous work has shown that poly (I:C) induced Interferon and ISG production upon stimulation of *in vitro* BM derived cells (216,217). However, my results showed that only BM-M and DN produced antiviral cytokines following poly (I:C) stimulation. Recent work that separate BM derived cells into DC and macrophages corroborated my results by showing that only the macrophage fraction produced cytokines when stimulated with TLR-4 agonist

LPS (207,218). Although the reason for the discrepancy is not clear, a plausible explanation may be similar to the situation seen in *in vitro* BM derived cell infection by Lassa fever virus, another Old World Arenavirus. In this case cytokine production was observed in macrophages and not in DC (81). Therefore, the cytokine production seen in previous BM derived cell infection may only be from BM-M and not BM-DC. However, because bulk cultures were initially analysed, we will not see the lack of cytokine production from the individual BM-DC population. Now that the heterogeneity of *in vitro* BM derived cells culture has been validated, there is a need to select the required or appropriate group of BM derived cells that corresponds to the desired experimental question.

Antigen presentation is a core function of DC. Previous studies have shown that LCMV impairs antigen presentation by DC (193,210). Helft et al. (2015) (154) showed that both subsets of cells (DC and macrophages) from GM-CSF stimulated BM derived cell cultures presented ovalbumin peptide effectively to T cells, but only DC could present ovalbumin proteins. To understand the effect of LCMV on the antigen presentation function of the three subsets of BM derived cells I studied, I co-cultured infected and uninfected cells from the three groups with T cell hybridoma cells and measured activation of the T cells. Note, I added LCMV specific peptides to the uninfected cells before adding the T cells. When uninfected cells from the three groups of BM derived cells were fed LCMV peptides (GP61-80), BM-DC were more efficient than BM-M and DN in antigen presentation as shown by the expression of CD25 on the T cells. This corroborated previous work that confirmed that DC are better antigen presenting cells than macrophages (213,219). However, LCMV infected cells from the three groups of BM derived cells were unable to present antigen to the T cell hybridoma, as demonstrated by lack of CD25 expression. This corroborated other work that has shown that LCMV and most Old World Arenaviruses impair antigen presentation to T cells (190). This has been postulated as one of the mechanisms driving apoptosis of T cells, due to lack of proliferation (220). I measured the expression of co-stimulatory receptors which are involved in T cell stimulation. The co-stimulatory receptors were down-regulated in the three subsets following LCMV infection compared to the uninfected BM derived cells. The down-regulation of these co-stimulatory markers signifies that there will be failure of APC maturation and presentation of the antigen to T cells (164,221).

My data revealed that both viral strains can impair cytokine and antigen presentation functions from the three groups of BMDC.

### 3.5 Conclusion

My research and other studies have validated the heterogeneity of APC from BM derived cell cultures that used GM-CSF to differentiate the cells. I confirmed that this heterogeneity existed across other growth factors, not just GM-CSF. I also showed that there was a functional difference in the response of the three groups of BM derived cells to LCMV and dsRNA. While BM-DC were better at antigen presentation to T cells, BM-M were efficient cytokine producers. However, both strains of LCMV can impair cytokine production and antigen presentation function by all three groups of BM derived cells. The impaired cytokine production is temporary in the BM-M and permanent in the BM-DC. The reason for this variation will require further elucidation. Also, the mechanism for LCMV impaired antigen presentation is not clear, but my data suggest that it may be due to downregulation of co-stimulatory receptors on the BMDCs.

My findings ascertain the division of labour among the cells generated from *in vitro* BM derived cell culture and highlights the need for caution in the interpretation of data generated from bulk *in vitro* BM derived APC cultures. In the era of immunotherapy using *in vitro* or *ex vivo* differentiated DC cultures, it is important to precisely define the population of cells used for different therapeutic applications.

# Chapter 4

## Dissecting LCMV *In vivo* Infection of APC using Single Cell RNA Sequencing

### 4.1 Background

The immune system is a dynamic system and the immune response seen phenotypically is a combination of individual cellular and molecular activities aimed at resolving an insult or injury. Until recently, studies looked at the overall cellular immune response. This does not give information on the state and contribution of single cells (222). Even in similar conditions, individual cell responses to infection differ. Similarly, the contribution of bystander cells and uninfected cells to the immune response is usually masked in this bulk analysis. For example, in a viral infection, part of the anti-viral interferon produced is from bystander cells responding to constitutive activation from the interferon released in the system (223,224). LCMV does not infect T cells; however, lack of antigen presentation from APC causes up-regulation of immunosuppressive receptors on T cells, T cell exhaustion and bystander apoptosis of the T cells (189). All these responses from T cells contribute to the generalised immunosuppression seen in persistent LCMV infection. Therefore, a good understanding of host-pathogen pathophysiology requires looking at the contribution of individual cells (uninfected, infected, bystander cells) to the bulk immune response.

The advent of single-cell technology has revolutionised the way we analyse an immune response. We can now differentiate responses from bystander and infected cells. Also, we can monitor immune response kinetics over time (225,226).

The LCMV mouse model has contributed immensely to the field of immunology and virology; one of its major contributions is the discovery of T cell restriction to the major histocompatibility complex (209). The LCMV model also helped us decipher the dual role of interferon both in controlling virus replication as well as fostering viral persistence (227). One of the advantages of the LCMV model is the availability of different strains of the virus. Also it is not a cytolytic virus, thus, infected cells can be recovered and interrogated. A review of LCMV and Arenaviruses is presented in chapter 1.

LCMV is known to infect antigen-presenting cells (APC), mainly dendritic cells (DC), and macrophages. There are two established strains of LCMV: the acute strain, Armstrong (ARM), and the persistent strain, clone 13, and they both infect and replicate in APC. Previous studies have shown that clone 13 preferentially infects CD11c<sup>+</sup>, DEC-205<sup>+</sup> DCs in the marginal zone of the spleen while the ARM strain infects F4/80 expressing cells, mainly in the red pulp (193).

Furthermore, in the spleen, LCMV clone 13 preferentially induces and sustains the expression of immunosuppressive receptors, including PD-L1 in CD8a<sup>-</sup> DC but not in CD8a<sup>+</sup> DC. Note, most of these previous studies were analysed in bulk cells; hence the exact cellular niche of LCMV has yet to be elucidated, and the cytokine response from the individual cells is not known. For example, does LCMV induced immunosuppression impair antigen presentation by DC. Is there immunosuppressive cytokine release from only infected cells? What is the role of bystander cells in the immunosuppressive immune response? Are all DCs and macrophages infected and do they all contribute to the immunosuppression?

Using RNA sequencing single-cell technology, I aimed to identify the *in vivo* cellular niche of LCMV and their cytokine profile in acute and persistent infection. I also investigated if LCMV infection affected the response of APC to secondary activation by poly (I:C).

## **4.2 Materials and Methods**

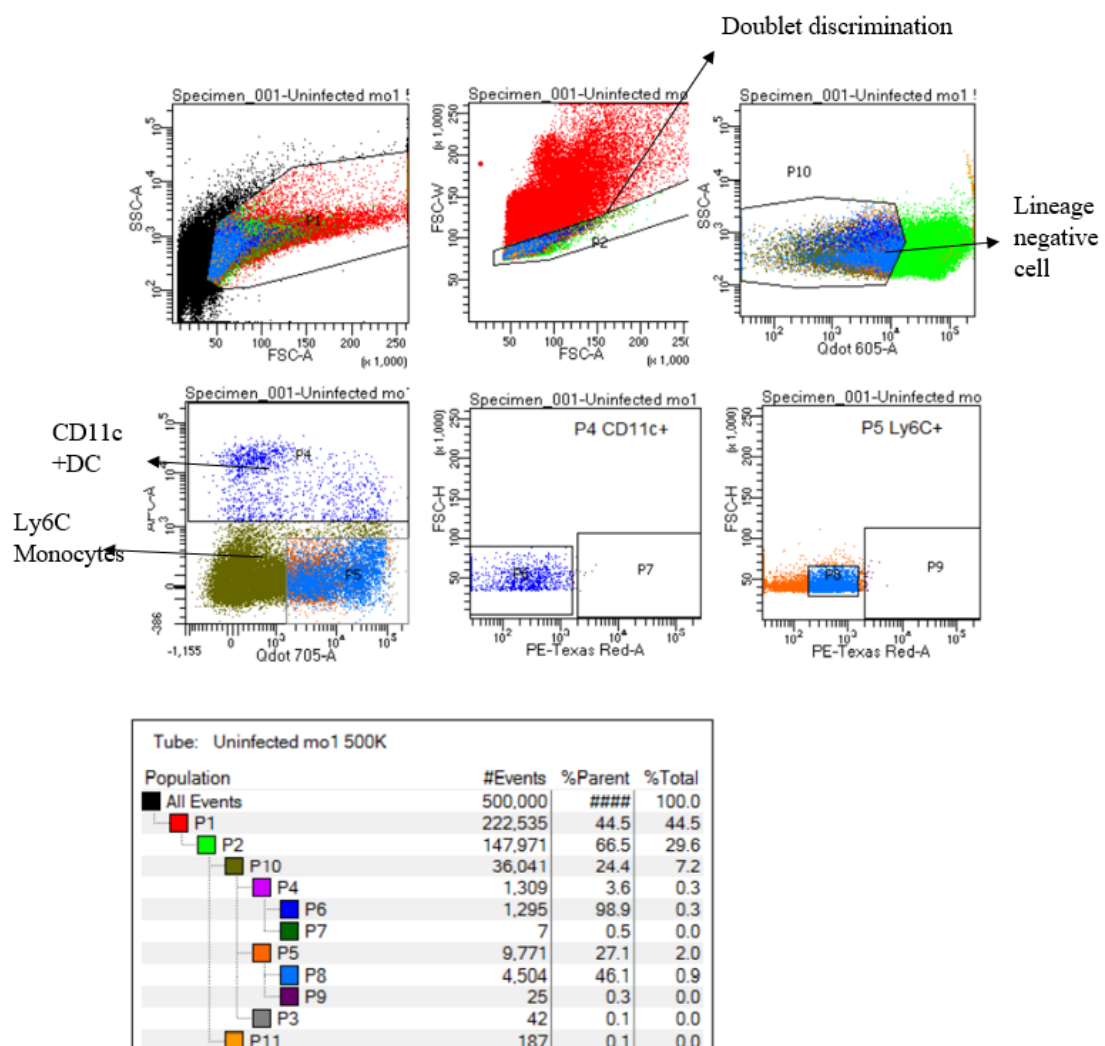
### **4.2.1 Animals**

Adult C57BL/6J (Rosa26floxedSTOPtdTomato) mice, age range between 6 to 14 weeks, were used in the study (see chapter 2 section 2.2).

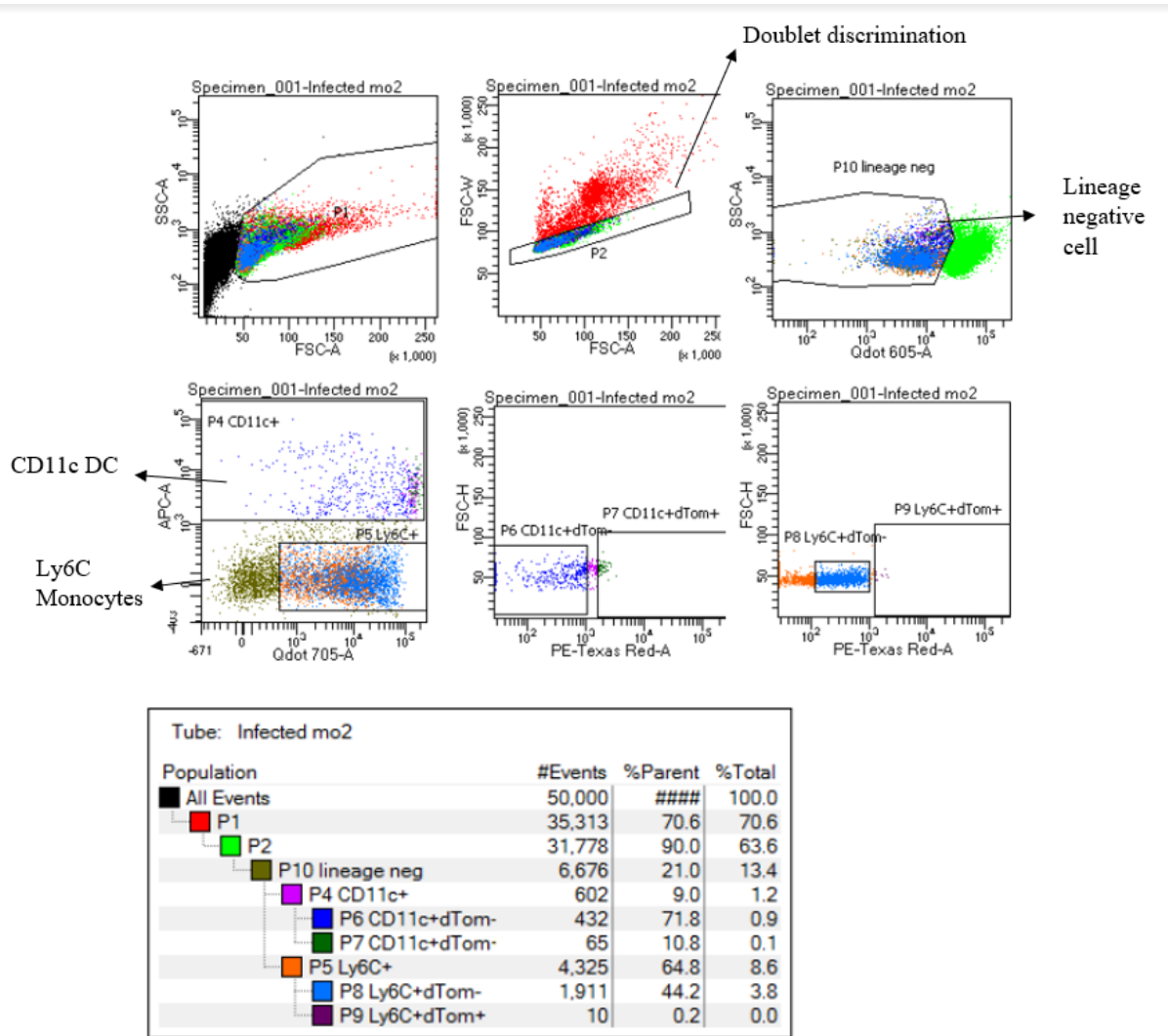
### **4.2.2 Experimental procedure**

The Rosa26floxedSTOPtdTomato mice were divided into six groups with four mice per group. Group 1 mice were given PBS (uninfected group), group 2 were infected intraperitoneally with r3LCMV/ Cl 13 Cre for 48 h (acute infection group), group 3 mice were injected intraperitoneally with poly (I:C) for 24 h, group 4 mice were infected intraperitoneally with r3LCMV cl 13 cre for two weeks (persistent infection group), group 5 mice were infected r3LCMV cl 13 cre for two weeks and poly (I:C) was injected for 24 h

(persistent infection plus poly (I:C)), while group 6 mice were given poly I:C for 24 h followed by r3LCMV cl 13 cre for 48 h (poly I:C plus LCMV infection). After infection, the mice were sacrificed, and the spleen harvested for single cell sorting. Infected cells expressed dTomato while non-red cells in infected mice were bystander cells. Using fluorescent activated cell sorting (see Table 2.2 and Figure 4.1 for list of antibodies used and FACS sorting set up and), 16000 cells from each mouse were sorted into polypropylene FACS tubes and sent to Cancer Research UK (CRUK) for library preparation and sequencing. See Table 4.1 for a summary of the experimental procedure.



28: Figure 4.1A Uninfected Mouse Splenic Cells Sorting Procedure



29: Figure 4.1B Infected Mouse Splenic Cells Sorting Procedure

### Figure 4.1. Mouse Splenic Cell Sorting Procedure

Mouse splenic DC and monocytes were sorted using Aria III flow cytometer (BD Biosciences, CA). Cells were selected by the size (FSC-A) and molecular granularity (SSC-A). After removal of debris, and doublet cells, lineage marker negative cells (CD45R/B220, Anti CD3, CD19, NK1.1, Ly6G, Siglec F) were all put into the Brilliant Violet 605 channel) were sorted into DC and monocytes using expression of Ly6C or CD11c. These cells were further separated using dTomato expression. Sorted cells were counted and resuspended in 50 ml of FACS buffer for further analysis.

### 4.2.3 Hashtag labelling of mouse splenic cells

Splenic cells resuspended in FACS buffer as previously described (see chapter 2 subsection 2.6.1) were stained with antibody cocktails (containing both anti-surface marker and specific TotalSeq™-A Hashtag antibodies (Biolegend) prepared in FACS buffer. TotalSeq™ anti-mouse Hashtag reagent contains two monoclonal antibodies specific against mouse CD45 and MHC class I (of a, b, d, j, k, s, and u haplotypes) and conjugated to an oligonucleotide barcode that can be sequenced(228). The hashtag antibody -oligonucleotide (HTO) conjugates allows for pooling of different experimental samples together in one library for single cell RNA sequencing (cell hashing)(229). The barcode antibody will enable demultiplexing of the experimental samples after sequencing. Stained cells were incubated in the dark at 4 ° C, 30 min. Cells were washed and re-suspended with FACS buffer for single cell sorting (see table 2.2 and 4.1 for the list of the hashtags and experimental groups respectively).

**8: Table 4.1. Treatment Groups and Their Hashtags (summary)**

Group 1 (Uninfected) Acute	Group 2 (Uninfected) Persistence	Group 3 (LCMV Infected) Acute	Group 4 (POLY I:C) Acute	Group 5 (LCMV Infected) Persistence	Group 6 (LCMV Infected + POLY I:C) persistence	Group 7 (POLY I:C + LCMV infected)
H1	H1	H14	H12	H8	H4	H4
		H13	H11	H7	H3	H5
		H2 (pilot)	H10	H6	H2	H6
		H3 (pilot)	H9	H5	H1	
			H2			
			H3			

#### **4.2.4. Sorting of Mouse Splenic DCs and Monocytes**

Cells were sorted into DC and monocytes using expression of Ly6C or CD11c (figure 4.1) using an Aria III flow cytometer (BD Biosciences, CA). These cells were further separated into infected and uninfected cells using dTomato expression. Sorted cells were counted and resuspended in 50 ml of FACS buffer then taken to the Cancer Research UK Cambridge Institute (CI-CRUK) Genomics Core facility, University of Cambridge for single cell RNA sequencing library preparation and sequencing.

#### **4.2.5 Library Preparation and Sequencing of Mouse Splenic Cells using the 10x Genomics Platform**

Single-cell RNA-seq libraries were prepared in the CI-CRUK Genomics Core Facility using the following: Chromium Single Cell 3' Library & Gel Bead Kit v3, Chromium Chip B Kit and Chromium Single Cell 3' Reagent Kits v3 User Guide (Manual Part CG000183 Rev C; 10X Genomics). Cell suspensions were loaded on the Chromium instrument with the expectation of collecting gel-bead emulsions containing single cells. RNA from the barcoded cells for each sample was subsequently reverse-transcribed in a C1000 Touch Thermal cycler (Bio-Rad) and all subsequent steps to generate single-cell libraries were performed according to the manufacturer's protocol with no modifications (14 cycles were used for cDNA amplification). Supernatant with antibody derived hashtags was saved and cleaned up after cDNA amplification PCR and hashtag libraries were constructed according to the manufacturer's protocol(230). cDNA quality and quantity were measured with an Agilent TapeStation 4200 (High Sensitivity 5000 ScreenTape) after which 25 % of the material was used for gene expression library preparation.

Library quality was confirmed with an Agilent TapeStation 4200 (High Sensitivity D1000 ScreenTape to evaluate library sizes) and Qubit 4.0 Fluorometer (ThermoFisher Qubit™ dsDNA HS Assay Kit to evaluate dsDNA quantity). Each sample was normalized and pooled in equal molar concentration (ratio between gene expression libraries and hashtag libraries was 19:1). To confirm concentration, pools were qPCRred using the KAPA Library Quantification Kit on QuantStudio 6 Flex before sequencing.

Sequencing was done on an Illumina NovaSeq6000 sequencer with the following parameters: 28 bp, read 1; 8 bp, i7 index; and 91 bp, read 2 (the pilot was run on 1 lane of an SP flowcell, 6 samples submitted after were sequenced on 2 lanes of the S1 flowcell).

#### 4.2.6 Bioinformatics and data analysis

The data were first processed through cellranger (v3.1) to generate the matrix of cell barcodes and features. Cellranger demultiplexes the cell data and aligns the reads to the mouse genome (Mus Musculus 38, Ensembl release 97 with added viral sequence to identify the infected cell using the dTomato gene). For the oligo-antibody hashtags (HTO), the software (Hoochm/CITE-seq-Count: 1.4.2) was used to generate the matrix barcodes for the hashtag data(231). This will allow the matching of the hashtag used to the matrix of cell data such that cells in a group can be isolated with a hashtag. For each library 39,000 cells were loaded in the 10X chromium instrument with an expected return of 19,000 sequenced cells. Overall, the performance of the libraries varied greatly from one to the next. Libraries with a lower than expected number of cells were excluded from further analysis. The cell ranger summary and library performance is presented in table 4.3. Once generated, both matrices were processed using the R statistical software (R Core Team 2018), with the Seurat package (Stuart et al. 2018). For the attribution of cell types to the clusters, I used the software SCSA (Cao et al., (2020)) to perform some automated annotations (232).

Seurat does include some filtering when loading the data; features detected in less than 3 cells were excluded and cells with less than 200 feature (genes) detected, along with cells with more than 6,000 features were excluded. These cells are likely to be doublet or triplet cells. These criteria were combined with mitochondrial filtering, removing cells with more than 5 % mitochondrial reads. These cells are likely to be dying. A summary of the libraries loaded on to Seurat is presented in table 4.2.

**9: Table 4.2 Summary of Cellranger and Library Performance**

	Pilot library	Library 1(SIGA F8)	Library 2 (SIGAD 10)	Library 3 (SIGAE)	Library 4 (SIGAF 12)	Library 5 (SIGAG 12)	Library 6 (SIGAG H12)
--	---------------	--------------------	----------------------	-------------------	----------------------	----------------------	-----------------------

Estimated number of cells	5832	909	15,396	1,716	9,945	3,613	17,123
Actual number of cells	5811	901	13824	1422	9632	3587	17081
Mean reads/ Cell	83612	291,963	20819	196616	26786	72981	14577
median genes detected	1677	1,855	1379	1379	1264	1448	1150
Number of reads generated	487,625,151	265,394,375	320,532,397	337,393,761	266,390,984	263,679,368	249,600,033
valid barcodes	97.6%	97.6%	97.7%	97.6%	97.9%	98.1%	97.7%
valid UMIs.	100%	100%	100%	100%	100%	100%	100%
% reaching Q30	93%	95.8%	96%	95.9%	96%	95.9%	96%
% reads mapping to genome	81.5%	81.5%	81.7%	79.8%	82%	84%	83.2%

% reads mapping to the transcriptome	56%	60.5%	58%	57.5%	57.4%	59.3%	57.3%
Comment	The number of single cell sequences is not enough for analysis	Number of single cell sequences is too low for analysis	The number of single cell sequences is not enough for analysis	Number of single cell sequences is too low for analysis	The number of single cell sequences is not enough for analysis	The number of single cell sequences is not enough for analysis	The number of single cell sequences is not enough for analysis

Once generated in CITE-Seq-count, the HTO matrix can be merged with matrix generated for the cells. This will remove any cells that have no barcode in common with the HTO library. For the hashtag demultiplexing, I used the HTODemux function which identifies positive hashtag data using the following procedure:

- I performed a k-medoid clustering on the normalized hashtag values, which initially separates cells into  $K(\# \text{ of samples})+1$  clusters.
- I calculated a ‘negative’ distribution for hashtags. For each hashtag, we used the cluster with the lowest average value as the negative group.
- For each hashtag, I fitted a negative binomial distribution to the negative cluster. I used the 0.99 quantile of this distribution as a threshold.

Based on these thresholds, each cell is classified as positive or negative for each hashtag. Singlet cells were cells tagged by a single hashtag, doublet were the ones tagged by two hashtags and negative cells were the cells that did not pass the threshold for hashtag selection. Both negative and doublet cells were removed from the set. The number of singlet hashtags was very high, which was a sign of good HTO labelling of the cells that were sorted.

For each library, clustering was performed using the UMAP algorithm and the “find cluster” function of the Seurat package. Once the clustering was performed, the next step was the identification of the different types of cells present in each of the libraries. Two different strategies were used, one based on genes in published work to identify genes in mouse spleen samples, the other using the SCSA software (Cao et al., (2020)) to identify cell types automatically (232). This software uses a database for gene expression linked to cell types in mouse (or human) to identify the clusters of cells given by the Seurat package. The software was set to use the whole mouse tissue database first and then the specific spleen database to identify the different cell types. These three methods of clustering were then aggregated to produce putative clusters. After reviewing the clusters, the final cell types were assigned to the clusters based on their five top expressed genes (fold change log2) (table 4.4). The cells were partitioned into categories according to 3 factors:

- Cell type (clusters)
- Hashtags (for uninfected, infected/bystander and poly (I:C))
- Infected status

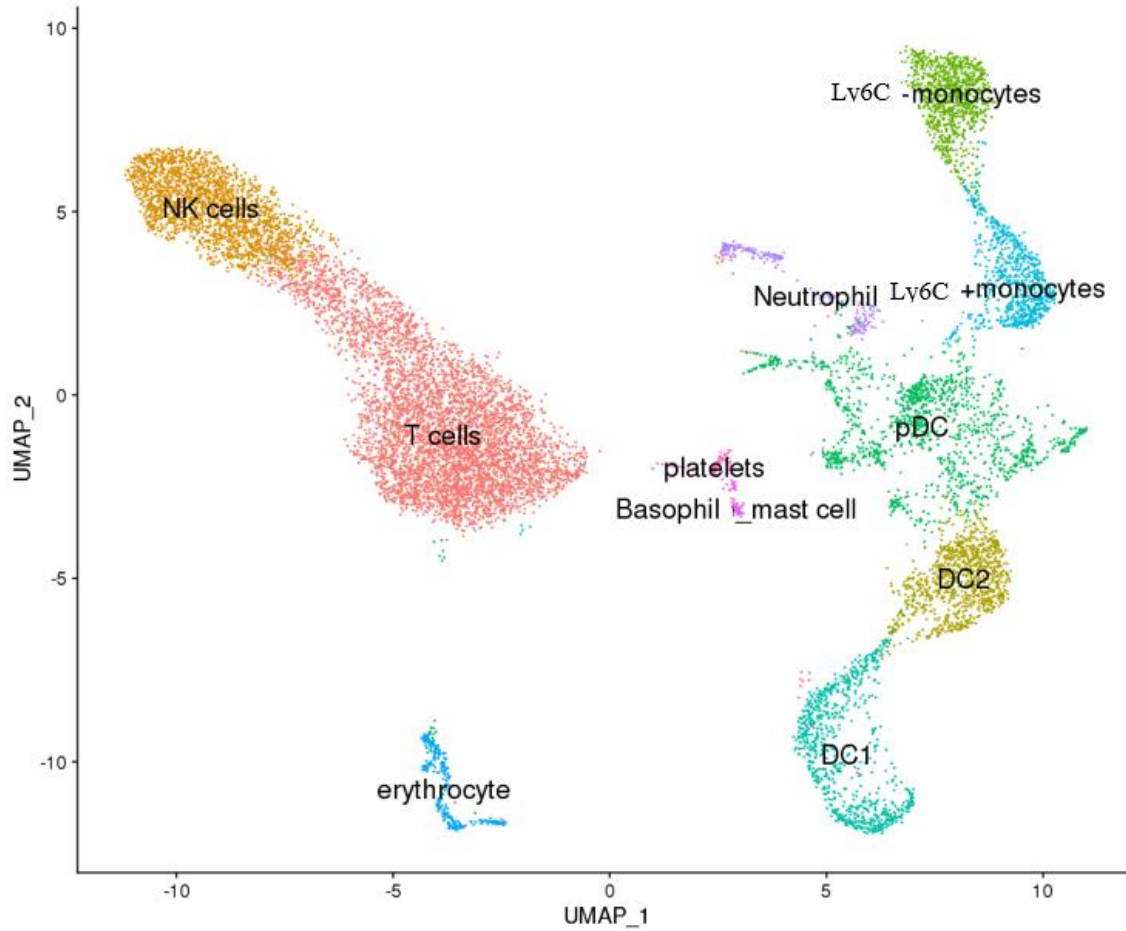
In all the experimental samples, average of twelve cell clusters were identified (DC1, DC2, pDC, MLy6C+monocytes, Ly6C-monocytes, Tcells, NK cells, platelets, Basophils, Mast cells, erythrocytes, Neutrophils) (figure 4.2).

**10: Table 4.3 Summary of Cell Clusters and Their Top Five Genes (fold change log2)**

DC1	DC2	Ly6C-MQ	Ly6C+MQ	pDC	T cells	NK cells	Neutrophil	Basophil	Platelets	Erythrocytes
Apol7c.5	H2-Ab1.2	ApoE.2	Lyz2.7	Cst3.7	Dapl1	Gzma.1	Prtn3	Prss34	Pf4	Hbb-bs.8

Gadd45 b.5	H2- Aa.2	Cebp b.3	Fn1.3	Naaa .6	Rpl 12	Ccl5. 1	Elane	Mcpt 8	Nrgn	Hba- a1.5
Il4i1.4	Cd7 4.2	Gngt 2.2	Wfdc 17.7	Ppt1. 5	Lef 1	Nkg7 .1	Mpo	Ccl3. 1	Tsc22 d1.2	Hbb- bt.1
Tbc1d4. 5	H2- Ea- ps.2	Hpg d.3	Plac8. 6	Stmn 1.7	Cd 3d	Lgals 1.1	Ctsg	Ifitm 1.2	Gng11	Hba-a2
Tmem1 76a.6	Ffar 2.2	Ace. 3	Ifitm3 .5	Pclaf	Tcf 7	Klrc1 .1	Hmgb 2.6	Ccl4. 11	Rgs18 .6	Car2

The libraries that met all the necessary criteria for cell clustering proceeded for further analysis (cell cluster comparison) (see table 4.1 for the libraries and experimental samples distribution). Unfortunately, for Library 1 and 3 the number of cells successfully tagged by HTO is too low to get meaningful clusters, they were excluded from further analysis.



**30: Figure 4.2 Mouse Splenic Cell Clustering**

For each library, clustering was performed using the UMAP algorithm and the “find cluster” function of the Seurat package. The cell clusters were identified manually (top 5 expressed genes (fold change log2) and automatically using the SCSA software (Cao et al., (2020)). This software uses a database for gene expression linked to cell types in mouse (or human) to identify the clusters of cells given by the Seurat package. The software was set to use the whole mouse tissue database first and then the specific spleen database to identify the different cell types. In all the experimental samples, average of twelve cell clusters were identified: DC1, DC2, pDC, Ly6C+monocytes, Ly6C-monocytes, Tcells, NK cells, platelets, Basophils, Mast cells, erythrocytes, Neutrophils.

#### **4.2.7 Comparison between the clusters and treatment**

Comparisons were performed between cell cluster from different experimental treatment (see table 4.1). The p-values were corrected using the false discovery rate (FDR). The summary gave the number of genes significant expressed (upregulated or downregulated) at a 5 % or 1 % significance threshold (FDR corrected p-value below 0.05 or 0.01). Positive value corresponds to the first member of the comparison while a negative value corresponds to the second member of the comparison. A summary table for all the comparisons between different cell clusters and treatments is present in appendix 1.

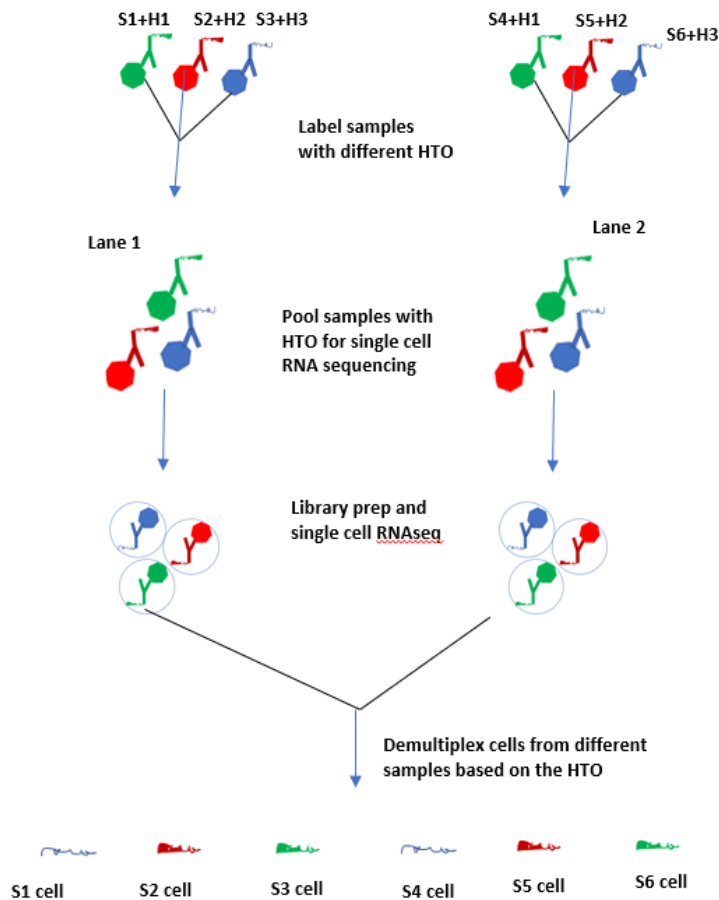
#### **4.2.8 Statistical Analysis**

Statistical analysis and generation of graphs was performed using GraphPad Prism 6 (GraphPad Prism Software, CA) or Microsoft Excel (Microsoft, WA).

### **4.3 Results**

#### **4.3.1 Cell hashing approach in single cell RNA sequencing**

Cell hashing involves the use of oligonucleotide-tagged antibodies (hashtags oligonucleotide HTO) to pool different cells from different experimental conditions for single cell RNA sequencing(229). The principle is the fact that the oligonucleotide or barcode can convert the antibody detection of cell surface protein into a readout alongside scRNA-seq(228). This readout can then be used to identify each cell from different experiment in a library during bioinformatics analysis (figure 4.3). I used 15 hashtags to label 30 mice divided across 7 different treatment groups (see subsection 4.2.2). I pooled all the cells in 6 libraries for sequencing. Each mouse has a specific hashtag thus all the splenic cells can be identified by that hashtag. With the hashtags, I was able to demultiplex the libraries into different treatments groups during analysis. For example, in library 2, all the cells with hashtag 1 are from uninfected mouse, the cells with hashtag 12 were from the mouse treated with poly: IC and those with hashtag 8 were persistently infected with LCMV clone 13 (see table 4.1).



### 31: Figure 4.3 Cell Hashing Approach in Single Cell RNA Sequencing

Cell hashing involves the use of oligonucleotide-tagged antibodies (hashtags oligonucleotide HTO) to pool different cells from different experimental conditions for single cell RNA sequencing. The principle is the fact that the oligonucleotide or barcode can convert the antibody detection of cell surface protein into a readout alongside scRNA-seq. This readout can then be used to identify each cell from different experiment in a library during bioinformatics analysis. Hashtag reagent contains two monoclonal antibodies specific against mouse CD45 and MHC class I (of a, b, d, j, k, s, and u haplotypes) and conjugated to an oligonucleotide barcode that can be sequenced. Here six samples (S1-6) were tagged with 3 HTO and pooled together for single cell RNA-seq.

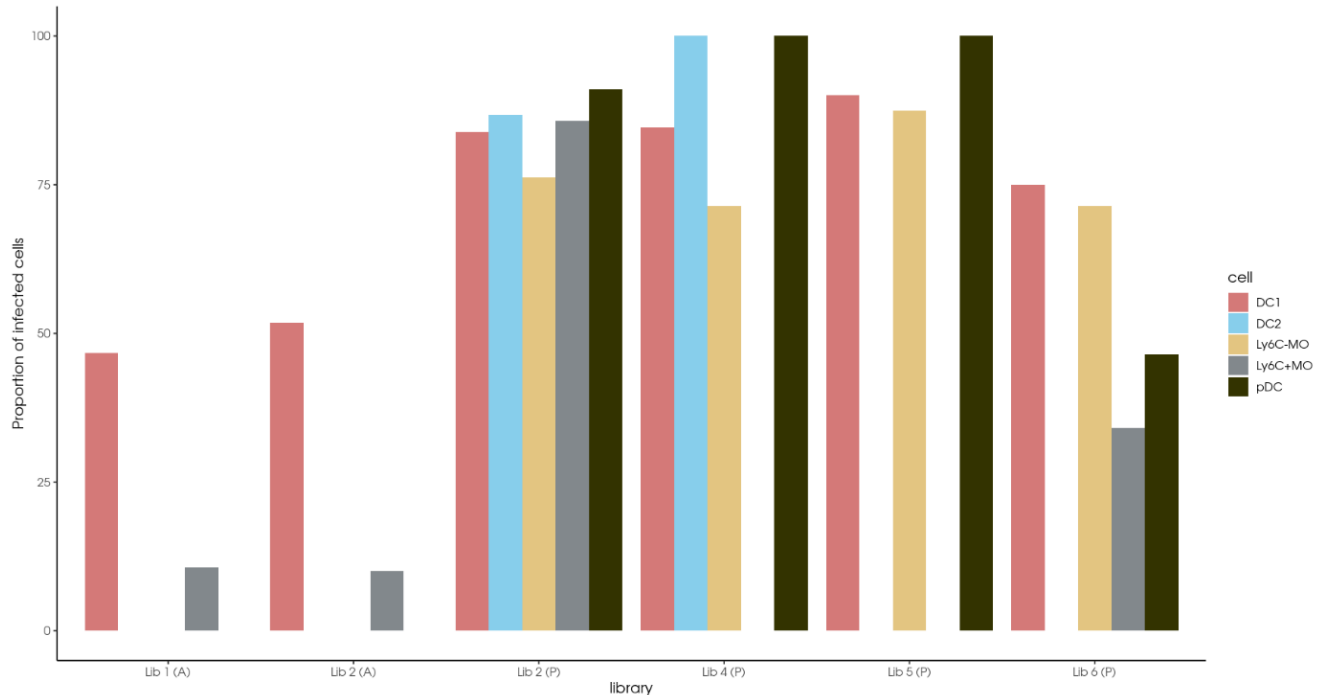
#### 4.3.2 LCMV Infects all Splenic DC and Monocytes

Previous studies showed that LCMV preferentially infects antigen presenting cells, DC and macrophages. While LCMV clone 13 infects DC, LCMV ARM infects macrophages (193). Using the mouse Cre-LoxP system and single cell technology, I aimed to establish the cellular niche for LCMV clone 13 in both acute and persistent infection. I used tripartite LCMV clone 13 expressing a Cre recombinase to infect mice with a LoxP site and dTomato gene such that interaction of the Cre recombinase and the LoxP site will activate the promoter driving expression of the dTomato gene. This protein expression can then be detected using fluorescent activated cell sorter (FACS) using a yellow green laser (561 nm). Thus, mouse splenic cells with dTomato gene expression were assumed to be infected cells. This system helped to differentiate between cells with only viral RNA (bystander cells) and those with productive infections (233).

I used the expression of Ly6C and CD11c to select monocytes and DC respectively by flow cytometry (see Table 2.2 and Figure 4.1 for flow cytometer set up and list of antibodies). I initially used the expression of dTomato protein (using a yellow green laser (561nm) to sort infected cells. However, the dTomato protein expressing cells were low in number so I decided to just select Ly6C positive and negative monocytes and CD11c DC for single cell RNA sequencing.

I used 10x Genomics chromium platform for scRNAseq to generate the gene profile of the cells. The cells were clustered into cell types and annotated both manually and by automation using the SCA software and twelve clusters of cells were identified based on the expression of cell specific markers (See table 4.4 and figure 4.2 for the summary of the cell clusters and surface markers used for their identification). The clusters were DC1, DC2, plasmacytoid DC, Ly6C<sup>+</sup> monocytes, Ly6C<sup>-</sup> monocytes, T cells, B cells, NK cells, neutrophils, erythrocytes, basophils, and platelets. This was unexpected because I used exclusion of the lineage markers (CD45R/B220, Anti CD3, CD19, NK1.1, Ly6G, Siglec F) and the expression of Ly6C and CD11c to enrich for DC and monocytes. However, during bioinformatics analysis other cell clusters were identified showing that our enrichment was not efficient. Due to time and the focus of my research, I selected all subsets of DC and monocytes for further analysis. I used the dTomato gene expression to identify infected cells and separate them from bystander cells and uninfected cells. I compared all the clusters and different treatments. My results showed that all subsets of DC (DC1, DC2, plasmacytoid DC) and monocytes were infected by LCMV clone 13, both in acute and persistent infection (by expression of the

dTomato gene). Plasmacytoid DC had the highest proportion of infected cells whilst Ly6C<sup>+</sup> monocytes had the lowest proportion of infected cells (figure 4.4).



### 32: Figure 4.4 LCMV clone 13 Infection of DC and Monocytes Subsets In vivo

The proportion of LCMV clone 13 infected DC and monocyte cells were analysed using dTomato gene expression both in acute (48 hours) and persistence (14 days) infection. Only the cells that passed the bioinformatics quality control were used for this analysis. Each colour depicts a cell type. Two libraries from acute infection (Lib1(A) and Lib2(A)) and 4 from persistent infection (Lib2,4,5,6(P)) were analysed.

### 4.3.3 Cytokine Gene Expression Kinetics of DC and Monocytes Following LCMV clone 13 Infection

LCMV is known to cause immunosuppression in mice by impairing cytokine production and antigen presentation by APC. My *in vitro* data showed that this impairment was temporary and could be reactivated by secondary exposure to an RNA virus mimic such as poly (I:C) (see chapter 3). Most previous *in vivo* infection of mice by LCMV used bulk data or focused

on one or a few cell types thus limiting the ability to identify individual cell responses from different APC. Also, the response of bystander cells and uninfected cells is masked in a bulk analysis.

To characterize this response systematically, I calculated the differential gene expression between splenic cell populations from LCMV and/or poly (I:C) treated, and control mice for each of the subsets of DC and monocytes selected. I selected over 100 genes that were differentially expressed significantly (up or downregulated) across all the comparisons (adjusted p value less than 0.005). Using, ShinyGO version 0.61 software (<http://bioinformatics.sdstate.edu/go/>), I grouped these genes into three categories – antiviral genes, antigen presentation genes and inflammatory genes (figure 4.5 A-C).

#### **4.3.3.1 Antiviral Genes**

My results showed antiviral interferon stimulated genes (ISG) among the genes showing significantly increased expression. These ISGs were seen mostly in cells from poly (I:C) treated mice compared to cells from virus infected mice. The ISGs commonly upregulated were *ISG15*, *ISG20*, *IFITM3*, and *BST2* (see figure 4.5A). Increased expression was mostly seen with ISGs in pDC and Ly6C<sup>+</sup> monocytes; very few were upregulated in the conventional DC subsets.

#### **4.3.3.2 Antigen Presentation Genes**

Next, I looked at the genes involved in antigen presentation. My results showed that they were mostly upregulated in DC and not in monocytes. Interestingly, the significantly upregulated genes were expressed in pDC compared to conventional DC. These genes were upregulated in persistent infection and stimulation with poly I:C but not in acute LCMV infection (Figure 4.5).

#### **4.3.3.3 Inflammatory Genes**

Several genes involved in both pro and anti-inflammatory responses were significantly upregulated in my data. However, these genes were upregulated mostly in pDC and only when poly: (I:C) is given before LCMV clone 13 infection. The exception is the anti-inflammatory genes *HMOX1* upregulated only in Ly6C<sup>+</sup> monocytes.

1		Mouse Treatment					Gene
2	Cell cluster comparison	Acute LCMV	Acute poly (I:C)	Persistent LCMV	Persistent LCMV + poly (I:C)	poly (I:C) + Persistent LCMV	
3	DC1 vs Non infected DC1	NA	NA	NA	NA	NA	<i>ISG15</i>
4	DC2 vs Non infected DC2	NA	NA	NA	0.96	NA	
5	pDC vs Non infected pDC	NA	1.75	NA	NA	2.17	
6	Ly6C- MO vs Non infected Ly6C- MO	NA	NA	NA	NA	NA	
7	Ly6C+ MO vs Non infected Ly6 MO+	NA	1.13	NA	NA	1.07	
8							
9	DC1 vs Non infected DC1	NA	NA	NA	NA	NA	<i>ISG20</i>
10	DC2 vs Non infected DC2	NA	NA	NA	0.73	NA	
11	pDC vs Non infected pDC	NA	1.12	NA	NA	1.57	
12	Ly6C- MO vs Non infected Ly6C- MO	NA	NA	NA	NA	NA	
13	Ly6C+ MO vs Non infected Ly6 MO+	NA	0.82	NA	NA	0.77	
14							
15	DC1 vs Non infected DC1	NA	NA	NA	NA	NA	<i>IFITM3</i>
16	DC2 vs Non infected DC2	NA	NA	NA	0.73	NA	
17	pDC vs Non infected pDC	NA	NA	NA	NA	2.58	
18	Ly6C- MO vs Non infected Ly6C- MO	NA	NA	NA	1.82	NA	
19	Ly6C+ MO vs Non infected Ly6 MO+	NA	NA	NA	NA	NA	
20							
21	DC1 vs Non infected DC1	NA	NA	NA	0.58	NA	<i>BST2</i>
22	DC2 vs Non infected DC2	NA	NA	NA	NA	NA	
23	pDC vs Non infected pDC	NA	2.06	NA	NA	1.73	
24	Ly6C- MO vs Non infected Ly6C- MO	NA	NA	NA	NA	NA	
25	Ly6C+ MO vs Non infected Ly6 MO+	NA	0.99	NA	NA	0.75	
26							
27	DC1 vs Non infected DC1	NA	NA	NA	NA	NA	<i>ZBP1</i>
28	DC2 vs Non infected DC2	NA	NA	NA	0.43	NA	
29	pDC vs Non infected pDC	NA	1.22	NA	NA	1.31	
30	Ly6C- MO vs Non infected Ly6C- MO	NA	NA	NA	NA	NA	
31	Ly6C+ MO vs Non infected Ly6 MO+	NA	0.77	NA	NA	0.82	
32							
33	DC1 vs Non infected DC1	NA	NA	NA	0.71	NA	<i>lfi2712a</i>
34	DC2 vs Non infected DC2	NA	NA	NA	1.23	NA	
35	pDC vs Non infected pDC	NA	1.74	NA	NA	2.10	
36	Ly6C- MO vs Non infected Ly6C- MO	NA	NA	NA	NA	NA	
37	Ly6C+ MO vs Non infected Ly6 MO+	NA	1.05	1.85	NA	0.87	
38							
39	DC1 vs Non infected DC1	NA	NA	NA	NA	NA	<i>lfit3</i>
40	DC2 vs Non infected DC2	NA	NA	NA	0.94	NA	
41	pDC vs Non infected pDC	NA	1.66	NA	NA	1.65	
42	Ly6C- MO vs Non infected Ly6C- MO	NA	NA	NA	NA	NA	
43	Ly6C+ MO vs Non infected Ly6 MO+	NA	0.96	NA	NA	1.13	
44							
45	DC1 vs Non infected DC1	NA	NA	NA	NA	NA	<i>OAS3</i>
46	DC2 vs Non infected DC2	NA	NA	NA	NA	NA	
47	pDC vs Non infected pDC	NA	NA	NA	NA	1.27	
48	Ly6C- MO vs Non infected Ly6C- MO	NA	NA	1.31	NA	NA	
49	Ly6C+ MO vs Non infected Ly6 MO+	NA	NA	NA	NA	NA	
50							
51	DC1 vs Non infected DC1	NA	NA	NA	NA	NA	<i>OAS1</i>
52	DC2 vs Non infected DC2	NA	NA	NA	NA	NA	
53	pDC vs Non infected pDC	NA	NA	NA	NA	0.96	
54	Ly6C- MO vs Non infected Ly6C- MO	NA	NA	NA	NA	NA	
55	Ly6C+ MO vs Non infected Ly6 MO+	NA	NA	NA	NA	NA	
56							
57	DC1 vs Non infected DC1	NA	NA	NA	NA	NA	<i>OASL1</i>
58	DC2 vs Non infected DC2	NA	NA	NA	NA	NA	
59	pDC vs Non infected pDC	NA	NA	NA	NA	1.11	
60	Ly6C- MO vs Non infected Ly6C- MO	NA	NA	NA	NA	NA	
61	Ly6C+ MO vs Non infected Ly6 MO+	NA	NA	NA	NA	NA	
62							
63	DC1 vs Non infected DC1	NA	NA	NA	NA	NA	<i>MX1</i>
64	DC2 vs Non infected DC2	NA	NA	NA	NA	NA	
65	pDC vs Non infected pDC	NA	NA	NA	NA	0.90	
66	Ly6C- MO vs Non infected Ly6C- MO	NA	NA	NA	NA	NA	
67	Ly6C+ MO vs Non infected Ly6 MO+	NA	NA	NA	NA	NA	
68							
69	DC1 vs Non infected DC1	NA	NA	NA	NA	NA	<i>LY6E</i>
70	DC2 vs Non infected DC2	NA	NA	NA	NA	NA	
71	pDC vs Non infected pDC	NA	NA	NA	NA	0.83	
72	Ly6C- MO vs Non infected Ly6C- MO	NA	NA	NA	NA	NA	
73	Ly6C+ MO vs Non infected Ly6 MO+	NA	NA	NA	NA	NA	
74							

75	DC1 vs Non infected DC1	NA	NA	NA	NA	NA	<i>RSAD2</i>
76	DC2 vs Non infected DC2	NA	NA	NA	NA	NA	
77	pDC vs Non infected pDC	NA	NA	NA	NA	1.08	
78	Ly6C- MO vs Non infected Ly6C- MO	NA	NA	NA	NA	NA	
79	Ly6C+ MO vs Non infected Ly6 MO+	NA	NA	NA	NA	NA	
80							
81	DC1 vs Non infected DC1	NA	NA	NA	NA	NA	<i>IRF7</i>
82	DC2 vs Non infected DC2	NA	NA	NA	NA	NA	
83	pDC vs Non infected pDC	NA	NA	NA	NA	1.69	
84	Ly6C- MO vs Non infected Ly6C- MO	NA	NA	NA	NA	NA	
85	Ly6C+ MO vs Non infected Ly6 MO+	NA	NA	NA	NA	NA	
86							
87	DC1 vs Non infected DC1	NA	NA	NA	NA	NA	<i>STAT1</i>
88	DC2 vs Non infected DC2	NA	NA	NA	0.38	NA	
89	pDC vs Non infected pDC	NA	1.05	NA	NA	0.83	
90	Ly6C- MO vs Non infected Ly6C- MO	NA	NA	NA	NA	NA	
91	Ly6C+ MO vs Non infected Ly6 MO+	NA	0.64	NA	NA	NA	

### 33: Figure 4.5A Antiviral Gene Expression (fold change Log2)

1	2	3 Mouse Treatment					Gene
		4 Acute LCMV	5 Acute poly (I:C)	6 Persistent LCMV	7 Persistent LCMV + poly (I:C)	8 poly (I:C) + Persistent LCMV	
3	DC1 vs Non infected DC1	NA	1.97	2.09	2.19	NA	RELB
4	DC2 vs Non infected DC2	NA	NA	1.18	1.41	NA	
5	pDC vs Non infected pDC	NA	NA	NA	NA	NA	
6	Ly6C- MO vs Non infected Ly6C-	NA	NA	NA	NA	NA	
7	Ly6C+ MO vs Non infected Ly6 M NA	NA	NA	NA	NA	NA	
8							
9	DC1 vs Non infected DC1	NA	NA	NA	NA	NA	CD74
10	DC2 vs Non infected DC2	NA	NA	NA	NA	NA	
11	pDC vs Non infected pDC	NA	NA	NA	NA	3.77	
12	Ly6C- MO vs Non infected Ly6C-	NA	NA	NA	NA	NA	
13	Ly6C+ MO vs Non infected Ly6 M NA	NA	NA	NA	NA	NA	
14							
15	DC1 vs Non infected DC1	NA	NA	NA	NA	NA	CD40
16	DC2 vs Non infected DC2	NA	NA	NA	NA	NA	
17	pDC vs Non infected pDC	NA	NA	NA	NA	0.82	
18	Ly6C- MO vs Non infected Ly6C-	NA	NA	NA	NA	NA	
19	Ly6C+ MO vs Non infected Ly6 M NA	NA	NA	NA	NA	NA	
20							
21	DC1 vs Non infected DC1	NA	NA	NA	NA	NA	H2-D1
22	DC2 vs Non infected DC2	NA	NA	NA	NA	NA	
23	pDC vs Non infected pDC	NA	0.31	NA	NA	0.34	
24	Ly6C- MO vs Non infected Ly6C-	NA	NA	NA	NA	NA	
25	Ly6C+ MO vs Non infected Ly6 M NA	NA	NA	NA	NA	NA	
26							
27	DC1 vs Non infected DC1	NA	NA	NA	NA	NA	H2-K
28	DC2 vs Non infected DC2	NA	NA	NA	NA	NA	
29	pDC vs Non infected pDC	NA	0.41	NA	NA	0.34	
30	Ly6C- MO vs Non infected Ly6C-	NA	NA	NA	NA	NA	
31	Ly6C+ MO vs Non infected Ly6 M NA	NA	NA	NA	NA	NA	
32							
33	DC1 vs Non infected DC1	NA	NA	NA	NA	NA	H2-Aa
34	DC2 vs Non infected DC2	NA	NA	NA	NA	NA	
35	pDC vs Non infected pDC	NA	NA	NA	NA	3.02	
36	Ly6C- MO vs Non infected Ly6C-	NA	NA	NA	NA	NA	
37	Ly6C+ MO vs Non infected Ly6 M NA	NA	NA	NA	NA	NA	
38							
39	DC1 vs Non infected DC1	NA	NA	NA	NA	NA	H2-AB
40	DC2 vs Non infected DC2	NA	NA	NA	NA	NA	
41	pDC vs Non infected pDC	NA	NA	NA	NA	3.01	
42	Ly6C- MO vs Non infected Ly6C-	NA	NA	NA	NA	NA	
43	Ly6C+ MO vs Non infected Ly6 M NA	NA	NA	NA	NA	NA	
44							
45	DC1 vs Non infected DC1	NA	NA	NA	NA	NA	H2-Ea
46	DC2 vs Non infected DC2	NA	NA	NA	NA	NA	
47	pDC vs Non infected pDC	NA	NA	NA	NA	1.05	
48	Ly6C- MO vs Non infected Ly6C-	NA	NA	NA	NA	NA	
49	Ly6C+ MO vs Non infected Ly6 M NA	NA	NA	NA	NA	NA	
50							

34: Figure 4.5B Antigen presentation gene expression (fold change Log2)

1	Cell cluster comparison	Mouse Treatment				Gene
		Acute LCMV	Acute poly (I:C)	Persistent LCMV	Persistent LCMV + poly (I:C)	
2	DC1 vs Non infected DC1	NA	NA	NA	NA	<i>CCL5</i>
3	DC2 vs Non infected DC2	NA	NA	NA	NA	
4	pDC vs Non infected pDC	NA	NA	NA	NA	1.17
5	Ly6C- MO vs Non infected Ly6C- MO	NA	NA	NA	NA	
6	Ly6C+ MO vs Non infected Ly6 MO+	NA	NA	NA	NA	
7						
8	DC1 vs Non infected DC1	NA	NA	NA	NA	<i>CCL6</i>
9	DC2 vs Non infected DC2	NA	NA	NA	NA	
10	pDC vs Non infected pDC	NA	NA	NA	NA	0.85
11	Ly6C- MO vs Non infected Ly6C- MO	NA	NA	NA	NA	
12	Ly6C+ MO vs Non infected Ly6 MO+	NA	NA	NA	NA	
13						
14	DC1 vs Non infected DC1	NA	NA	NA	NA	<i>CXCL10</i>
15	DC2 vs Non infected DC2	NA	NA	NA	NA	
16	pDC vs Non infected pDC	NA	NA	NA	NA	1.69
17	Ly6C- MO vs Non infected Ly6C- MO	NA	NA	NA	NA	
18	Ly6C+ MO vs Non infected Ly6 MO+	NA	NA	NA	NA	
19						
20	DC1 vs Non infected DC1	NA	NA	NA	NA	<i>ANXA5</i>
21	DC2 vs Non infected DC2	NA	NA	NA	NA	
22	pDC vs Non infected pDC	NA	NA	NA	NA	0.82
23	Ly6C- MO vs Non infected Ly6C- MO	NA	NA	NA	NA	
24	Ly6C+ MO vs Non infected Ly6 MO+	NA	NA	NA	NA	
25						
26						
27	DC1 vs Non infected DC1	NA	NA	NA	NA	<i>Mapkapk2</i>
28	DC2 vs Non infected DC2	NA	NA	NA	NA	
29	pDC vs Non infected pDC	NA	NA	NA	NA	1.10
30	Ly6C- MO vs Non infected Ly6C- MO	NA	NA	NA	NA	
31	Ly6C+ MO vs Non infected Ly6 MO+	NA	NA	NA	NA	
32						
33	DC1 vs Non infected DC1	NA	NA	NA	NA	<i>APOE</i>
34	DC2 vs Non infected DC2	NA	NA	NA	NA	
35	pDC vs Non infected pDC	NA	NA	NA	NA	1.28
36	Ly6C- MO vs Non infected Ly6C- MO	NA	NA	NA	NA	
37	Ly6C+ MO vs Non infected Ly6 MO+	NA	NA	NA	NA	
38						
39	DC1 vs Non infected DC1	NA	NA	NA	NA	<i>TGFB</i>
40	DC2 vs Non infected DC2	NA	NA	NA	NA	
41	pDC vs Non infected pDC	NA	NA	NA	NA	0.88
42	Ly6C- MO vs Non infected Ly6C- MO	NA	NA	NA	NA	
43	Ly6C+ MO vs Non infected Ly6 MO+	NA	NA	NA	NA	
44						
45	DC1 vs Non infected DC1	NA	NA	NA	NA	<i>HMOX1</i>
46	DC2 vs Non infected DC2	NA	NA	NA	NA	
47	pDC vs Non infected pDC	NA	NA	NA	NA	
48	Ly6C- MO vs Non infected Ly6C- MO	NA	NA	NA	NA	
49	Ly6C+ MO vs Non infected Ly6 MO+	NA	NA	NA	NA	0.65

### 35: Figure 4.5C Inflammatory gene expression (fold change Log2)

#### Figure 4.5(A-C) Single cell RNA sequencing and gene expression analysis of DC and Monocytes subsets infected with LCMV clone 13 (GFP) and or stimulated with poly (I:C) in vivo

Mouse splenic cells (DC and monocytes) sorted from LCMV clone 13 infected and uninfected mice as well as poly (I:C) treated mice. Single cell RNA sequencing was carried out on these cells using the 10X genomics platform. Expression of transcripts from the libraries were analysed and expressed as log2 difference in gene expression between infected and uninfected cells. Selected genes that were differentially expressed significantly (up or

downregulated) across all the comparisons (adjusted p value less than 0.005) were grouped into three categories (A-antiviral, B-antigen presentation and C- inflammatory genes) using ShinyGO version 0.61 software (<http://bioinformatics.sdstate.edu/go/>). Positive value (coloured) depicts upregulation while NA is non significantly expressed values.

Note: Only the library that passed the QC were analysed and only the genes that were differentially expressed significantly are shown.

### **4.3.3 Biological consequences of LCMV infection in APC**

I submitted mouse splenic tissues for histopathology to compare the pathological changes associated with acute and persistent LCMV infection as well as the effect this has on a secondary stimulation with poly (I:C). Due to COVID19 lockdown and travel restrictions, I was unable to analyse these samples within the time frame provided to complete my thesis.

## **4.4 Discussion**

LCMV preferentially infects APC. In the spleen, LCMV clone 13 preferentially infects DEC205<sup>+</sup> DC, while the Armstrong strain has a greater tropism for F4/80 positive macrophages in the red pulp of the spleen (193). Thus, there is heterogeneity in the interaction of LCMV with different APCs. However, how this is reflected in the individual subsets of APC is not clear. The effect of LCMV on different subsets is also variable; eg LCMV clone 13 preferentially induced and sustained the expression of immunosuppressive receptors including PD-L1 in CD8 $\alpha$ <sup>-</sup> DC (DC2) but not in CD8 $\alpha$ <sup>+</sup> DC (DC1). In my *in vitro* data, I demonstrated the heterogeneity of the BMDC cellular response to both LCMV clone 13 and Armstrong (see chapter 3). In the work in this chapter, I used a mouse Cre-LoxP system and single cell RNA sequencing technology to determine the cellular niche of LCMV among different splenic APC. I also described the variation and kinetics of cytokine gene expression from different APC at the single cell level. I further analysed the impact of a primary LCMV clone 13 infection on splenic APCs to secondary activation by a TLR-3 agonist (poly (I:C)).

I used the expression of Ly6C and CD11c to select all splenic DC and monocytes subsets for analysis by RNA-seq (See figure 4.1 for FACS sorting procedure). I also used specific

surface lineage markers (CD3, CD19, NK1.1, Ly6G, Siglec F) to exclude other cells leaving only DC and monocytes. However, from the gene expression analysis and clustering, apart from DC and monocytes, other cells like T cells, NK cells, and B cells were also recovered. This may be due to the lack of fine specificity of the expression of certain of surface markers that can be shared by one or two different cell types. It may also be due to poor enrichment for selected cells during sorting. I used the gene expression transcripts both manually and automated (using the SCSA software (Cao et al., (2020)) to identify the cell clusters (see table 4.6). I selected the cell clusters based on top five expressed genes and compared it with the clusters selected by SCSA software. This approach seem more accurate than the use of surface marker expression however, some of the genes are not specific to a particular cells and some are shared by two or three different cells. For example, *Ifitm* is highly expressed Ly6<sup>+</sup>MO and basophils. For future studies, I will recommend a system that combines both the surface marker expression and genes transcript expression during FACS to identify cell types example single-cell mRNA sequencing (scmRNAseq) and cytometry by time-of-flight (CyTOF)(29).

Using RNAseq data, dTomato gene expression was detected in all subsets of splenic DC and monocytes showing that all APC subsets can be infected by LCMV clone 13 (figure 4.4). No dTomato gene expression was seen in T cells, NK cells or B cells (data shown). Plasmacytoid DC had the highest proportion of cells infected whilst Ly6C<sup>-</sup> monocytes the least. This result agrees with previous data showing preferential infection by LCMV clone 13 of pDC generated *in vitro* and in an *in vivo* infection (234). However, the reason for preferential infection by LCMV clone 13 of pDC is yet to be elucidated and will require further studies. A caveat to the preferential infection of pDC by LCMV clone 13 in my result is that only the cells that passed the sequencing and bioinformatics QC were analysed so other factors may have affected my result.

Furthermore, my *in vitro* LCMV infection of APC study showed impaired cytokine production from both DC and macrophages (see chapter 3). Similar results have been demonstrated in an *in vivo* study as well. LCMV impaired cytokine production and antigen presentation in all APC by 5 days post infection(215). However, all these data were produced from bulk analysis of different splenic APCs. Whether this impaired cytokine production is seen in individual cells including infected and bystander cells is not known. Using hashtag antibody labelling of cells from individual mice and single cell RNA sequencing, I interrogated individual splenic APC cells and described their cytokine gene expression.

Following infection with LCMV clone 13 and/or treatment with poly (I:C), I selected the genes that were differentially expressed (upregulated or downregulated when compared with uninfected cells) from all the comparisons and grouped them into three categories for analysis (antiviral genes, antigen presentation genes and inflammatory genes) (Figure 4.4 A-C).

My results agreed with the data from *in vitro* LCMV infection of APC. There was no induction of antiviral inflammatory cytokine gene expression in all the subsets of splenic DC and monocytes by acute or persistent LCMV clone 13 infection. However, when stimulated with poly (I:C), antiviral cytokine genes were upregulated in most of the cells. Most upregulation of the antiviral cytokines was seen in plasmacytoid DC and Ly6C<sup>+</sup> monocytes and not from DC1 and DC2. The antiviral ISGs upregulated in DC1 are *BST2* and *Ifi2712a*. A previous study demonstrated that most antiviral ISGs and inflammatory cytokine mRNAs are present as early as day 1 post infection with LCMV clone 13 and are mainly produced by plasmacytoid DC and less from conventional DC (234). The lack of antiviral cytokines from LCMV infected group in my experiment may be due to the timing. I harvested the splenic cells 48 h post infection instead of the 24 h as seen in the previous experiment. However, at 24 h post infection in my experiment, I was unable to detect infected cells by dTomato expression by FACS and I did not assess the dTomato transcripts after 24 hours by RNAseq. Because I harvested splenic cells 48 h post infection (which is the time required for enough dTomato protein to be expressed), I may not see cytokine gene upregulation both from infected and bystander cells. For future studies using the LCMV model, infected cells should be assessed at 24 hours post infection using gene transcript from RNAseq. Even though, the dTomato protein may be low or non-detectable at 24 hours post infection, their gene transcript will be expressed and used to select infected cells. The advantage of this approach is that the dTomato genes are only expressed following integration of the Cre recombinase from the virus and the LoxP site on the mouse cell thus depicts an active infection which can be differentiated from bystander cells with just viral gene signature(233).

Immunosuppression by LCMV clone 13 is associated with impaired inflammatory cytokine response and antigen presentation by APC(235). My results showed no upregulation of pro and anti-inflammatory cytokine genes following both acute and persistent LCMV clone 13 infection. However, in the presence of poly: (IC) some inflammatory chemokine genes (*CCL5, CCL6, CXCL10, ANXA*) were upregulated in pDC and they were not downregulated by infection with LCMV clone 13. A previous study implicated pDC as the major source of pro inflammatory cytokine response 18 hours post infection with LCMV clone 13 and Armstrong

thereby agreeing with my result(143). The two anti-inflammatory that were significantly upregulated were *HMOX1* in Ly6C<sup>+</sup> monocytes and *TGFB* in pDC (see figure 4.4C). Further studies to elucidate the role and dynamics of pro versus anti inflammatory cytokines in LCMV infection is necessary.

On the other hand, genes associated with antigen presentation function were mostly upregulated in DC compared to monocytes. Surprisingly, most of them were upregulated in pDC especially following poly: (I:C) treatment. pDC is specialised in interferon production while conventional DC are known for antigen presentation(20). The reason for the upregulation of genes associated with antigen presentation in pDC and not conventional DC is not clear from my results and will require further studies to elucidate their roles in pDC. A previous study has attributed the antigen presentation role of pDC to contamination by a rare subset of DC called pre-DC in human so it is possible that this may be the case with my result(29).

However, note that none of the genes associated with antigen presentation were upregulated following acute and persistent LCMV clone 13 infection. This is in line with my *in vitro* result showing that LCMV infection impairs expression of antigen presentation markers in DC and macrophage (see chapter 3).

Having established the impairment of cytokine production from APC by LCMV clone 13 in both *in vitro* and *in vivo* infection, I investigated the effect of this impairment on secondary stimulation by a RNA virus mimic. A previous study by Zuniga et al. (2008) showed that primary infection by LCMV clone 13 impaired secondary interferon responses to cytomegalovirus (236). My *in vivo* result did not correlate with this. When LCMV clone 13 infected mice were stimulated with poly (I:C) both antiviral ISG and inflammatory cytokines were upregulated in plasmacytoid DC and Ly6C<sup>+</sup> monocytes. Also, subsequent infection with LCMV clone 13 after 24 h pre-stimulation with poly (I:C) did not impair or reduce antiviral ISG and inflammatory gene expression. The reason for the difference in the effect of LCMV clone 13 on response to a secondary stimulation is not clear but may be due to different stimulator and gene expression pathways (synthetic agonist versus pathogen and TLR-3 versus TLR-9 pathway). However, my results correlated with what was seen in my *in vitro* LCMV infection, antigen presentation genes were mostly upregulated in DC while antiviral and inflammatory cytokines were upregulated in pDC and monocytes. With LCMV

infection, both antigen presentation and cytokine production are impaired, but the impairment is not permanent and can be overridden by stimulation with poly (I:C).

## 4.5 Conclusion

A lot of immunology and virology research has been based on the LCMV model which has contributed immensely to the field. Previous studies described different strains of LCMV and also showed preferential cellular niches for the different strains. LCMV clone 13 causes expression of immunosuppressive cytokines thereby impairing T cell responses. However, most of the data from the LCMV model are from bulk or specific cell analysis. This system obliterates the contribution of the individual cell to the collective immune response. For example, in bulk analysis bystander cell responses are masked (222). In this chapter, I used a combination of a Cre-LoxP system and RNA single cell sequencing to separate bystander cells from infected cells. I used the expression of Ly6C and CD11c to select all splenic DC and monocytes for analysis by RNA-seq. I also used specific surface lineage markers (CD3, CD19, NK1.1, Ly6G, Siglec F) to exclude other cells leaving only DC and monocytes. However, from the gene expression analysis and clustering, apart from DC and monocytes, other cells like T cells, NK cells, and B cells were also recovered. This may be due to non specificity in the expression of many of surface markers which is shared by one or two different cells. It may also be due to poor enrichment for selected cells during sorting. I suggested a system that combines both surface marker and gene expression transcript for identification of cells from RNAseq data.

For the purpose of my thesis, and the limited availability of time, I focused on only DC and monocytes. It will be interesting to analyse gene expression of other splenic cells following LCMV and or poly (I:C) treatment. This will be undertaken for publication post PhD.

My results confirmed the preferential infection of APC by LCMV clone 13 and showed that the plasmacytoid DC is the major cell infected among the DC and monocytes. It also validated the impaired cytokine response associated with LCMV infection of APC and further confirmed that this impairment is temporary and can be overridden by a TLR-3 agonist poly (I:C). Furthermore, both my *in vitro* and *in vivo* LCMV infection emphasises the division of labour among the splenic APC; while conventional DC focus on antigen

presentation, antiviral and inflammatory cytokine production is the function of plasmacytoid DC and monocytes.

My results and other studies have further emphasised the importance of studying cell pathogen interactions at the single cell level (237,238). Thus, there is need a to revisit some of the previously published data generated from bulk cell analysis if we consider the dynamic nature of the immune system. In the era of 'omics and high throughput technology, understanding the cellular immune response at the single cell level will help us to be precise in designing therapeutics and vaccines using different immune components.

# Chapter 5

## General Discussion and Concluding remarks

### 5.1 Summary of results

This thesis set out to explain virus-host interaction with a focus on antigen-presenting cells (APC) and the LCMV model. The population of different APC play a significant role in the immune response, being the first cells that detect pathogen invasion and present the antigen to the cells of the adaptive immune system for activation and clearance of the pathogen (2). Thus, their unique function as the receptionist and in early induction of both innate and adaptive immunity makes them critical players in directing the outcome of an immune response. The LCMV model, on the other hand, is a well established model system for studying the immune system and its interaction with pathogen. It has contributed to some fundamental discoveries in the field of immunology and virology; for example, understanding the role of the major histocompatibility complex (209).

In this thesis, I investigated the interaction of APC (DC and macrophage/monocytes) with LCMV at the *in vitro*, *in vivo* and single-cell level. Though the LCMV model has been a critical player in the field of immunology and virology, most of the data from the model are from bulk analyses and made use of available resources at the time. At the time of conceiving this project, an important publication by Helft *et al.* (2015) (154) showed that GM-CSF treated *in vitro* BM derived cells are a heterogeneous mix of both DC and macrophages as opposed to the previous view that they were mainly DC whilst macrophages are generated only by M-CSF growth factor.

I began by validating the heterogeneity of *in vitro* BM derived cells. My result confirmed the heterogeneity that Helft *et al.* (2015) had shown and that it was present after differentiating cells in the presence of all the growth factors commonly used for generating *in vitro* BM-DC. Using LCMV and poly (I:C), I also confirmed functional differences between the DC (BM-DC) and macrophage (BM-M) subsets. While BM-DC were better at antigen presentation to T cells, BM-M were more efficient cytokine producers. Interestingly, I identified a previously

unrecognised third subset which neither expressed surface marker CD11c nor MHC class II. This third subset I termed the double negative group (DN), and transcriptional and functional profiling suggested that it may be an immature form of the BM-M subset. Given the timeline of my thesis, after graduation I will explore this new subset, to confirm the identity of the double negative subsets and their functional profile.

Both acute (Armstrong) and chronic (clone 13) strains of LCMV impaired cytokine production and antigen presentation in all three groups of BM-derived cells. My findings suggested that this impairment was temporary in the BM-M and permanent in the BM-DC populations. The BM-M group produced antiviral cytokine genes following secondary stimulation with poly (I:C) while the BM-DC group did not, likely due to their terminally differentiated state. The reason for this variation will also require further elucidation.

Furthermore, using a Cre-LoxP system and single-cell RNA sequencing, I undertook the study of LCMV infection of APC *in vivo*. In this case, I only used the LCMV clone 13. The Cre-LoxP system helped me to differentiate a productively infected cell from bystander cells using the cellular RNA signature. My *in vivo* result correlated with the *in vitro* result, LCMV clone 13 infected all subsets of splenic DC and macrophages. Similarly, to a previous study, plasmacytoid DC were the most infected of all the splenic DC and monocytes (234). This is interesting because plasmacytoid DC are the major Type 1 interferon producing population of cells and this important antiviral cytokine has been demonstrated to control LCMV and other RNA viruses including SARS-CoV-2(239,240). Understanding the factors that make plasmacytoid DC more receptive to LCMV clone 13 will be an excellent future study.

LCMV clone 13 also impaired expression of antiviral and inflammatory cytokine genes as well as antigen presentation genes in APC *in vivo*. Similar, to my *in vitro* result, this impairment was temporary and was overridden by secondary stimulation with poly (I:C). This result contrasted with a previous study where primary infection with LCMV clone 13 impaired cytokine responses following secondary infection by cytomegalovirus (236). The reason for the variation in outcome is not known and may be due to difference in the type of stimulating agent (pathogen versus synthetic mimetic). Cytomegalovirus itself has been shown to induce immunosuppression following superinfection with influenza virus (241).

Furthermore, in this thesis, I utilised a new approach to multiplexing complex cell populations and experimental conditions known as cell hashing. Cell hashing involves the use of oligonucleotide-tagged antibodies (hashtags oligonucleotide HTO) to pool different cells

from different experimental conditions for single cell RNA sequencing. It is easy, and efficient and complex biological questions can be answered quickly.

Taken together, this thesis has shown the division of labour among APC in their interaction with the virus. It also demonstrated the power of single-cell sequencing technology and how it is helping to recognise the dynamic nature of the immune response even at the single-cell transcriptome level. It also demonstrated the power of the cell hashing approach in multiplexing complex experimental conditions. With more availability of high-throughput technology, there is a need to revisit some of the previous studies that were based on bulk analyses of the immune response. Understanding immunity, at the single-cell level, will help us target immune components efficiently and understand pathogen invasion precisely in different tissues and immune environments.

## **5.2 Limitations to this study**

There were several challenges during this project. The primary objectives of this thesis were to describe the interaction of APC with the RNA virus LCMV at different levels – *in vitro* and *in vivo* in specific single cell types. I managed to finish the *in vitro* part of the study, though a change of government in my country affected the funding for this study. My scholarship was halted for over two years, making it difficult to continue with the work. During this time, the BSL3 unit at the Cambridge Biomedical Services (CBS) (the only available BSL3 unit for *in vivo* BSL3 virus infection) was unavailable. It took nine months to reactivate this CL3 animal lab, which further delayed commencing the *in vivo* aspect of this project. Despite all of these drawbacks, I persisted and focussed on the main objective of the thesis. I used the available time to characterise the working virus stock from the isolate kindly provided by Prof. Juan Carlos de la Torre (The Scripps Research Institute, La Jolla, CA). I also bred enough Adult C57BL/6J (Rosa26floxedSTOPtdTomato) mice ready for the study. However, by the time my funding problem was resolved, and the BSL3 CBS unit was ready, I had lost over two years of the time allocated for this project. This did not deter me, and I went on to perform the *in vivo* experiment, which went very well. Tragically the COVID-19 pandemic delayed the time from sequencing to availability of my data for analysis.

There are some aspects of the thesis that I was unable to execute because of these setbacks. For example, I was unable to validate the data from the single-cell RNA sequencing in another system such as PCR or even at the protein level. Also, I could not process the

histopathology slides I would have liked, to demonstrate the pathology of the LCMV virus in the spleen both as primary infection and the effects on secondary stimulation with poly (I:C).

Furthermore, it would have been nice to also look at the gene profile of other splenic cells such as T cells, B cells and NK cells following LCMV infection. I was not able to look at these other cell populations because of the deadline to submit this thesis.

Other limitations were associated with the technology and experimental design utilised for this study. The single cell RNA sequencing technology has revolutionised the way we do science(226,238). However, this comes with certain challenges. For this study, FACS sorting was used to recover rare cell populations from the spleen for single cell RNA-seq. However, this introduced processing delays as well as perturbations of the cells. The impact of this on the gene expression of the cell is not known considering that immune response or cell pathogen interactions is dynamic and happens in real time. The cell hashing approach is an efficient way of pooling different cells from different experimental conditions for single cell RNAseq. However, it comes with its own challenges. For example, some HTO may not have tagged cells properly or may be transferred to other cells and this will appear as non-tagged cells or infected cells carrying a hashtag that was used to tag an uninfected cell. These cells will not pass the bioinformatic analysis QC and will be excluded from further analysis. For example, in my study, I excluded Library 1 and 3 because they have low number of hashtag positive cells.

Furthermore, the Cre-LoxP system enabled me to differentiate between infected cells and bystander cells using the expression of the dTomato. However, there was limitation with this system because it takes about 48 hours to for dTomato to be fully expressed and by then the interferon cytokine response would have waned. Also, how much cre is needed for dTomato to be switched on ie what level of replication is needed to see red cells. Could I have relied on the LCMV RNA signature or dTomato gene expression and will that be available at 24 hours post infection when the interferon cytokines are detected?

Overall, despite the delays and setbacks, I was able to validate the heterogeneity of *in vitro* BMDC and their functional responses. Previous work has only used synthetic mimics and had focused only on one of the growth factors. My results not only confirmed this heterogeneity across all the growth factors commonly used to generate BMDC, but also showed that there were functional differences in the response to actual pathogen, and not just synthetic mimics such as poly (I:C). Furthermore, my *in vivo* experiment has now become the foundation and

pilot for working with BSL3 pathogens in the high containment animal lab and in establishing the *in vivo* single-cell level RNA-seq technology in the lab.

## **5.5 Concluding remarks and future work**

The LCMV model has had a major impact on the field of immunology and virology. This thesis has taken this model further by incorporating single cell RNA sequencing technology in the study of immune function using this animal model.

This project has been a great learning process for me. I have acquired excellent skills working with a virus at high containment and the application of cutting-edge techniques in this environment. I can grow and propagate viruses in high containment and use them for both *in vitro* and *in vivo* infections. I have also acquired knowledge and skills in flow cytometric analysis and RNA single-cell sorting and analysis of immune cells.

LCMV may not be a highly contagious or pathogenic virus, as the potential risks are mostly seen in immunocompromised patients, however, another old-world Arenavirus which shares about 60 % homology with LCMV is Lassa fever virus (LASV). LASV is a major viral haemorrhagic fever (VHF) agent endemic in West Africa. LASV accounts for more than 300,000 cases of LF and up to 5,000 - 10,000 deaths per year in West Africa (242).

LCMV presents an excellent model to study the biology and interaction of Lassa fever with the host. In the near future, I will apply these skills and knowledge to an ongoing BBSRC funded project looking at the immune correlates of protection to LASV in Nigeria. This project is using methodologies from my thesis to study the interaction of LASV and immune cells at the single cell level. Thus, my thesis has provided a solid foundation for studying a highly pathogenic, high consequence human Arenaviruses such as Lassa fever virus.

Finally, this thesis has further emphasised the need to consider the dynamic nature and contribution of an individual APC to the overall immune response. With more advancement in single-cell technology, we can be precise and efficient in understanding and therapeutically targeting APC tropic RNA viruses.

# Bibliography

1. Parkin J, Cohen B. An overview of the immune system. *Lancet*. 2001;357:1777–89.
2. Chaplin DD. Overview of the immune response. *J Allergy Clin Immunol* [Internet]. 2010;125(2):S3–23. Available from: <http://dx.doi.org/10.1016/j.jaci.2009.12.980>
3. Turvey SE, Broide DH. Innate immunity. *J Allergy Clin Immunol* [Internet]. 2010;125(2):S24–32. Available from: <http://dx.doi.org/10.1016/j.jaci.2009.07.016>
4. Loré K, Lin A. Granulocytes : New Members of the Antigen-Presenting Cell Family. *Front Immunol*. 2017;8(1781):1–8.
5. Reis E Sousa C. Dendritic cells in a mature age. *Nat Rev Immunol*. 2006;6(6):476–83.
6. Steinman RM, Gutchinov B, Witmer MD, Nussenzweig MC. Dendritic cells are the principle stimulators mixed leukocyte reaction of the primary in mice. *J Exp MED*. 1983;157(February):613–27.
7. Pozzi L-AM, Maciaszek JW, Rock KL. Both Dendritic Cells and Macrophages Can Stimulate Naive CD8 T Cells In Vivo to Proliferate, Develop Effector Function, and Differentiate into Memory Cells. *J Immunol*. 2005;175(4):2071–81.
8. Delamarre L, Pack M, Chang H, Mellman I, Trombetta ES. Differential lysosomal proteolysis in antigen-presenting cells determines antigen fate. *Science* (80- ). 2005;307(5715):1630–4.
9. Mccurley N, Mellman I. Monocyte-derived dendritic cells exhibit increased levels of lysosomal proteolysis as compared to other human dendritic cell populations. *PLoS One*. 2010;5(8):e11949.
10. Alculumbre SG, Saint-andré V, Domizio J Di, Vargas P, Sirven P, Bost P, et al. Diversification of human plasmacytoid predendritic cells in response to a single stimulus. *Nat Immunol* [Internet]. 2018;19:63–75. Available from: <http://dx.doi.org/10.1038/s41590-017-0012-z>
11. Jakubzick C V, Randolph GJ, Henson PM. Monocyte differentiation and antigen-presenting functions. *Nat Publ Gr* [Internet]. 2017;17(6):349–62. Available from: <http://dx.doi.org/10.1038/nri.2017.28>

12. Steinman RM. Decisions about dendritic cells: past, present, and future. *Annu Rev Immunol* [Internet]. 2012 Jan [cited 2013 Nov 7];30:1–22. Available from: <http://www.ncbi.nlm.nih.gov/pubmed/22136168>
13. Liu YJ. Dendritic cell subsets and lineages, and their functions in innate and adaptive immunity. *Cell* [Internet]. 2001;106(3):259–62. Available from: <http://www.ncbi.nlm.nih.gov/pubmed/11509173>
14. Unanue ER, Turk V, Neefjes J. Variations in MHC Class II Antigen Processing and Presentation in Health and Disease. *Annu Rev Immunol*. 2016;34:265–97.
15. Pearce EJ, Everts B. Dendritic cell metabolism. *Nat Rev Immunol* [Internet]. 2015;15(1):18–29. Available from: <http://dx.doi.org/10.1038/nri3771>
16. Onai N, Ohteki T. Bipotent or Oligopotent? A Macrophage and DC Progenitor Revisited. *Immunity* [Internet]. 2014;41(1):5–7. Available from: <http://dx.doi.org/10.1016/j.immuni.2014.07.004>
17. Sathe P, Metcalf D, Vremec D, Naik SH, Langdon WY, Huntington ND, et al. Lymphoid Tissue and Plasmacytoid Dendritic Cells and Macrophages Do Not Share a Common Macrophage-Dendritic Cell-Restricted Progenitor. *Immunity*. 2014;41(1):104–15.
18. Bagadia P, Huang X, Liu T, Durai V, Grajales-reyes GE, Nitschké M, et al. An Nfil3–Zeb2–Id2 pathway imposes Irf8 enhancer switching during cDC1 development. *Nat Immunol* [Internet]. 2019;20:1174–85. Available from: <http://dx.doi.org/10.1038/s41590-019-0449-3>
19. MacDonald KPA, Munster DJ, Clark GJ, Dzionek A, Schmitz J, Hart DNJ. Characterization of human blood dendritic cell subsets. *Blood* [Internet]. 2002 [cited 2013 Nov 22];100(13):4512–20. Available from: <http://www.ncbi.nlm.nih.gov/pubmed/12393628>
20. Shortman K, Liu Y-J. Mouse and human dendritic cell subtypes. *Nat Rev Immunol*. 2002;2(3):151–61.
21. Cisse B, Caton ML, Lehner M, Maeda T, Scheu S, Locksley R, et al. Transcription Factor E2-2 Is an Essential and Specific Regulator of Plasmacytoid Dendritic Cell Development. *Cell*. 2008;135(1):37–48.

22. Swiecki M, Colonna M. The multifaceted biology of plasmacytoid dendritic cells. *Nat Rev Immunol* [Internet]. 2015;15:471–485. Available from: <http://www.nature.com/doifinder/10.1038/nri3865>
23. Reizis B, Colonna M, Trinchieri G, Barrat F, Gilliet M. Plasmacytoid dendritic cells: one-trick ponies or workhorses of the immune system? *Nat Rev Immunol* [Internet]. 2011;11(8):558–65. Available from: <http://dx.doi.org/10.1038/nri3027>
24. Dasgupta S, Erturk-Hasdemir D, Ochoa-Reparaz J, Reinecker H-C, Kasper DL. Plasmacytoid dendritic cells mediate anti-inflammatory responses to a gut commensal molecule via both innate and adaptive mechanisms. *Cell Host Microbe* [Internet]. 2014;15(4):413–23. Available from: <http://www.ncbi.nlm.nih.gov/pubmed/24721570>
25. Koblansky AA, Jankovic D, Oh H, Hieny S, Sungnak W, Mathur R, et al. Recognition of Profilin by Toll-like Receptor 12 is Critical for Host Resistance to *Toxoplasma gondii*. *Immunity*. 2013;38(1):119–30.
26. Kim T, Pazhoor S, Bao M, Zhang Z, Hanabuchi S, Facchinetti V, et al. Aspartate-glutamate-alanine-histidine box motif (DEAH)/RNA helicase A helicases sense microbial DNA in human plasmacytoid dendritic cells. *Proc Natl Acad Sci U S A*. 2010;107(34):15181–6.
27. Crow YJ. Type I interferonopathies: A novel set of inborn errors of immunity. *Ann N Y Acad Sci*. 2011;1238(1):91–8.
28. Chappell CP, Giltiay N V, Draves KE, Chen C, Hayden-Ledbetter MS, Shlomchik MJ, et al. Targeting antigens through blood dendritic cell antigen 2 on plasmacytoid dendritic cells promotes immunologic tolerance. *J Immunol* [Internet]. 2014;192(12):5789–801. Available from: <http://www.ncbi.nlm.nih.gov/pubmed/24829416>
29. See P, Dutertre CA, Chen J, Günther P, McGovern N, Irac SE, et al. Mapping the human DC lineage through the integration of high-dimensional techniques. *Science* (80- ). 2017;356(6342):1044.
30. Villani A, Satija R, Reynolds G, Sarkizova S, Shekhar K, Fletcher J, et al. Single-cell RNA-seq reveals new types of human blood dendritic cells, monocytes, and progenitors. *Science* (80- ). 2017;356(283):4573.

31. Sichien D, Lambrecht BN, Williams M, Scott CL. Development of conventional dendritic cells : from common bone marrow progenitors to multiple subsets in peripheral tissues. *Mucosal Immunol* [Internet]. 2017;10(4):831–44. Available from: <http://dx.doi.org/10.1038/mi.2017.8>
32. Hashimoto D, Miller J, Merad M. Dendritic cell and macrophage heterogeneity in vivo. *Immunity* [Internet]. 2011 [cited 2013 Nov 6];35(3):323–35. Available from: <http://www.ncbi.nlm.nih.gov/pubmed/21943488>
33. Merad M, Sathe P, Helft J, Miller J, Mortha A. The dendritic cell lineage: ontogeny and function of dendritic cells and their subsets in the steady state and the inflamed setting. *Annu Rev Immunol* [Internet]. 2013 [cited 2013 Nov 7];31:563–604. Available from: <http://www.ncbi.nlm.nih.gov/pubmed/23516985>
34. Mildner A, Jung S. Development and function of dendritic cell subsets. *Immunity* [Internet]. 2014;40(5):642–56. Available from: <http://dx.doi.org/10.1016/j.immuni.2014.04.016>
35. Schraml BU, Reis e Sousa C. Defining dendritic cells. *Curr Opin Immunol* [Internet]. 2015 [cited 2014 Dec 8];32:13–20. Available from: <http://linkinghub.elsevier.com/retrieve/pii/S0952791514001484>
36. Kurotaki D, Yamamoto M, Nishiyama A, Uno K, Ban T, Ichino M, et al. IRF8 inhibits C/EBP $\alpha$  activity to restrain mononuclear phagocyte progenitors from differentiating into neutrophils. *Nat Commun* [Internet]. 2014;5:1–15. Available from: <http://dx.doi.org/10.1038/ncomms5978>
37. Bachem A, Güttler S, Hartung E, Ebstein F, Schaefer M, Tannert A, et al. Superior antigen cross-presentation and XCR1 expression define human CD11c+CD141+ cells as homologues of mouse CD8+ dendritic cells. *J Exp Med*. 2010;207(6):1273–81.
38. Crozat K, Guiton R, Contreras V, Feuillet V, Dutertre C-A, Ventre E, et al. The XC chemokine receptor 1 is a conserved selective marker of mammalian cells homologous to mouse CD8 $\alpha$ + dendritic cells. *J Exp Med*. 2010;207(6):1283–92.
39. Schlitzer A, Ginhoux F. Organization of the mouse and human DC network. *Curr Opin Immunol* [Internet]. 2014 [cited 2013 Dec 19];26:90–9. Available from: <http://www.sciencedirect.com/science/article/pii/S0952791513002124>

40. Lewis KL, Caton ML, Bogunovic M, Greter M, Grajkowska LT, Ng D, et al. Notch2 receptor signaling controls functional differentiation of dendritic cells in the spleen and intestine. *Immunity* [Internet]. 2011;35(5):780–91. Available from: <http://dx.doi.org/10.1016/j.immuni.2011.08.013>
41. Woodruff MC, Heesters BA, Herndon CN, Groom JR, Thomas PG, Luster AD, et al. Trans-nodal migration of resident dendritic cells into medullary interfollicular regions initiates immunity to influenza vaccine. *J Exp Med* [Internet]. 2014;211(8):1611–21. Available from: <http://www.jem.org/lookup/doi/10.1084/jem.20132327>
42. Meyer B, Ly H. Inhibition of Innate Immune Responses Is Key to Pathogenesis by Arenaviruses. *J Virol* [Internet]. 2016;90(8):3810–8. Available from: <http://jvi.asm.org/lookup/doi/10.1128/JVI.03049-15>
43. Plantinga M, Guilliams M, Vanheerswynghe M, Deswarte K, Branco-madeira F, Toussaint W, et al. Conventional and Monocyte-Derived CD11b+ Dendritic Cells Initiate and Maintain T Helper 2 Cell-Mediated Immunity to House Dust Mite Allergen. *Immunity* [Internet]. 2013;38(2):322–35. Available from: <http://dx.doi.org/10.1016/j.immuni.2012.10.016>
44. Segura E, Touzot M, Bohineust A, Cappuccio A, Chiocchia G, Hosmalin A, et al. Human inflammatory dendritic cells induce Th17 cell differentiation. *Immunity* [Internet]. 2013 [cited 2013 Nov 10];38(2):336–48. Available from: <http://www.ncbi.nlm.nih.gov/pubmed/23352235>
45. Hammad H, Plantinga M, Deswarte K, Pouliot P, Willart MAM, Kool M, et al. Inflammatory dendritic cells--not basophils--are necessary and sufficient for induction of Th2 immunity to inhaled house dust mite allergen. *J Exp Med* [Internet]. 2010 [cited 2013 Nov 7];207(10):2097–111. Available from: <http://www.pubmedcentral.nih.gov/articlerender.fcgi?artid=2947072&tool=pmcentrez&rendertype=abstract>
46. Nakano H, Lin KL, Yanagita M, Charbonneau C, Cook DN, Kakiuchi T, et al. Blood-derived inflammatory dendritic cells in lymph nodes stimulate acute T helper type 1 immune responses. *Nat Immunol*. 2009;10(4):394–402.
47. Meredith MM, Liu K, Darrasse-Jeze G, Kamphorst AO, Schreiber HA, Guermonprez P, et al. Expression of the zinc finger transcription factor zDC (Zbtb46, Btbd4) defines

- the classical dendritic cell lineage. *J Exp Med* [Internet]. 2012;209(6):1153–65. Available from: <http://www.jem.org/lookup/doi/10.1084/jem.20112675>
48. Satpathy AT, KC W, Albring JC, Edelson BT, Kretzer NM, Bhattacharya D, et al. *Zbtb46* expression distinguishes classical dendritic cells and their committed progenitors from other immune lineages. *J Exp Med* [Internet]. 2012;209(6):1135–52. Available from: <http://www.jem.org/lookup/doi/10.1084/jem.20120030>
49. Serbina N V, Salazar-Mather TP, Biron CA, Kuziel WA, Pamer EG. TNF/iNOS-Producing Dendritic Cells Mediate Innate Immune Defense against Bacterial Infection. *Immunity* [Internet]. 2003 [cited 2013 Nov 25];19(1):59–70. Available from: <http://www.sciencedirect.com/science/article/pii/S1074761303001717>
50. Tamoutounour S, Guilliams M, Montanana SF, Liu H, Terhorst D, Malosse C, et al. Origins and Functional Specialization of Macrophages and of Conventional and Monocyte-Derived Dendritic Cells in Mouse Skin. *Immunity*. 2013;39:925–38.
51. Hänsel A, Günther C, Ingwersen J, Starke J, Schmitz M, Bachmann M, et al. Human slan (6-sulfo LacNAc) dendritic cells are inflammatory dermal dendritic cells in psoriasis and drive strong TH17/TH1 T-cell responses. *J Allergy Clin Immunol* [Internet]. 2011 Mar 1 [cited 2013 Nov 17];127(3):787-94.e1-9. Available from: [http://www.jacionline.org/article/S0091-6749\(10\)01948-2/abstract](http://www.jacionline.org/article/S0091-6749(10)01948-2/abstract)
52. Wollenberg A, Kraft S, Hanau D, Bieber T. Immunomorphological and ultrastructural characterization of Langerhans cells and a novel, inflammatory dendritic epidermal cell (IDEC) population in lesional skin of atopic eczema. *J Invest Dermatol* [Internet]. 1996;106(3):446–53. Available from: <http://dx.doi.org/10.1111/1523-1747.ep12343596>
53. Kashem SW, Haniffa M, Kaplan DH. Antigen-Presenting Cells in the Skin. *Annu Rev Immunol*. 2017;35:469–99.
54. Romani N, Clausen BE, Stoitzner P. Langerhans cells and more: langerin-expressing dendritic cell subsets in the skin. *Immunol Rev* [Internet]. 2010 [cited 2013 Dec 19];234(1):120–41. Available from: <http://www.pubmedcentral.nih.gov/articlerender.fcgi?artid=2907488&tool=pmcentrez&rendertype=abstract>

55. Hoeffel G, Wang Y, Greter M, See P, Teo P, Malleret B, et al. Adult Langerhans cells derive predominantly from embryonic fetal liver monocytes with a minor contribution of yolk sac-derived macrophages. *J Exp Med*. 2012;209(6):1167–81.
56. Ginhoux F, Liu K, Helft J, Bogunovic M, Greter M, Hashimoto D, et al. The origin and development of nonlymphoid tissue CD103<sup>+</sup> DCs. *J Exp Med*. 2009;206(13):3115–30.
57. Doebel T, Voisin B, Nagao K. Langerhans Cells – The Macrophage in Dendritic Cell Clothing. *Trends Immunol* [Internet]. 2017;38(11):817–28. Available from: <http://dx.doi.org/10.1016/j.it.2017.06.008>
58. Igyártó BZ, Haley K, Ortner D, Bobr A, Gerami-Nejad M, Edelson BT, et al. Skin-Resident Murine Dendritic Cell Subsets Promote Distinct and Opposing Antigen-Specific T Helper Cell Responses. *Immunity*. 2011;35(2):260–72.
59. de Jong A, Peña-Cruz V, Cheng T-Y, Clark RA, Van Rhijn I, Moody DB. CD1a-autoreactive T cells are a normal component of the human  $\alpha\beta$  T cell repertoire. *Nat Immunol* [Internet]. 2010;11(12):1102–9. Available from: <http://www.nature.com/doi/10.1038/ni.1956>
60. Miller JC, Brown BD, Shay T, Gautier EL, Jovic V, Cohain A, et al. Deciphering the transcriptional network of the dendritic cell lineage. *Nat Immunol* [Internet]. 2012 [cited 2013 Nov 7];13(9):888–99. Available from: <http://dx.doi.org/10.1038/ni.2370>
61. Wu X, Briseño CG, Durai V, Albring JC, Haldar M, Bagadia P, et al. *Mafb* lineage tracing to distinguish macrophages from other immune lineages reveals dual identity of Langerhans cells. *J Exp Med* [Internet]. 2016;213(12):2553–65. Available from: <http://www.jem.org/lookup/doi/10.1084/jem.20160600>
62. Heesters BA, Myers RC, Carroll MC. Follicular dendritic cells : dynamic antigen libraries. *Nat Rev Immunol*. 2014;14:495–504.
63. Gordon S. Phagocytosis: The Legacy of Metchnikoff. *Cell* [Internet]. 2016;166(5):1065–8. Available from: <http://dx.doi.org/10.1016/j.cell.2016.08.017>
64. Tauber AI. Metchnikoff and the phagocytosis theory. *Nat Rev Mol Cell Biol*. 2003;4(11):897–901.
65. Wynn TA, Chawla A, Pollard JW. Macrophage biology in development, homeostasis

- and disease. *Nature* [Internet]. 2013;496(7446):445–55. Available from:  
<http://www.ncbi.nlm.nih.gov/pubmed/23619691>
66. Davies LC, Jenkins SJ, Allen JE, Taylor PR. Tissue-resident macrophages. *Nat Immunol* [Internet]. 2013;14(10):986–95. Available from:  
<http://www.pubmedcentral.nih.gov/articlerender.fcgi?artid=4045180&tool=pmcentrez&rendertype=abstract>
  67. Hettinger J, Richards DM, Hansson J, Barra MM, Joschko A-C, Krijgsveld J, et al. Origin of monocytes and macrophages in a committed progenitor. *Nat Immunol* [Internet]. 2013;14(8):821–30. Available from:  
<http://www.nature.com/doifinder/10.1038/ni.2638>
  68. Gordon S, Taylor PR. Monocyte and macrophage heterogeneity. *Nat Rev Immunol* [Internet]. 2005;5(12):953–64. Available from:  
<http://www.nature.com/doifinder/10.1038/nri1733>
  69. Gosselin D, Link VM, Romanoski CE, Fonseca GJ, Eichenfield DZ, Spann NJ, et al. Environment drives selection and function of enhancers controlling tissue-specific macrophage identities. *Cell* [Internet]. 2014;159(6):1327–40. Available from:  
<http://dx.doi.org/10.1016/j.cell.2014.11.023>
  70. Phan AT, Goldrath AW, Glass CK. Metabolic and Epigenetic Coordination of T Cell and Macrophage Immunity. *Immunity* [Internet]. 2017;46(5):714–29. Available from:  
<http://dx.doi.org/10.1016/j.immuni.2017.04.016>
  71. Okabe Y, Medzhitov R. Tissue biology perspective on macrophages. *Nat Immunol* [Internet]. 2015;17(1):9–17. Available from:  
<http://www.nature.com/doifinder/10.1038/ni.3320>
  72. Butovsky O, Jedrychowski MP, Moore CS, Cialic R, Lanser AJ, Gabriely G, et al. Identification of a unique TGF- $\beta$ -dependent molecular and functional signature in microglia. *Nat Neurosci*. 2014;17(1):131–43.
  73. Murray PJ, Wynn T a. Protective and pathogenic functions of macrophage subsets. *Nat Rev Immunol* [Internet]. 2011;11(11):723–37. Available from:  
<http://www.pubmedcentral.nih.gov/articlerender.fcgi?artid=3422549&tool=pmcentrez&rendertype=abstract>

74. Gordon S, Plüddemann A. Tissue macrophages : heterogeneity and functions. *BMC Biol.* 2017;15(53):1–18.
75. Ginhoux F, Jung S. Monocytes and macrophages: developmental pathways and tissue homeostasis. *Nat Rev Immunol* [Internet]. 2014;14(6):392–404. Available from: <http://www.nature.com/doifinder/10.1038/nri3671>
76. Ingersoll M, Spanbroek R, Lottaz C, Gautier E, Frankenberger M, Hoffmann R, et al. Comparison of gene expression profiles between human and mouse monocyte subsets. *Blood* [Internet]. 2010;115(3):10–20. Available from: <http://bloodjournal.hematologylibrary.org/content/115/3/e10.short>
77. Sehgal M, Khan ZK, Talal AH, Jain P. Dendritic cells in HIV-1 and HCV infection: Can they help win the battle? *Viol Res Treat.* 2013;4:1–25.
78. Wu L, KewalRamani VN. Dendritic-cell interactions with HIV: Infection and viral dissemination. *Nat Rev Immunol.* 2006;6(11):859–68.
79. Spörri R, Reis e Sousa C. Inflammatory mediators are insufficient for full dendritic cell activation and promote expansion of CD4+ T cell populations lacking helper function. *Nat Immunol.* 2005;6(2):163–70.
80. Martinez O, Leung LW, Basler CF. The role of antigen-presenting cells in filoviral hemorrhagic fever: Gaps in current knowledge. Vol. 93, *Antiviral Research.* 2012. p. 416–28.
81. Pannetier D, Faure C, Deubel V, Baize S. Human Macrophages , but Not Dendritic Cells , Are Activated and Produce Alpha / Beta Interferons in Response to Mopeia Virus Infection. 2004;78(19):10516–24.
82. McDermott DS, Weiss KA, Knudson CJ, Varga SM. Response During Respiratory Syncytial Virus Infection. *Future Virol.* 2011;6(8):963–73.
83. Mintern JD, Villadangos JA. Antigen-presenting cells look within during influenza infection. *Nat Med.* 2015;21(10):1123–5.
84. Akira S, Uematsu S, Takeuchi O. Pathogen Recognition and Innate Immunity. *Cell* [Internet]. 2006;124(4):783–801. Available from: <http://linkinghub.elsevier.com/retrieve/pii/S0092867406001905>

85. Pichlmair A, Sousa CRE. Review Innate Recognition of Viruses. *Immunity*. 2007;27:370–83.
86. Takaoka A, Wang Z, Choi MK, Yanai H, Negishi H, Ban T, et al. DAI (DLM-1/ZBP1) is a cytosolic DNA sensor and an activator of innate immune response. *Nature*. 2007;448(7152):501–5.
87. Yoneyama M, Kikuchi M, Matsumoto K, Imaizumi T, Miyagishi M, Taira K, et al. Shared and unique functions of the DExD/H-box helicases RIG-I, MDA5, and LGP2 in antiviral innate immunity. *J Immunol*. 2005;175(5):2851–8.
88. Zhang Z, Kim T, Bao M, Facchinetti V, Jung SY, Ghaffari AA, et al. DDX1, DDX21, and DHX36 Helicases Form a Complex with the Adaptor Molecule TRIF to Sense dsRNA in Dendritic Cells. *Immunity* [Internet]. 2011;34(6):866–78. Available from: <http://dx.doi.org/10.1016/j.immuni.2011.03.027>
89. Jensen S, Thomsen AR. Sensing of RNA Viruses: a Review of Innate Immune Receptors Involved in Recognizing RNA Virus Invasion. *J Virol*. 2012;86(6):2900–10.
90. Dalod M, Chelbi R, Malissen B, Lawrence T. Dendritic cell maturation: Functional specialization through signaling specificity and transcriptional programming. *EMBO J*. 2014;33(10):1104–16.
91. Boltjes A, van Wijk F. Human dendritic cell functional specialization in steady-state and inflammation. *Front Immunol*. 2014;5(APR):1–13.
92. Durand M, Segura E. The Known Unknowns of the Human Dendritic Cell Network. *Front Immunol* [Internet]. 2015;6(129):2–8. Available from: <http://journal.frontiersin.org/article/10.3389/fimmu.2015.00129>
93. Huang X, Yang Y. Review Innate Immune Recognition of Viruses and Viral Vectors. *Hum Gene Ther*. 2009;20(141):293–301.
94. Diebold SS, Massacrier C, Akira S, Patrel C, Morel Y, Reis e Sousa C. Nucleic acid agonists for Toll-like receptor 7 are defined by the presence of uridine ribonucleotides. *Eur J Immunol*. 2006;36(12):3256–67.
95. Heil F, Hemmi H, Hochrein H, Ampenberger F, Kirschning C, Akira S, et al. Species-Specific Recognition of Single-Stranded RNA via Toll-like Receptor 7 and 8. *Science* (80- ). 2004;303:4–8.

96. Jurk M, Heil F, Vollmer J, Schetter C, Krieg AM, Wagner H, et al. Human TLR7 or TLR8 independently confer responsiveness to the antiviral compound R-848. *Nat Immunol.* 2002;3(6):499.
97. Schulz O, Diebold SS, Chen M, Naslund TI, Nolte MA, Alexopoulou L, et al. Toll-like receptor 3 promotes cross-priming to virus-infected cells. *Nature.* 2005;433(24):887–92.
98. Bieback K, Lien E, Klagge IM, Avota E, Schneider-schaulies J, Duprex WP, et al. Hemagglutinin Protein of Wild-Type Measles Virus Activates Toll-Like Receptor Hemagglutinin Protein of Wild-Type Measles Virus Activates Toll-Like Receptor 2 Signaling. *J Virol.* 2002;76(17):8729–36.
99. Burzyn D, Rassa JC, Kim D, Nepomnaschy I, Ross SR, Piazzon I. Toll-like receptor 4-dependent activation of dendritic cells by a retrovirus. *J Virol.* 2004;78(2):576–84.
100. Richer MJ, Fang D, Shanina I, Horwitz MS. Toll-like receptor 4-induced cytokine production circumvents protection conferred by TGF- $\beta$  in coxsackievirus-mediated autoimmune myocarditis. *Clin Immunol.* 2006;121(3):339–49.
101. Henao-Restrepo AM, Camacho A, Longini IM, Watson CH, Edmunds WJ, Egger M, et al. Efficacy and effectiveness of an rVSV-vectored vaccine in preventing Ebola virus disease: final results from the Guinea ring vaccination, open-label, cluster-randomised trial (Ebola Ça Suffit!). *Lancet.* 2017;389(10068):505–18.
102. Lai C, Strange DP, Wong TAS, Lehrer AT, Verma S. Ebola Virus Glycoprotein Induces an Innate Immune Response In vivo via TLR4. *Front Immunol.* 2017;8(1571):1–15.
103. Kato H, Sato S, Yoneyama M, Yamamoto M, Uematsu S, Matsui K, et al. Cell type-specific involvement of RIG-I in antiviral response. *Immunity.* 2005;23(1):19–28.
104. Bryan MA, Giordano D, Draves KE, Green R, Gale M, Clark EA. Splenic macrophages are required for protective innate immunity against West Nile virus. *PLoS One.* 2018;13(2):1–24.
105. Baum A, Sachidanandam R, García-Sastre A. Preference of RIG-I for short viral RNA molecules in infected cells revealed by next-generation sequencing. *Proc Natl Acad Sci U S A.* 2010;107(37):16303–8.

106. Hornung V, Kato H, Poeck H, Akira S, Conzelmann K, Schlee M. Ligand for RIG-I. *Science* (80- ). 2010;994(2006):1–5.
107. Pichlmair A, Schulz O, Tan C-P, Rehwinkel J, Kato H, Takeuchi O, et al. Activation of MDA5 requires higher-order RNA structures generated during virus infection. *J Virol*. 2009;83(20):10761–9.
108. Wu B, Peisley A, Richards C, Yao H, Zeng X, Lin C, et al. Structural basis for dsRNA recognition, filament formation, and antiviral signal activation by MDA5. *Cell* [Internet]. 2013;152(1–2):276–89. Available from: <http://dx.doi.org/10.1016/j.cell.2012.11.048>
109. Cárdenas WB, Loo Y-M, Gale M, Hartman AL, Kimberlin CR, Martínez-Sobrido L, et al. Ebola virus VP35 protein binds double-stranded RNA and inhibits alpha/beta interferon production induced by RIG-I signaling. *J Virol*. 2006;80(11):5168–78.
110. Yen B, Mulder LCF, Martinez O, Basler CF. Molecular basis for ebolavirus VP35 suppression of human dendritic cell maturation. *J Virol* [Internet]. 2014 [cited 2014 Dec 4];88(21):12500–10. Available from: <http://www.ncbi.nlm.nih.gov/pubmed/25142601>
111. Venkataraman T, Valdes M, Elsby R, Kakuta S, Caceres G, Saijo S, et al. Loss of DExD/H box RNA helicase LGP2 manifests disparate antiviral responses. *J Immunol*. 2007;178(10):6444–55.
112. Rodriguez KR, Bruns AM, Horvath CM. MDA5 and LGP2: Accomplices and Antagonists of Antiviral Signal Transduction. *J Virol* [Internet]. 2014;88(15):8194–200. Available from: <http://www.ncbi.nlm.nih.gov/pubmed/24850739>
113. Trotard M, Tsooulidis N, Tibroni N, Willemsen J, Binder M, Ruggieri A, et al. Sensing of HIV-1 Infection in Tzm-bl Cells with Reconstituted Expression of STING. *J Virol*. 2016;90(4):2064–76.
114. Dixit E, Boulant S, Zhang Y, Lee ASY, Odendall C, Shum B, et al. Peroxisomes Are Signaling Platforms for Antiviral Innate Immunity. *Cell* [Internet]. 2010;141(4):668–81. Available from: <http://dx.doi.org/10.1016/j.cell.2010.04.018>
115. Pestka S, Krause CD, Walter MR. Interferons, interferon-like cytokines, and their receptors. *Immunol Rev*. 2004;202:8–32.

116. Nan Y, Nan G, Zhang Y-J. Interferon Induction by RNA Viruses and Antagonism by Viral Pathogens. *Viruses* [Internet]. 2014;6(12):4999–5027. Available from: <http://www.mdpi.com/1999-4915/6/12/4999/>
117. Fensterl V, Sen GC. Interferons and viral infections. *BioFactors*. 2009;35(1):14–20.
118. Ito T, Kanzler H, Duramad O, Cao W, Liu YJ. Specialization, kinetics, and repertoire of type I interferon responses by human plasmacytoid dendritic cells. *Blood*. 2006;107(6):2423–31.
119. Ingle H, Peterson S, Baldrige M. Distinct Effects of Type I and III Interferons on Enteric Viruses. *Viruses* [Internet]. 2018;10(1):46. Available from: <http://www.mdpi.com/1999-4915/10/1/46>
120. Fitzgerald-Bocarsly P, Dai J, Singh S. Plasmacytoid Dendritic Cells and Type I IFN: 50 Years of Convergent History. *Cytokine Growth Factor Rev* [Internet]. 2008 [cited 2013 Nov 22];19(1):3–19. Available from: <http://www.pubmedcentral.nih.gov/articlerender.fcgi?artid=2277216&tool=pmcentrez&rendertype=abstract>
121. Kotenko S V., Durbin JE. Contribution of type III interferons to antiviral immunity: Location, location, location. *J Biol Chem*. 2017;292(18):7295–303.
122. Sommereyns C, Paul S, Staeheli P, Michiels T. IFN-lambda (IFN- $\lambda$ ) is expressed in a tissue-dependent fashion and primarily acts on epithelial cells in vivo. *PLoS Pathog*. 2008;4(3):1–12.
123. Arimoto K-I, Miyauchi S, Stoner SA, Fan J-B, Zhang D-E. Negative regulation of type I IFN signaling. *J Leukoc Biol* [Internet]. 2018;1–18. Available from: <http://doi.wiley.com/10.1002/JLB.2MIR0817-342R>
124. Au-Yeung N, Mandhana R, Horvath CM. Transcriptional regulation by STAT1 and STAT2 in the interferon JAK-STAT pathway. *Jak-Stat* [Internet]. 2013;2(3):e23931. Available from: <http://www.tandfonline.com/doi/abs/10.4161/jkst.23931>
125. Schindler C, Levy DE, Decker T. JAK-STAT signaling: From interferons to cytokines. *J Biol Chem*. 2007;282(28):20059–63.
126. Alsharifi M, Müllbacher A, Regner M. Interferon type I responses in primary and secondary infections. *Immunol Cell Biol*. 2008;86(3):239–45.

127. McFadden G, Mohamed MR, Rahman MM, Bartee E. Cytokine determinants of viral tropism. *Nat Rev Immunol* [Internet]. 2009;9(9):645–55. Available from: <http://dx.doi.org/10.1038/nri2623>
128. Raniga K, Liang C. Interferons: Reprogramming the metabolic network against viral infection. *Viruses*. 2018;10(1):1–21.
129. Li MMH, MacDonald MR, Rice CM. To translate, or not to translate: Viral and host mRNA regulation by interferon-stimulated genes. *Trends Cell Biol* [Internet]. 2015;25(6):320–9. Available from: <http://dx.doi.org/10.1016/j.tcb.2015.02.001>
130. Schneider WM, Chevillotte MD, Rice CM. Interferon-Stimulated Genes: A Complex Web of Host Defenses. *Annu Rev Immunol* [Internet]. 2014;32(1):513–45. Available from: <http://www.annualreviews.org/doi/10.1146/annurev-immunol-032713-120231>
131. Helbig KJ, Beard MR. The role of viperin in the innate antiviral response. *J Mol Biol* [Internet]. 2014;426(6):1210–9. Available from: <http://dx.doi.org/10.1016/j.jmb.2013.10.019>
132. Tian J, Zhang X, Wu H, Liu C, Li Z, Hu X, et al. Blocking the PI3K/AKT pathway enhances mammalian reovirus replication by repressing IFN-stimulated genes. *Front Microbiol*. 2015;6(886):1–14.
133. Liu SY, Aliyari R, Chikere K, Li G, Marsden MD, Smith JK, et al. Interferon-Inducible Cholesterol-25-Hydroxylase Broadly Inhibits Viral Entry by Production of 25-Hydroxycholesterol. *Immunity* [Internet]. 2013;38(1):92–105. Available from: <http://dx.doi.org/10.1016/j.immuni.2012.11.005>
134. Anggakusuma, Romero-Brey I, Berger C, Colpitts CC, Boldanova T, Engelmann M, et al. Interferon-inducible cholesterol-25-hydroxylase restricts hepatitis C virus replication through blockage of membranous web formation. *Hepatology*. 2015;62(3):702–14.
135. Zang R, Case JB, Yutuc E, Ma X, Shen S, Castro MFG, et al. Cholesterol 25-hydroxylase suppresses SARS-CoV-2 replication by blocking membrane fusion. *Proc Natl Acad Sci U S A*. 2020;117(50):32105–13.
136. Civra A, Cagno V, Donalisio M, Biasi F, Leonarduzzi G, Poli G, et al. Inhibition of pathogenic non-enveloped viruses by 25-hydroxycholesterol and 27-

- hydroxycholesterol. *Sci Rep*. 2014;4:1–6.
137. Nice TJ, Robinson BA, Van Winkle JA. The Role of Interferon in Persistent Viral Infection: Insights from Murine Norovirus. *Trends Microbiol* [Internet]. 2017;26(6):510–24. Available from: <http://dx.doi.org/10.1016/j.tim.2017.10.010>
  138. Pulverer JE, Rand U, Lienenklaus S, Kugel D, Zietara N, Kochs G, et al. Temporal and Spatial Resolution of Type I and III Interferon Responses In Vivo. *J Virol* [Internet]. 2010;84(17):8626–38. Available from: <http://jvi.asm.org/cgi/doi/10.1128/JVI.00303-10>
  139. Baldrige MT, Lee S, Brown JJ, McAllister N, Urbanek K, Dermody TS, et al. Expression of *Ifnlr1* on Intestinal Epithelial Cells Is Critical to the Antiviral Effects of Interferon Lambda against Norovirus and Reovirus. *J Virol* [Internet]. 2017;91(7):e02079-16. Available from: <http://jvi.asm.org/lookup/doi/10.1128/JVI.02079-16>
  140. Mahlaköiv T, Hernandez P, Gronke K, Diefenbach A, Staeheli P. Leukocyte-Derived IFN- $\alpha/\beta$  and Epithelial IFN- $\lambda$  Constitute a Compartmentalized Mucosal Defense System that Restricts Enteric Virus Infections. *PLoS Pathog*. 2015;11(4):1–19.
  141. Voigt EA, Yin J. Kinetic Differences and Synergistic Antiviral Effects Between Type I and Type III Interferon Signaling Indicate Pathway Independence. *J Interf Cytokine Res* [Internet]. 2015;35(9):734–47. Available from: <http://online.liebertpub.com/doi/10.1089/jir.2015.0008>
  142. Sandler NG, Bosinger SE, Estes JD, Zhu RTR, Tharp GK, Boritz E, et al. Type I interferon responses in rhesus macaques prevent SIV infection and slow disease progression. *Nature* [Internet]. 2014;511(7511):601–5. Available from: <http://dx.doi.org/10.1038/nature13554>
  143. Teijaro JR, Ng C, Lee AM, Sullivan BM, Sheehan KCF, Welch M, et al. Persistent LCMV infection is controlled by blockade of type I interferon signaling. *Science* (80- ) [Internet]. 2013;340(6129):207–11. Available from: <http://www.pubmedcentral.nih.gov/articlerender.fcgi?artid=3640797&tool=pmcentrez&rendertype=abstract>
  144. Zitvogel L, Galluzzi L, Kepp O, Smyth MJ, Kroemer G. Type I interferons in

- anticancer immunity. *Nat Rev Immunol* [Internet]. 2015;15(7):405–14. Available from: <http://www.nature.com/doi/10.1038/nri3845>
145. Kalkavan H, Sharma P, Kasper S, Helfrich I, Pandya AA, Gassa A, et al. Spatiotemporally restricted arenavirus replication induces immune surveillance and type I interferon-dependent tumour regression. *Nat Commun*. 2017;8(14447):1–14.
146. Lee-Kirsch MA. The Type I Interferonopathies. *Annu Rev Med* [Internet]. 2017;68(1):297–315. Available from: <http://www.annualreviews.org/doi/10.1146/annurev-med-050715-104506>
147. Ng CT, Oldstone MB a. Infected CD8 $\alpha$ - dendritic cells are the predominant source of IL-10 during establishment of persistent viral infection. *Proc Natl Acad Sci U S A* [Internet]. 2012;109(35):14116–21. Available from: <http://www.pubmedcentral.nih.gov/articlerender.fcgi?artid=3435180&tool=pmcentrez&rendertype=abstract>
148. Izquierdo-Useros N, Lorizate M, Puertas MC, Rodriguez-Plata MT, Zangger N, Erikson E, et al. Siglec-1 Is a Novel Dendritic Cell Receptor That Mediates HIV-1 Trans-Infection Through Recognition of Viral Membrane Gangliosides. *PLoS Biol*. 2012;10(12):1–13.
149. Boggiano C, Manel N, Littman DR. Dendritic Cell-Mediated trans-Enhancement of Human Immunodeficiency Virus Type 1 Infectivity Is Independent of DC-SIGN. *J Virol* [Internet]. 2007;81(5):2519–23. Available from: <http://jvi.asm.org/cgi/doi/10.1128/JVI.01661-06>
150. Nobile C, Petit C, Moris A, Abastado J, Mammano F, Schwartz O, et al. Covert Human Immunodeficiency Virus Replication in Dendritic Cells and in DC-SIGN-Expressing Cells Promotes Long-Term Transmission to Lymphocytes. *J Virol*. 2005;79(9):5386–99.
151. Steinman RM, Kaplan G, Witmer MD, Cohn ZA. Identification of a novel cell type in peripheral lymphoid organs of mice. I. Morphology, quantitation, tissue distribution. *J Exp Med*. 1979;137(5):1142–62.
152. Inaba K, Steinman RM, Inaba M, Romani N, Aya H, Deguchi M, et al. Generation of Large Numbers of Dendritic Cells from Mouse Bone Marrow Cultures Supplemented

- with Granulocyte/Macrophage Colony-stimulating Factor. *J Exp Med*. 1992;176(6):1693–702.
153. Palucka K, Banchereau J. Cancer immunotherapy via dendritic cells. *Nat Rev Immunol*. 2012;12(4):265–77.
  154. Helft J, Böttcher J, Chakravarty P, Zelenay S, Huotari J, Schraml BU, et al. GM-CSF Mouse Bone Marrow Cultures Comprise a Heterogeneous Population of CD11c+MHCII+ Macrophages and Dendritic Cells. *Immunity* [Internet]. 2015;42(6):1197–211. Available from: <http://www.sciencedirect.com/science/article/pii/S1074761315002162>  
<http://linkinghub.elsevier.com/retrieve/pii/S1074761315002162>
  155. Huang C, Kolokoltsova O a., Yun NE, Seregin A V., Ronca S, Koma T, et al. Highly pathogenic New World and Old World human arenaviruses induce distinct interferon responses in human cells. *J Virol* [Internet]. 2015;89(14):7079–88. Available from: <http://jvi.asm.org/lookup/doi/10.1128/JVI.00526-15>
  156. Sarute N, Ross SR. New World Arenavirus Biology. *Annu Rev Virol* [Internet]. 2017;4(1):141–58. Available from: <http://www.annualreviews.org/doi/10.1146/annurev-virology-101416-042001>
  157. Wright R, Johnson D, Neumann M, Ksiazek TG, Rollin P, Keech R V, et al. Congenital Lymphocytic Choriomeningitis Virus Syndrome : A Disease That Mimics Congenital Toxoplasmosis or Cytomegalovirus Infection. *Pediatrics*. 1997;100(1):1–6.
  158. Lukashevich IS, Peters CJ, Salvato MS, Stenglein MD, Carlos J. Past, present, and future of arenavirus taxonomy. *Arch Virol*. 2015;160(7):1851–74.
  159. Irwin NR, Bayerlova M, Missa O, Martinkova N. Complex patterns of host switching in New World arenaviruses. *Mol Ecol*. 2012;21(16):4137–50.
  160. Charrel RN, Lamballerie X De, Emonet SF. Phylogeny of the genus Arenavirus. *Cuurent Opin Microbiol*. 2008;11(4):362–8.
  161. Stenglein MD, Jacobson ER, Chang L, Sanders C, Hawkins G, Guzman DS, et al. Widespread Recombination , Reassortment , and Transmission of Unbalanced Compound Viral Genotypes in Natural Arenavirus Infections. *PLoS Pathog*. 2015;11(5):1–26.

162. Zapata JC, Salvato MS. Arenavirus variations due to host-specific adaptation. *Viruses* [Internet]. 2013 [cited 2014 Nov 1];5(1):241–78. Available from: <http://www.pubmedcentral.nih.gov/articlerender.fcgi?artid=3564120&tool=pmcentrez&rendertype=abstract>
163. Gaudin R, Kirchhausen T. Superinfection exclusion is absent during acute Junin virus infection of Vero and A549 cells. *Sci Rep* [Internet]. 2015;5(15990):1–8. Available from: <http://dx.doi.org/10.1038/srep15990>
164. Xing J, Ly H, Liang Y. The Z Proteins of Pathogenic but Not Nonpathogenic Arenaviruses Inhibit RIG-i-Like Receptor-Dependent Interferon Production. *J Virol* [Internet]. 2015;89(5):2944–55. Available from: <http://jvi.asm.org/lookup/doi/10.1128/JVI.03349-14>
165. Paessler S, Walker DH. Pathogenesis of the viral hemorrhagic fevers. *Annu Rev Pathol Mech Dis* [Internet]. 2013 Jan 24 [cited 2014 Nov 13];8:411–40. Available from: <http://www.ncbi.nlm.nih.gov/pubmed/23121052>
166. Zinzula L, Tramontano E. Strategies of highly pathogenic RNA viruses to block dsRNA detection by RIG-I-like receptors: Hide, mask, hit. *Antiviral Res* [Internet]. 2013;100(3):615–35. Available from: <http://dx.doi.org/10.1016/j.antiviral.2013.10.002>
167. Peng R, Xu X, Jing J, Wang M, Peng Q, Liu S, et al. Structural insight into arenavirus replication machinery. *Nature* [Internet]. 2020;579:615–9. Available from: <http://dx.doi.org/10.1038/s41586-020-2114-2>
168. Maruyama J, Miyamoto H, Kajihara M, Ogawa H, Maeda K, Sakoda Y, et al. Characterization of the envelope glycoprotein of a novel filovirus, Ilovu virus. *J Virol* [Internet]. 2014 Jan [cited 2014 Oct 24];88(1):99–109. Available from: <http://www.pubmedcentral.nih.gov/articlerender.fcgi?artid=3911722&tool=pmcentrez&rendertype=abstract>
169. Fehling SK, Lennartz F, Strecker T. Multifunctional nature of the arenavirus RING finger protein Z. *Viruses* [Internet]. 2012 Nov [cited 2014 Oct 23];4(11):2973–3011. Available from: <http://www.pubmedcentral.nih.gov/articlerender.fcgi?artid=3509680&tool=pmcentrez&rendertype=abstract>

170. Urata S, Carlos J, Torre D. Arenavirus Budding. *Adv Virol.* 2011;2011:180326.
171. Ziegler CM, Eisenhauer P, Bruce EA, Weir ME, King R, Klaus JP, et al. The Lymphocytic Choriomeningitis Virus Matrix Protein PPXY Late Domain Drives the Production of Defective Interfering Particles. *PLoS Pathog.* 2016;12(3):1–29.
172. Hallam SJ, Koma T, Maruyama J, Paessler S, Ross SR. Review of Mammarenavirus Biology and Replication. *Front Microbiol.* 2018;9(1751):1–8.
173. Watanabe Y, Raghwani J, Allen JD, Seabright GE, Li S, Moser F. Structure of the Lassa virus glycan shield provides a model for immunological resistance. *Proc Natl Acad Sci U S A.* 2018;115(28):1–6.
174. Wilda M, Lopez N, Casabona JC, Franze-fernandez MT. Mapping of the Tacaribe Arenavirus Z-Protein Binding Sites on the L Protein Identified both Amino Acids within the Putative Polymerase Domain and a Region at the N Terminus of L That Are Critically Involved in Binding □. *J Virol.* 2008;82(22):11454–60.
175. Baseler L, Chertow DS, Johnson KM, Feldmann H, Morens DM. The Pathogenesis of Ebola Virus Disease. *Annu Rev Pathol Mech Dis [Internet].* 2017;12(1):387–418. Available from: <http://www.annualreviews.org/doi/10.1146/annurev-pathol-052016-100506>
176. Jae LT, Raaben M, Herbert AS, Kuehne AI, Wirchnianski AS, Soh TK, et al. Lassa virus entry requires a trigger-induced receptor switch. *Science (80- ).* 2014;344(6191):1506–10.
177. Ly H. Differential immune responses to new world and old world mammalian arenaviruses. *Int J Mol Sci.* 2017;18(5):1–10.
178. Heeney JL, Dalgleish AG, Weiss R a. Origins of HIV and the evolution of resistance to AIDS. *Science (80- ).* 2006;313(5786):462–6.
179. Zapata JC, Cox D, Salvato MS. The role of platelets in the pathogenesis of viral hemorrhagic fevers. *PLoS Negl Trop Dis [Internet].* 2014 [cited 2014 Sep 3];8(6):e2858. Available from: <http://www.pubmedcentral.nih.gov/articlerender.fcgi?artid=4055450&tool=pmcentrez&rendertype=abstract>
180. Saéz AM, Weiss S, Nowak K, Lapeyre V, Kaba M, Regnaut S, et al. Investigating the

- zoonotic origin of the West African Ebola epidemic. *Embo Mol Med*. 2014;7(1):17–23.
181. WHO. Ebola Virus Disease. <http://apps.who.int/ebola/ebola-situation-reports>. 2016;1–2.
182. Nigeria Centre for Disease Control N. 2018 Lassa Fever Outbreak in Nigeria. [www.ncdc.gov.ng](http://www.ncdc.gov.ng). 2018;1–5.
183. Vasconcelos PFC, Monath TP. Yellow Fever Remains a Potential Threat to Public Health. *Vector-Borne Zoonotic Dis*. 2016;16(8):566–7.
184. Basler CF. Molecular pathogenesis of viral hemorrhagic fever. *Semin Immunopathol*. 2017;39(5):551–61.
185. Feldmann H, Geisbert TW. Ebola haemorrhagic fever. *Lancet* [Internet]. 2011 [cited 2014 Aug 2];377(9768):849–62. Available from: <http://www.pubmedcentral.nih.gov/articlerender.fcgi?artid=3406178&tool=pmcentrez&rendertype=abstract>
186. Oldstone MBA. Anatomy of viral persistence. *PLoS Pathog*. 2009;5(7):5–8.
187. Zapata JC, Pauza CD, Djavani MM, Rodas JD, Moshkoff D, Bryant J, et al. Lymphocytic choriomeningitis virus (LCMV) infection of macaques: a model for Lassa fever. *Antiviral Res* [Internet]. 2011 [cited 2014 Nov 18];92(2):125–38. Available from: <http://www.pubmedcentral.nih.gov/articlerender.fcgi?artid=3209703&tool=pmcentrez&rendertype=abstract>
188. Oldstone MBA. Viral persistence: Parameters, mechanisms and future predictions. *Virology*. 2006;344(1):111–8.
189. Borrow P, Evans CF, Oldstone MBA. Virus-Induced Immunosuppression : Immune System-Mediated Destruction of Virus-Infected Dendritic Cells Results in Generalized Immune Suppression. *J Virol*. 1995;69(2):1059–70.
190. Sevilla N, Kunz S, Holz A, Lewicki H, Homann D, Yamada H, et al. Immunosuppression and resultant viral persistence by specific viral targeting of dendritic cells. *J Exp Med*. 2000;192(9):1249–60.

191. Teijaro JR. Type I interferons in viral control and immune regulation. *Curr Opin Virol* [Internet]. 2016;16:31–40. Available from: <http://linkinghub.elsevier.com/retrieve/pii/S1879625716000043>
192. Smelt SC, Borrow P, Kunz S, Cao WEI, Tishon A, Lewicki H, et al. Differences in Affinity of Binding of Lymphocytic Choriomeningitis Virus Strains to the Cellular Receptor  $\alpha$ -Dystroglycan Correlate with Viral Tropism and Disease Kinetics. *J Virol*. 2001;75(1):448–57.
193. Sevilla N, Kunz S, MCGAVERN D, Oldstone MBA. Infection of Dendritic Cells by Lymphocytic Choriomeningitis Virus. *Curr Top Microbiol Immunol*. 2003;276:125–44.
194. Velu V, Titanji K, Zhu B, Husain S, Pladevega A, Lai L, et al. Enhancing SIV-specific immunity in vivo by PD-1 blockade. *Nature* [Internet]. 2009;457(7235):206–10. Available from: <http://dx.doi.org/10.1038/nature07662>
195. Lukashevich IS, Djavani M, Shapiro K, Sanchez A, Ravkov E, Nichol ST, et al. The Lassa fever virus L gene : nucleotide sequence , comparison , and precipitation of a predicted 250 kDa protein with monospecific antiserum. *J Gen Virol*. 1997;78(PT3):547–51.
196. Oxenius A, Bachmann MF, Mathis D, Benoist C, Zinkernagel RM, Hengartner H. Functional In Vivo MHC Class II Loading by Endogenously Synthesized Glycoprotein During Viral Infection. *J Immunol*. 1997;158(12):5717–26.
197. Madisen L, Zwingman TA, Sunkin SM, Oh SW, Hatim A, Gu H, et al. A robust and high-throughput Cre reporting and characterization system for the whole mouse brain. *Nat Neurosci*. 2010;13(1):133–40.
198. Emonet SF, Garidou L, McGAVERN DB, de La Torre JC. Generation of recombinant lymphocytic choriomeningitis viruses with trisegmented genomes stably expressing two additional genes of interest. *Proc Natl Acad Sci U S A* [Internet]. 2009;106(9):3473–8. Available from: <http://eutils.ncbi.nlm.nih.gov/entrez/eutils/elink.fcgi?dbfrom=pubmed&id=19208813&retmode=ref&cmd=prlinks%5Cnpapers3://publication/doi/10.1073/pnas.0900088106>
199. Martínez-Sobrido L, de la Torre JC. Reporter-Expressing, Replicating-Competent

- Recombinant Arenaviruses. *Viruses*. 2016;8(7).
200. Popkin DL, Teijaro JR, Lee AM, Lewicki H, Emonet S, de la Torre JC, et al. Expanded potential for recombinant trisegmented lymphocytic choriomeningitis viruses: protein production, antibody production, and in vivo assessment of biological function of genes of interest. *J Virol* [Internet]. 2011;85(15):7928–32. Available from: <http://www.ncbi.nlm.nih.gov/pubmed/21613399><http://jvi.asm.org/content/85/15/7928.full.pdf>
  201. Livak KJ, Schmittgen TD. Analysis of relative gene expression data using real-time quantitative PCR and the 2- $\Delta\Delta$ CT method. *Methods*. 2001;25(4):402–8.
  202. Foulon E, Foucras G. Two populations of ovine bone marrow-derived dendritic cells can be generated with recombinant GM-CSF and separated on CD11b expression. *J Immunol Methods*. 2008;339(1):1–10.
  203. Bienzle D, Reggeti F, Clark ME, Chow C. Immunophenotype and functional properties of feline dendritic cells derived from blood and bone marrow. *Vet Immunol Immunopathol*. 2003;96(1–2):19–30.
  204. Gutzwiller MER, Moulin HR, Zurbriggen A, Roosje P, Summerfield A. Comparative analysis of canine monocyte- and bone-marrow-derived dendritic cells. *Vet Res*. 2010;41(4).
  205. Wu Z, Rothwell L, Young JR, Kaufman J, Butter C, Kaiser P. Generation and characterization of chicken bone marrow-derived dendritic cells. *J cells, Mol Syst Technol*. 1973;133–45.
  206. Jansen CA, Biggelaar RHG. van den, Arkesteijn GJ., Rutten VPM. In vitro Chicken Bone Marrow-Derived Dendritic Cells Comprise Subsets at Different States of Maturation. *Front Immunol*. 2020;11(February).
  207. Na YR, Jung D, Gu GJ, Seok SH. GM-CSF Grown Bone Marrow Derived Cells Are Composed of Phenotypically Different Dendritic Cells and Macrophages. *Mol Cells*. 2016;39(10):734–41.
  208. Wang J, Dai X, Hsu C, Ming C, He Y, Zhang JI, et al. Discrimination of the heterogeneity of bone marrow - derived dendritic cells. *Mol Med Rep*. 2017;6787–93.
  209. Abdel-Hakeem MS. Viruses teaching immunology: Role of LCMV model and human

- viral infections in immunological discoveries. *Viruses*. 2019;11(2).
210. Althage A, Odermatt B, Moskophidis D, Kiindig T, Hengartner H, Zinkernagel RM. Immunosuppression by lymphocytic choriomeningitis virus infection : competent effector T and B cells but impaired antigen present ation \*. *Eur J Immunol*. 1992;1803–12.
  211. Caruso A, Licenziati S, Corulli M, Canaris AD, Francesco MA De, Fiorentini S, et al. Flow Cytometric Analysis of Activation Markers on Stimulated T Cells and Their Correlation With Cell Proliferation. *Cytometry*. 1997;76:71–6.
  212. Cao W, Henry MD, Borrow P, Yamada H, Elder JH, Ravkov E V, et al. Identification of  $\alpha$ -Dystroglycan as a Receptor for Lymphocytic Choriomeningitis Virus and Lassa Fever Virus. *Science* (80- ). 1998;282(December):2079–82.
  213. Alothaimen T, Seaver K, Mulder R, Gee K, Basta S. Granulocyte/Macrophage Colony-Stimulating Factor-Derived Macrophages Exhibit Distinctive Early Immune Response to Lymphocytic Choriomeningitis Virus Infection. *Viral Immunol*. 2020;00(00):1–12.
  214. Sevilla BN, Kunz S, Holz A, Lewicki H, Homann D, Yamada H, et al. Immunosuppression and Resultant Viral Persistence by Specific Viral Targeting of Dendritic Cells. *J Exp Med*. 2000;192(9):1249–60.
  215. Che Mat NF, Siddiqui S, Mehta D, Seaver K, Banete A, Alothaimen T, et al. Lymphocytic choriomeningitis virus infection of dendritic cells interferes with TLR-induced IL-12/IL-23 cytokine production in an IL-10 independent manner. *Cytokine* [Internet]. 2018;108(March):105–14. Available from: <https://doi.org/10.1016/j.cyto.2018.03.017>
  216. Mian MF, Ahmed AN, Rad M, Babaian A, Bowdish D, Ashkar AA. Length of dsRNA ( poly I : C ) drives distinct innate immune responses , depending on the cell type. *J Leukoc Biol*. 2013;94(November):1025–36.
  217. Reimer T, Brcic M, Schweizer M, Jungi TW, The I-. poly ( I : C ) and LPS induce distinct IRF3 and NF- B signaling during type-I IFN and TNF responses in human macrophages. *J Leukoc Biol*. 2008;83(May):1249–57.
  218. Erlich Z, Shlomovitz I, Edry-botzer L, Cohen H, Frank D, Wang H, et al.

- Macrophages , rather than DCs , are responsible for inflammasome activity in the GM-CSF BMDC model. *Nat Immunol* [Internet]. 2019;20(April). Available from: <http://dx.doi.org/10.1038/s41590-019-0313-5>
219. Jin D, Sprent J. GM-CSF Culture Revisited: Preparation of Bulk Populations of Highly Pure Dendritic Cells from Mouse Bone Marrow. *J Immunol*. 2020;
  220. Yun NE, Walker DH. Pathogenesis of Lassa fever. *Viruses* [Internet]. 2012 Oct [cited 2014 Nov 26];4(10):2031–48. Available from: <http://www.pubmedcentral.nih.gov/articlerender.fcgi?artid=3497040&tool=pmcentrez&rendertype=abstract>
  221. Xing J, Chai Z, Ly H, Liang Y. Differential Inhibition of Macrophage Activation by Lymphocytic Choriomeningitis Virus and Pichinde Virus Is Mediated by the Z Protein N-Terminal Domain. *J Virol*. 2015;89(24):12513–7.
  222. Whiteside SK, Snook JP, Williams MA, Weis JJ. Bystander T Cells : A Balancing Act of Friends and Foes. *Trends Immunol* [Internet]. 2018;39(12):1021–35. Available from: <http://dx.doi.org/10.1016/j.it.2018.10.003>
  223. Suprunenko T, Hofer MJ. Complexities of type i interferon biology: Lessons from lcmv. *Viruses*. 2019;11(2):1–20.
  224. Bost P, Giladi A, Liu Y, Bendjelal Y, Xu G, David E, et al. Host-viral infection maps reveal signatures of severe COVID-19 patients. *Cell* [Internet]. 2020;181:1475–88. Available from: <https://doi.org/10.1016/j.cell.2020.05.006>
  225. Hwang B, Lee JH, Bang D. Single-cell RNA sequencing technologies and bioinformatics pipelines. *Exp Mol Med* [Internet]. 2018;50(96):1–14. Available from: <http://dx.doi.org/10.1038/s12276-018-0071-8>
  226. Lin WN, Tay MZ, Lu R, Liu Y, Chen C, Cheow LF. The Role of Single-Cell Technology in the Study and Control of Infectious Diseases. :1–28.
  227. Norris BA, Uebelhoer LS, Nakaya HI, Price AA, Grakoui A, Pulendran B. Polyphasic innate immune responses to acute and chronic LCMV infection: innate immunity to acute and chronic viral infection. *Immunity* [Internet]. 2013;38(2):309–21. Available from: <http://linkinghub.elsevier.com/retrieve/pii/S1074761313000551>
  228. Stoeckius M, Hafemeister C, Stephenson W, Houck-Loomis B, Chattopadhyay PK,

- Swerdlow H, et al. Simultaneous epitope and transcriptome measurement in single cells. *Nat Methods*. 2017;14(9):865–8.
229. Stoeckius M, Zheng S, Houck-Loomis B, Hao S, Yeung BZ, Mauck WM, et al. Cell Hashing with barcoded antibodies enables multiplexing and doublet detection for single cell genomics. *Genome Biol*. 2018;19(1):1–12.
230. Biolegend. TotalSeq™ -A0315 anti-mouse Hashtag 15 Antibody. Tech datasheet. 2018;1–2.
231. Mulè M, Martins A, Tsang J. Normalizing and denoising protein expression data from droplet-based single cell profiling. 2020;
232. Cao Y, Wang X, Peng G. SCSA: A cell type annotation tool for single-cell RNA-seq data. *Front Genet*. 2020;11(May):1–8.
233. Kim H, Kim M, Im S-K, Fang S. Mouse Cre-LoxP system: general principles to determine tissue-specific roles of target genes. *Lab Anim Res*. 2018;34(4):147.
234. Monica Macal, Gavin M. Lewis, Stefan Kunz, Richard Flavell, James A. Harker and EIZ. Plasmacytoid Dendritic Cells Are Productively Infected And Activated Through TLR-7 Early After Arenavirus Infection. *Cell Host Microbe*. 2012;11(6):617–30.
235. Sullivan BM, Teijaro JR, de la Torre JC, Oldstone MBA. Early Virus-Host Interactions Dictate the Course of a Persistent Infection. *PLoS Pathog*. 2015;11(1):1–14.
236. Zuniga EI, Liou L, Mack L, Mendoza M, Ba M. In vivo virus infection inhibits type I interferon production by plasmacytoid dendritic cells thereby facilitating opportunistic infections. *Cell Host Microbe*. 2008;4(4):374–86.
237. Argilaguet J, Pedragosa M, Esteve-codina A, Riera G, Vidal E, Peligero-cruz C, et al. Systems analysis reveals complex biological processes during virus infection fate decisions. :907–19.
238. Bolton DL, Roederer M, Chattopadhyay PK. A deadly dance: the choreography of host–pathogen interactions, as revealed by single-cell technologies. *Nat Commun* [Internet]. 2018;9(4638):1–11. Available from: <http://dx.doi.org/10.1038/s41467-018-06214-0>

239. Stanifer ML, Kee C, Cortese M, Zumarán CM, Triana S, Mukenhirn M, et al. Critical Role of Type III Interferon in Controlling SARS-CoV-2 Infection in Human Intestinal Epithelial Cells. *Cell Rep* [Internet]. 2020;32(1):107863. Available from: <https://doi.org/10.1016/j.celrep.2020.107863>
240. Ribero MS, Jouvenet N, Dreux M, Nisole S. Interplay between SARS-CoV-2 and the type I interferon response. *PLoS Pathog*. 2020;16(7):1–22.
241. Cicin-Sain L, Brien JD, Uhrlaub JL, Drabig A, Marandu TF, Nikolich-Zugich J. Cytomegalovirus Infection Impairs Immune Responses and Accentuates T-cell Pool Changes Observed in Mice with Aging. *PLoS Pathog*. 2012;8(8):1–15.
242. Geisbert TW. Predicting outcome and improving treatment for Lassa fever. *Lancet Infect Dis* [Internet]. 2018;18(6):594–5. Available from: [http://dx.doi.org/10.1016/S1473-3099\(18\)30116-6](http://dx.doi.org/10.1016/S1473-3099(18)30116-6)

# APPENDIX

## **Appendix 1. A summary table for all the comparisons between different cell clusters and treatments**

### **DC1 cells**

Summary for comparisons DC1 bystander vs MQ Ly6C - bystander: 5% significance level: 62 1% significance level: 43 Total genes tested: 2862 Link to table: [results table](#)

Summary for comparisons DC1 bystander vs MQ Ly6C + bystander: 5% significance level: 8 1% significance level: 8 Total genes tested: 3794 Link to table: [results table](#)

Summary for comparisons DC1 bystander vs pDC bystander: 5% significance level: 18 1% significance level: 6 Total genes tested: 3090 Link to table: [results table](#)

Summary for comparisons DC1 inf vs DC1 polyIC: 5% significance level: 11 1% significance level: 11 Total genes tested: 2362 Link to table: [results table](#)

Summary for comparisons DC1 Inf vs MQ Ly6C - Inf: 5% significance level: 665 1% significance level: 576 Total genes tested: 2281 Link to table: [results table](#)

Summary for comparisons DC1 Inf vs MQ Ly6C + Inf: 5% significance level: 614 1% significance level: 527 Total genes tested: 2608 Link to table: [results table](#)

Summary for comparisons DC1 Inf vs pDC Inf: 5% significance level: 1323 1% significance level: 1275 Total genes tested: 1895 Link to table: [results table](#)

Summary for comparisons DC1 non inf vs DC1 polyIC: 5% significance level: 10 1% significance level: 7 Total genes tested: 2141 Link to table: [results table](#)

Summary for comparisons DC1 non inf vs MQ Ly6C - non inf: 5% significance level: 581 1% significance level: 496 Total genes tested: 2164 Link to table: [results table](#)

Summary for comparisons DC1 non inf vs MQ Ly6C - non inf: 5% significance level: 333 1% significance level: 276 Total genes tested: 2444 Link to table: [results table](#)

Summary for comparisons DC1 non inf vs pDC non inf: 5% significance level: 405 1% significance level: 312 Total genes tested: 2296 Link to table: [results table](#)

Summary for comparisons DC1 polyIC vs MQ Ly6C - polyIC: 5% significance level: 7 1% significance level: 0 Total genes tested:3647 Link to table: [results table](#)

### **DC2 cells:**

Summary for comparisons DC2 bystander vs DC2 inf: 5% significance: 1 1% significance: 1 Total genes tested:1618 Link to table: [results table](#)

Summary for comparisons DC2 bystander vs MQ Ly6C - bystander: 5% significance: 28 1% significance: 17 Total genes tested:3113 Link to table: [results table](#)

Summary for comparisons DC2 bystander vs MQ Ly6C + bystander: 5% significance: 3 1% significance: 2 Total genes tested:4405 Link to table: [results table](#)

Summary for comparisons DC2 bystander vs pDC bystander: 5% significance: 0 1% significance: 0 Total genes tested:2830 Link to table: [results table](#)

Summary for comparisons DC2 Inf vs MQ Ly6C - Inf: 5% significance: 419 1% significance: 363 Total genes tested:1631 Link to table: [results table](#)

Summary for comparisons DC2 Inf vs MQ Ly6C + Inf: 5% significance: 351 1% significance: 295 Total genes tested:2165 Link to table: [results table](#)

Summary for comparisons DC2 Inf vs pDC Inf: 5% significance: 424 1% significance: 370 Total genes tested:872 Link to table: [results table](#)

Summary for comparisons DC2 non inf vs DC2 bystander: 5% significance: 1 1% significance: 0 Total genes tested:1478 Link to table: [results table](#)

Summary for comparisons DC2 non inf vs DC2 infected: 5% significance: 64 1% significance: 34 Total genes tested:722 Link to table: [results table](#)

Summary for comparisons DC2 non inf vs MQ Ly6C - non inf: 5% significance: 385 1% significance: 333 Total genes tested:1794 Link to table: [results table](#)

Summary for comparisons DC2 non inf vs MQ Ly6C + non inf: 5% significance: 239 1% significance: 192 Total genes tested:2347 Link to table: [results table](#)

Summary for comparisons DC2 non inf\_vs pDC no inf: 5% significance: 177 1% significance: 131 Total genes tested:2004 Link to table: [results table](#)

### **MQ Ly6C - cells**

Summary for comparisons MQ Ly6C - bystander vs MQ Ly6C - inf: 5% significance: : 1 1% significance: : 1 Total genes tested:1863 Link to table: [results table](#)

Summary for comparisons MQ Ly6C - inf vs MQ Ly6C - polyIC: 5% significance: : 1 1% significance: : 1 Total genes tested:2663 Link to table: [results table](#)

Summary for comparisons MQ Ly6C - non inf vs MQ Ly6C - bystander: 5% significance: : 2 1% significance: : 1 Total genes tested:1458 Link to table: [results table](#)

Summary for comparisons MQ Ly6C - non inf vs MQ Ly6C - infected: 5% significance: : 2 1% significance: : 1 Total genes tested:428 Link to table: [results table](#)

Summary for comparisons MQ Ly6C - non inf vs MQ Ly6C - polyIC: 5% significance: : 5 1% significance: : 3 Total genes tested:2284 Link to table: [results table](#)

### **MQ Ly6C + cells:**

Summary for comparisons MQ Ly6C plus non inf vs MQ Ly6C plus bystander: 5% significance: 5 1% significance: 3 Total genes tested:3147 Link to table: [results table](#)

Summary for comparisons MQ Ly6C plus non inf vs MQ Ly6C plus infected: 5% significance: 7 1% significance: 3 Total genes tested:1293 Link to table: [results table](#)

### **pDC cells:**

Summary for comparisons pDC bystander vs MQ Ly6C - bystander: 5% significance: 8 1% significance: 4 Total genes tested:3090 Link to table: [results table](#)

Summary for comparisons pDC bystander vs MQ Ly6C + bystander: 5% significance: 1 1% significance: 0 Total genes tested:4423 Link to table: [results table](#)

Summary for comparisons pDC bystander vs pDC inf: 5% significance: 2 1% significance: 1 Total genes tested:1440 Link to table: [results table](#)

Summary for comparisons pDC infected vs MQ Ly6C - infected: 5% significance: 420 1% significance: 348 Total genes tested:1494 Link to table: [results table](#)

Summary for comparisons pDC infected vs MQ Ly6C + infected: 5% significance: 142 1% significance: 119 Total genes tested:1510 Link to table: [results table](#)

Summary for comparisons pDC non inf vs pDC bystander: 5% significance: 2 1% significance: 2 Total genes tested:1709 Link to table: [results table](#)

Summary for comparisons pDC non inf vs pDC infected: 5% significance: 57 1% significance: 42 Total genes tested:222 Link to table: [results table](#)

Summary for comparisons pDC uninfected vs MQ Ly6C plus uninfected: 5% significance: 75 1% significance: 57 Total genes tested:1455 Link to table: [results table](#)

## 4.2.9.2 Library 4

### DC1 cells

Summary for comparisons DC1 Inf vs Ly6C - Inf: 5% significance: 0 1% significance: 0 Total genes tested:4243 Link to table: [results table](#)

Summary for comparisons DC1 Inf vs pDC Inf: 5% significance: 0 1% significance: 0 Total genes tested:4532 Link to table: [results table](#)

Summary for comparisons DC1 non inf vs DC1 infected: 5% significance: 4 1% significance: 4 Total genes tested:2245 Link to table: [results table](#)

Summary for comparisons DC1 non inf vs Ly6C - non inf: 5% significance: 188 1% significance: 137 Total genes tested:2433 Link to table: [results table](#)

Summary for comparisons DC1 non inf vs pDC non inf: 5% significance: 178 1% significance: 127 Total genes tested:2915 Link to table: [results table](#)

### DC2 cells

Summary for comparisons DC2 Inf vs Ly6C - Inf: 5% significance: 0 1% significance: 0 Total genes tested:4482 Link to table: [results table](#)

Summary for comparisons DC2 Inf vs pDC Inf: 5% significance: 0 1% significance: 0 Total genes tested:3968 Link to table: [results table](#)

Summary for comparisons DC2 non inf vs DC2 infected: 5% significance: 0 1% significance: 0 Total genes tested:3079 Link to table: [results table](#)

Summary for comparisons DC2 non inf vs Ly6C - non inf: 5% significance: 42 1% significance: 29 Total genes tested:2978 Link to table: [results table](#)

Summary for comparisons DC2 non inf vs pDC non inf: 5% significance: 0 1% significance: 0 Total genes tested:3286 Link to table: [results table](#)

## **MQ Ly6C - cells**

Summary for comparisons MQ Ly6C - non inf vs MQ Ly6C - infected: 5% significance: 9  
1% significance: 6 Total genes tested:3133 Link to table: [results table](#)

## **pDC cells**

Summary for comparisons pDC infected vs MQ Ly6C - infected: 5% significance: 0 1%  
significance: 0 Total genes tested:4812 Link to table: [results table](#)

Summary for comparisons pDC non inf vs pDC infected: 5% significance: 0 1% significance:  
0 Total genes tested:3779 Link to table: [results table](#)

Summary for comparisons pDC uninfected vs MQ Ly6C - uninfected: 5% significance: 4 1%  
significance: 1 Total genes tested:2795 Link to table: [results table](#)

## **4.2.9.3 Library 5**

### **DC1 cells**

Summary for comparisons DC1 bystander vs DC1 inf: 5% significance: 0 1% significance: 0  
Total genes tested:4347 Link to table: [results table](#)

Summary for comparisons DC1 Inf vs Ly6C -Inf: 5% significance: 51 1% significance: 37  
Total genes tested:3961 Link to table: [results table](#)

Summary for comparisons DC1 Inf vs pDC Inf: 5% significance: 289 1% significance: 225  
Total genes tested:2262 Link to table: [results table](#)

Summary for comparisons DC1 non inf vs DC1 bystander: 5% significance: 0 1%  
significance: 0 Total genes tested:4049 Link to table: [results table](#)

Summary for comparisons DC1 non inf vs DC1 infected: 5% significance: 0 1% significance:  
0 Total genes tested:4660 Link to table: [results table](#)

Summary for comparisons DC1 non inf vs Ly6C - non inf: 5% significance: 68 1%  
significance: 67 Total genes tested:4525 Link to table: [results table](#)

Summary for comparisons DC1 non inf vs pDC non inf: 5% significance: 0 1% significance:  
0 Total genes tested:3462 Link to table: [results table](#)

### **MQ Ly6C- cells**

Summary for comparisons MQ Ly6C - non inf vs MQ Ly6C - infected: 5% significance: 10  
1% significance: 8 Total genes tested:2719 Link to table: [results table](#)

### **pDC cells**

Summary for comparisons pDC infected vs MQ Ly6C - infected: 5% significance: 28 1%  
significance: 21 Total genes tested:3629 Link to table: [results table](#)

Summary for comparisons pDC non inf vs pDC infected: 5% significance: 84 1%  
significance: 60 Total genes tested:4220 Link to table: [results table](#)

Summary for comparisons pDC uninfected vs MQ Ly6C - uninfected: 5% significance: 57  
1% significance: 24 Total genes tested:3515 Link to table: [results table](#)

## **4.2.9.4 Library 6**

### **DC1 cells**

Summary for comparisons DC1 bystander vs DC1 inf: 5% significance: 1 1% significance: 0  
Total genes tested: 2111 Link to table: [results table](#)

Summary for comparisons DC1 bystander vs MQ Ly6C - bystander: 5% significance: 14 1%  
significance: 11 Total genes tested: 2678 Link to table: [results table](#)

Summary for comparisons DC1 bystander vs MQ Ly6C + bystander: 5% significance: 362  
1% significance: 332 Total genes tested: 2695 Link to table: [results table](#)

Summary for comparisons DC1 bystander vs pDC bystander: 5% significance: 132 1%  
significance: 77 Total genes tested: 2622 Link to table: [results table](#)

Summary for comparisons DC1 inf vs DC1 polyIC: 5% significance: 3 1% significance: 3  
Total genes tested: 1163 Link to table: [results table](#)

Summary for comparisons DC1 Inf vs MQ Ly6C - Inf: 5% significance: 88 1% significance:  
66 Total genes tested: 2289 Link to table: [results table](#)

Summary for comparisons DC1 Inf vs MQ Ly6C + Inf: 5% significance: 515 1%  
significance: 470 Total genes tested: 2538 Link to table: [results table](#)

Summary for comparisons DC1 non inf vs DC1 bystander: 5% significance: 0 1%  
significance: 0 Total genes tested: 3578 Link to table: [results table](#)

Summary for comparisons DC1 non inf vs DC1 infected: 5% significance: 1 1% significance: 0 Total genes tested: 3694 Link to table: [results table](#)

Summary for comparisons DC1 non inf vs DC1 polyIC: 5% significance: 5 1% significance: 1 Total genes tested: 3431 Link to table: [results table](#)

Summary for comparisons DC1 non inf vs MQ Ly6C - non inf: 5% significance: 0 1% significance: 0 Total genes tested: 4937 Link to table: [results table](#)

Summary for comparisons DC1 non inf vs MQ Ly6C + non inf: 5% significance: 30 1% significance: 27 Total genes tested: 3828 Link to table: [results table](#)

Summary for comparisons DC1 non inf vs pDC non inf: 5% significance: 113 1% significance: 106 Total genes tested: 3619 Link to table: [results table](#)

Summary for comparisons DC1 polyIC vs MQ Ly6C - polyIC: 5% significance: 272 1% significance: 224 Total genes tested: 2092 Link to table: [results table](#)

Summary for comparisons DC1 polyIC vs MQ Ly6C + polyIC: 5% significance: 1040 1% significance: 971 Total genes tested: 2462 Link to table: [results table](#)

Summary for comparisons DC1 polyIC vs pDC polyIC: 5% significance: 402 1% significance: 339 Total genes tested: 2395 Link to table: [results table](#)

### **MQ Ly6C - cells**

Summary for comparisons MQ Ly6C - bystander vs MQ Ly6C - inf: 5% significance: 1 1% significance: 1 Total genes tested: 1450 Link to table: [results table](#)

Summary for comparisons MQ Ly6C - inf vs MQ Ly6C - polyIC: 5% significance: 12 1% significance: 9 Total genes tested: 744 Link to table: [results table](#)

Summary for comparisons MQ Ly6C - non inf vs MQ Ly6C - bystander: 5% significance: 1 1% significance: 1 Total genes tested: 3661 Link to table: [results table](#)

Summary for comparisons MQ Ly6C - non inf vs MQ y6 - infected: 5% significance: 8 1% significance: 4 Total genes tested: 4146 Link to table: [results table](#)

Summary for comparisons MQ Ly6C - non inf vs MQ Ly6C - polyIC: 5% significance: 11 1% significance: 9 Total genes tested: 3680 Link to table: [results table](#)

### **MQ Ly6C + cells**

Summary for comparisons MQ Ly6C + bystander vs MQ Ly6C + inf: 5% significance: 1 1% significance: 1 Total genes tested: 59 Link to table: [results table](#)

Summary for comparisons MQ Ly6C + inf vs MQ Ly6C + polyIC: 5% significance: 18 1% significance: 15 Total genes tested: 73 Link to table: [results table](#)

Summary for comparisons MQ Ly6C + non inf vs MQ Ly6C + bystander: 5% significance: 20 1% significance: 15 Total genes tested: 801 Link to table: [results table](#)

Summary for comparisons MQ Ly6C + non inf vs MQ Ly6C + infected: 5% significance: 13 1% significance: 10 Total genes tested: 897 Link to table: [results table](#)

Summary for comparisons MQ Ly6C + non inf vs MQ Ly6C + polyIC: 5% significance: 23 1% significance: 16 Total genes tested: 801 Link to table: [results table](#)

### **pDC cells**

Summary for comparisons pDC polyIC vs MQ Ly6C - polyIC: 5% significance: 242 1% significance: 201 Total genes tested: 1608 Link to table: [results table](#)

Summary for comparisons pDC polyIC vs MQ Ly6C + polyIC: 5% significance: 251 1% significance: 230 Total genes tested: 900 Link to table: [results table](#)

Summary for comparisons pDC bystander vs MQ Ly6C - bystander: 5% significance: 41 1% significance: 31 Total genes tested: 1636 Link to table: [results table](#)

Summary for comparisons pDC bystander vs MQ Ly6C + bystander: 5% significance: 512 1% significance: 462 Total genes tested: 1490 Link to table: [results table](#)

Summary for comparisons pDC bystander vs pDC inf: 5% significance: 3 1% significance: 1 Total genes tested: 781 Link to table: [results table](#)

Summary for comparisons pDC infected vs MQ Ly6C - infected: 5% significance: 128 1% significance: 94 Total genes tested: 1142 Link to table: [results table](#)

Summary for comparisons pDC infected vs MQ Ly6C + infected: 5% significance: 618 1% significance: 525 Total genes tested: 1634 Link to table: [results table](#)

Summary for comparisons pDC inf vs pDC polyIC: 5% significance: 173 1% significance: 129 Total genes tested: 1251 Link to table: [results table](#)

Summary for comparisons pDC non inf vs pDC bystander: 5% significance: 171 1%

significance: 123 Total genes tested: 1613 Link to table: [results table](#)

Summary for comparisons pDC non inf vs pDC infected: 5% significance: 391 1%

significance: 339 Total genes tested: 1782 Link to table: [results table](#)

Summary for comparisons pDC non inf vs pDC polyIC: 5% significance: 76 1% significance:

62 Total genes tested: 1029 Link to table: [results table](#)

Summary for comparisons pDC uninfected vs MQ Ly6C - uninfected: 5% significance: 63

1% significance: 55 Total genes tested: 3572 Link to table: [results table](#)

Summary for comparisons pDC uninfected vs MQ Ly6C + uninfected: 5% significance: 4 1%

significance: 3 Total genes tested: 1081 Link to table: [results table](#)